DELIVERABLE D.T3.3.1

ACTIVITY REPORT ON 3D MODELLING

Part 2: Detailed description of numerical models including estimation of errors

08 2019

Authors

C. Steiner[1], J. Švasta[2], M. Janža[3], D. Šram[3] and B. Ciapała[4]

[1]Geologicial Survey of Austria

[2] State Geological Institute of Dionýz Štúr, Slovakia

[3] Geological Survey of Slovenia

[4] AGH University of Science and Technology

The involved GeoPLASMA-CE team

PP Acronym	**Person and task**
LP - GBA	Cornelia Steiner (compilation and reporting of numerical model pilot area Vienna) Martin Fuchsluger (input for numerical model pilot areas Vienna)
PP06 – SGIDS	Jaromír Švasta (reporting of model for pilot area Bratislava-Hainburg)
PP07 – GeoZS	Mitja Janža (reporting of model for pilot area Ljubljana) Dejan Šram (reporting of model for pilot area Ljubljana)
PP09 – AGH-UST	Bartłomiej Ciapała (reporting of model for pilot area Krakow)

1. Introduction

1.1. Aim and scope of this deliverable

This report summarizes all numerical modelling activities in the urban areas that were in the scope of the project GeoPLASMA-CE. It describes the conceptual models, model setup, and discusses model results. The GeoPLASMA-CE team elaborated 3D numerical models for the pilot areas Vienna, Ljubljana, Bratislava-Hainburg and Krakow. We prepared the models with the numerical modelling software systems MODFLOW (pilot area Krakow) and FEFLOW (pilot areas Vienna, Ljubljana and Bratislava-Hainburg).

All models compile existing hydrogeological and geological data as well as new measurements performed within GeoPLASMA-CE. Geological 3D models (D.T3.3.1 - 3D modelling report part 1) provide input data for 3D structure and material properties of the numerical models. Hydrogeological data such as hydraulic conductivity, existing groundwater contour maps and groundwater level and temperature measurements are used as input data as well as calibration targets of the models.

Basic goal of modelling was to generate a map of mean groundwater level, which serves as input data for calculations of shallow geothermal potential open loop and closed loop systems in the pilot areas. In Vienna and Ljubljana, we additionally set-up heat transport models to simulate thermal conditions in shallow aquifers located in urban environments.

2. Activity report numeric process modelling

2.1. Pilot area Ljubljana

2.1.1. Introduction

Ljubljana pilot area was divided into three major units regarding the hydrogeological and geothermal conditions (Figure 1):

1. Ljubljansko polje; Holocene (mostly) unconsolidated sediments, unconfined extensive and highly productive intergranular aquifer,
2. Ljubljansko barje; Pleistocene-Holocene lacustrine and marsh deposits, aquitards overlying moderately productive aquifer and
3. Surrounding hilly area; Carboniferous to Holocene, minor aquifers with local and limited groundwater resources to moderately productive aquifers.

The far most productive aquifer in the Ljubljana pilot area is Ljubljansko polje aquifer with relative fast groundwater flow (up to 20 m/day) which significantly contributes to higher geothermal potential. Previous studies (Janža, 2015) and recent observations of groundwater level and temperature (Šram et al., 2019 b) show high groundwater recharge from River Sava (around 2/3) on the North and the rest from precipitation (around 1/3). While the groundwater dynamic was relatively intensively investigated in the past (Janža, 2015), the information on temperature conditions was scarce.

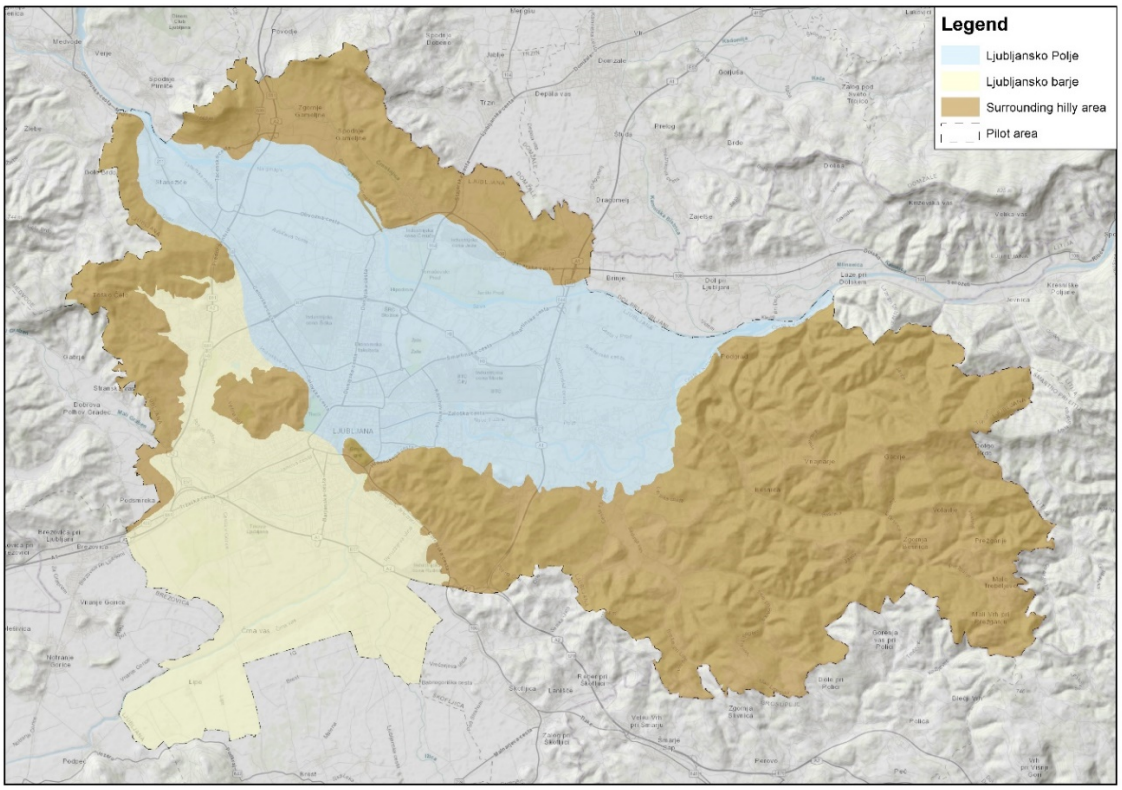

Figure 1. Geological units in the pilot area Ljubljana.

Aim of numerical modelling in GeoPLASMA-CE project was to upgrade the existing hydrological model (Janža, 2015) with the heat transport modelling and get an insight on shallow geothermal conditions, with special focus on most urbanised part of pilot area - Ljubljansko polje area.

In scope of GeoPLASMA-CE a project partner PP03 preformed TRT measurement at the Ljubljansko polje (Rehabilitacijski center Soča). The results from TRT were used as a target in calibration of heat transfer rate of the borehole heat exchanger (BHE) and further for estimation of contribution of groundwater flow to the heat transfer rate. Results for TRT model are presented in special report Annex 1 "NUMERICAL MODELLING OF TRT MEASURMENTS AND ESTIMATION OF HEAT EXTRACTION CAPACITY". Numerical modelling was done with software FEFLOW (Diersch, 2009).

2.1.2. Input data

Data used in the model is based on 3D geological model created in the previous stage of modelling and temperature measurements performed during the GeoPLASMA-CE project (Šram et al., 2019a).

JewelSuite (Baker Hughes, 2014) and ArcMAP software were applied for structural 3D modelling and FEFLOW and ArcMAP (ESRI, 2014) for numerical modelling.

Input data for numerical model:

1. 3D geological model created within GeoPLASMA-CE WPT3 (Šram et. al., 2019a)
2. Measured thermal conductivity and thermal diffusivity (Šram et al., 2019b)
3. Measured groundwater temperature (Šram et al., 2019b and archive data),
4. Hydrological data: Rivers, precipitation, groundwater elevation, hydraulic conductivity (data are obtained from different archive and sources)

5. hydrological data from existing hydrological model (Janža, 2015)

2.1.3. Conceptual model

2.1.3.1. Modelling domain

Pilot area was divided into smaller numerical models according to hydrogeological characteristics and its modelling purposes. Modelling areas are presented in Figure 2. Combined they correspond to area of unconfined aquifer Ljubljansko polje which lies in the central part of the pilot area. Numerical model 1 (Figure 2) covers the central part of Ljubljansko polje aquifer where temperature is relatively constant in time. Numerical model 2 (Figure 2) focuses on the simulation of inflow from river Sava in the North of the model and groundwater temperature fluctuation (Janža et. al. 2017). Numerical model 3 is local model in the area of the performed TRT (Figure 2).

All three models have same setup in FEFLOW regarding the vertical extent and hydrogeological attributes. In vertical direction model extends from around 330 m a.s.l. to 50 m a.s.l. and it is divided into two lithological units: bedrock and quaternary sediments (saturated and unsaturated zone) (Figure 3).

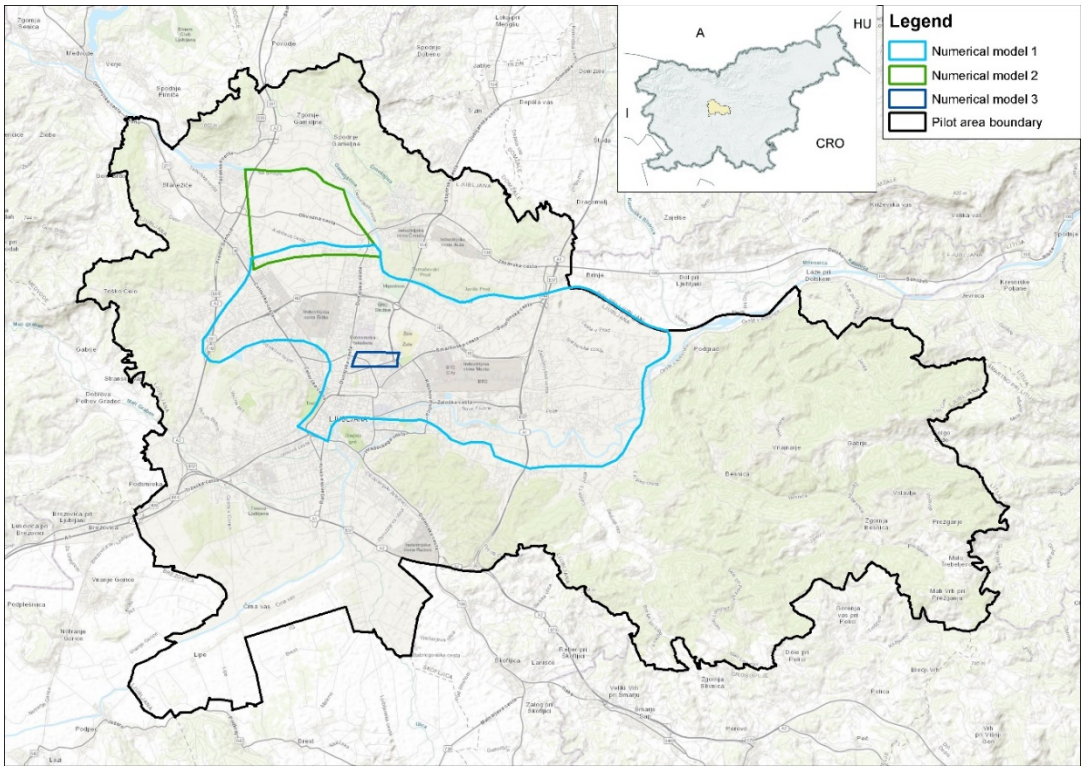

Figure 2. Modelling domains.

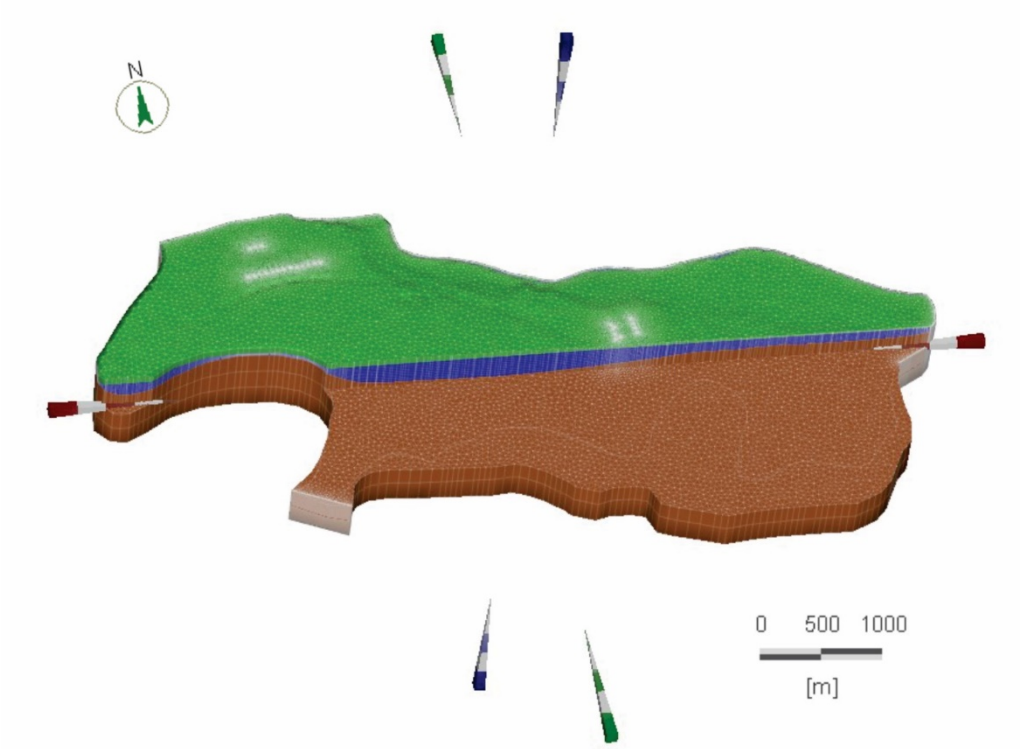

Figure 3. Lithological zone in the model (Unsaturated zone – green, Saturated zone – blue and bedrock – brown) Southern part of the aquifer is clipped.

Quaternary aquifer is in regional sense relatively homogeneous and it was considered as one layer although locally conglomerate lenses and perched aquifers are present (Šram et. al 2012, Janža et. al 2015). Heterogeneity was represented in the model with alternating hydraulic conductivities. Nevertheless, it is further divided into unsaturated and saturated part based on mean groundwater level. Bottom bedrock layer is considered as homogenous layer with uniform properties.

2.1.3.2. Modelling objectives

Major urbanised part of Ljubljana is built on Ljubljansko polje area. The knowledge about Ljubljansko polje hydrogeological settings is relatively good, while thermal characteristic are not well known.

Aquifer of Ljubljansko barje has a complex structure of alternating layers of low permeable clays and sands with higher hydraulic conductivity. Aquifer is confined, especially in the pilot area, except a small part in the Northern part of pilot area. Since 2012 in this area only closed loop geothermal systems are allowed (Decree, 2012).

Hilly areas surrounding both aquifers on pilot area have minor settlements and are poorly investigated, especially in depth. The structure is complex due to faulted carbonated rocks of Triassic and Jurassic ages thrusted over Permian quartz conglomerates and shale.

The aim of numerical modelling was to get a better insight into geothermal conditions and processes in the pilot area. Modelling focused on Ljubljansko polje area, which is the most urbanised part of the city of Ljubljana and where the highest shallow geothermal potential is expected. A regional numerical model of Ljubljansko polje enables a simulation of groundwater flow and heat transport.

2.1.4. Numerical model

2.1.4.1. Model setup

For all numerical models the hydraulic model is steady state, while heat transport model is transient. Hydraulic model is calibrated to the hydraulic conditions in August 2016. Layers in the model, defining its 3D structure were prepared in previous steps, described in the Part 1 of this report. Geological layers were imported into FEFLOW as xyz points.

2.1.4.2. 3D configuration

Horizontal scale of the modelling area is around 14 km x 10 km (E-W x N-S). Vertically the model extends from 330 m a.s.l. to 50 m a. s. l. and is divided into two layers which represent bedrock and quaternary aquifer. To reach a numerical stability of the model, all geological layers are divided further into additional layers.

2.1.4.3. Process variables

2.1.4.3.1. Process variables - Fluid flow

- Groundwater table

For the initial groundwater table we took groundwater level on date 08.06.2016. Based on data from 40 observation points groundwater table in raster format was created in ArcGIS using interpolation method "topo to raster".

2.1.4.3.2. Process variables - Heat transport

- Temperature

Initial uniform temperature of 12 °C was set to whole model.

2.1.4.4. Boundary conditions

2.1.4.4.1. Boundary conditions - Fluid flow

1. River Sava is presented as Constant head

River Sava recharges the aquifer of Ljubljansko polje most intensively at the NW part (Janža et. al. 2015). Boundary condition was set to head elevation which corresponds to groundwater head elevation for mean water level (Figure 4).

2. Constant flow from Ljubljansko barje is set as Fluid flux (Figure 4)

3.

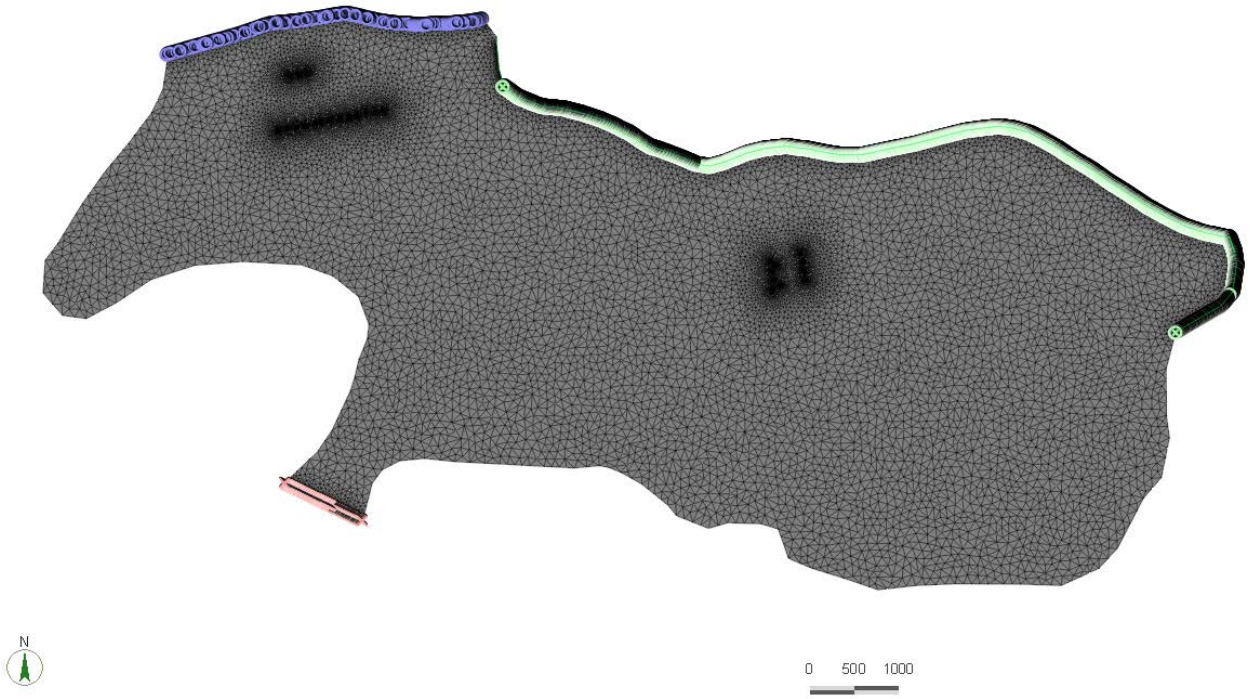

Figure 4. Hydraulic boundary conditions for model 1. Purple – Constant hydraulic head BC (groundwater flow), green – fluid transfer BC (River Sava), pink – fluid-flux BC (constant flow from Barje).

4. Infiltration is set as inflow on the top of the layer

Infiltration from precipitation at Ljubljansko polje represents around 1/3 of all recharge. Yearly average infiltration excluding the evapotranspiration is estimated to 300 mm per year.

5. Wells

Average pumping rates (m^3/day) from the wells were applied in the model.

2.1.4.4.2. Boundary conditions – Heat transport

1. Temperature on the top and bottom of the model

In the Ljubljana pilot area, the meteorological station Ljubljana-Bežigrad registers air temperature at 2 m above ground and soil temperature at different depths up to 1 m daily. We compared air temperature and soil temperatures in 10 cm depth. In time period 2001-2016 the average temperature is 11.6 °C and 12.6 °C respectively. In transient model the daily average temperature of soil at 10 cm depth was used. Temperature at the bottom of the model in depth 250 m was set to 17 °C, which is estimated based on the average heat flux (75 mW/m^2) in the pilot area. Figure 5 shows the model nodes with temperature boundary conditions.

2. Transient temperature for River Sava

Data for average daily temperature for River Sava were obtained from Environmental agency (Web 1) and were used in transient model.

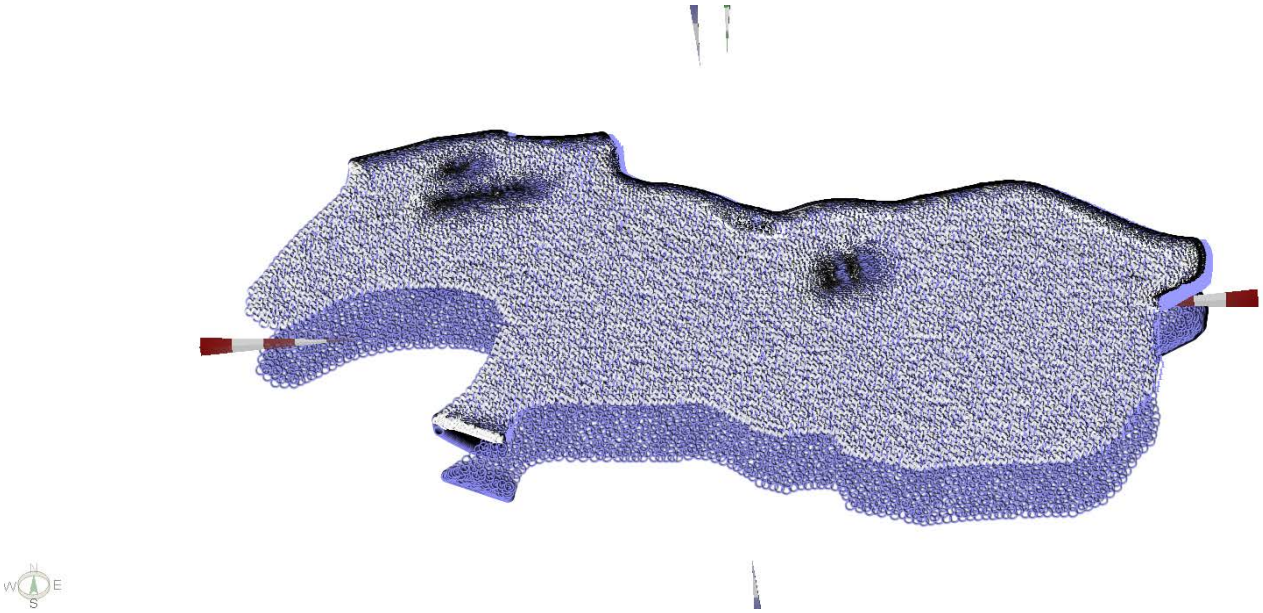

Figure 5. Violet points are model nodes with temperature boundary conditions.

2.1.4.5. Meshing

The mesh is denser around the pumping wells and River Sava (Figure 6 and Figure 7). Figures for total elements, nodes per layer and total area are shown in Table 1.

Table 1. Model 1 and Model 2 geometrical properties.

	Model 1	Model 2
Elements per layer	71216	9320
Nodes per slice	37930	5185
Total area [km²]	50.2	7.5

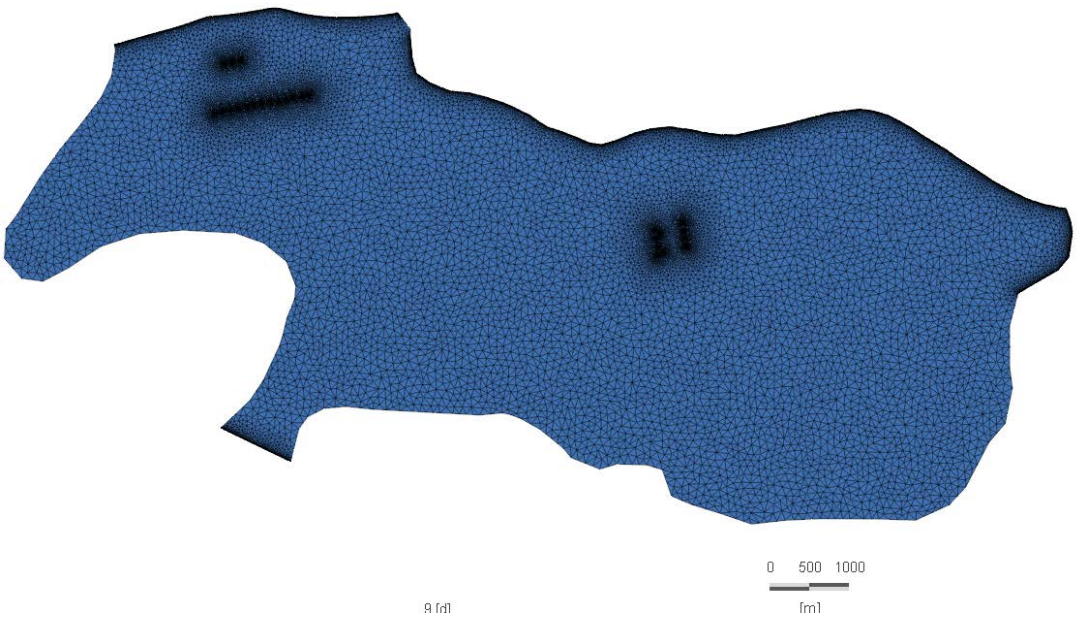

Figure 6. Meshing properties for model 1.

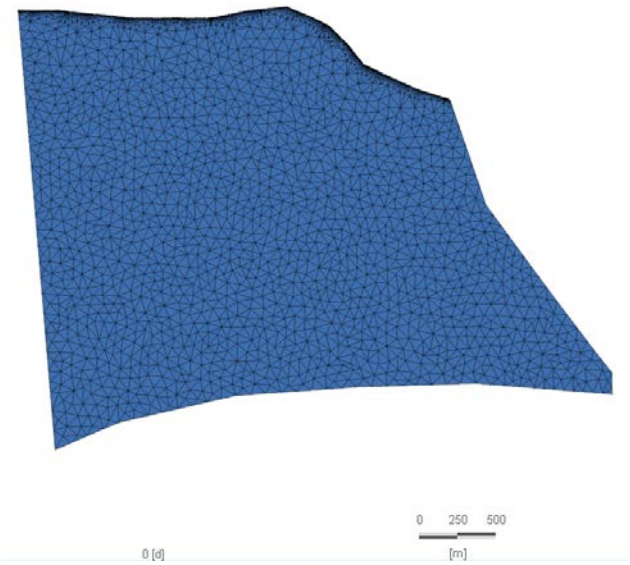

Figure 7. Meshing properties for model 2.

2.1.4.6. Material properties

2.1.4.6.1. Material properties – fluid flow

1. River conductance (In/Out transfer rate)

The transfer rate is a conductance term describing the properties of a clogging layer. It is defined as:

$\Phi = K/d$

where

K: hydraulic conductivity of the clogging layer

d: thickness of the clogging layer

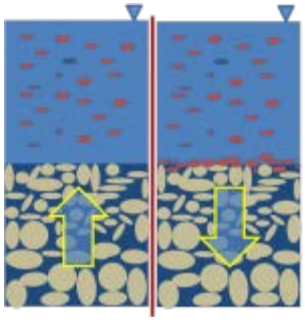

FEFLOW distinguishes between two different transfer rates for infiltration from surface water (Transfer rate in) and exfiltration to surface water (Transfer rate out). According to the gradient direction, FEFLOW automatically chooses the correct value.

Typically, the transfer rate out (left image – web 2) is larger than the transfer rate in (right image – web 2) as clean groundwater 'flushes' the pore space in the clogging layer. In contrast, infiltrating surface water that is typically rich in suspended material tends to clog the pore space (web 2).

Because the river bottom hydraulic conductivity is parameter which is hard to measure, was the value for In/Out transfer rate was estimated with FePEST based on the values for hydraulic conductivity and goundwater elevation.

2. Hydraulic conductivity

Data for hydraulic conductivity were gathered from reports available at archive of Geological Survey of Slovenia. The initial values for hydraulic conductivity were set from $2x10^{-2}$ m/s to $1x10^{-5}$ m/s.

2.1.4.6.2. Material properties – heat transport

1. Thermal conductivity and diffusivity

Thermal conductivity and diffusivity were measured on the 27 different lithological units at least 2 samples (if possible) from same unit were collected and measured (Janža et. al. 2017). Average values for each lithological unit was used as input values for modelling (Figure 8).

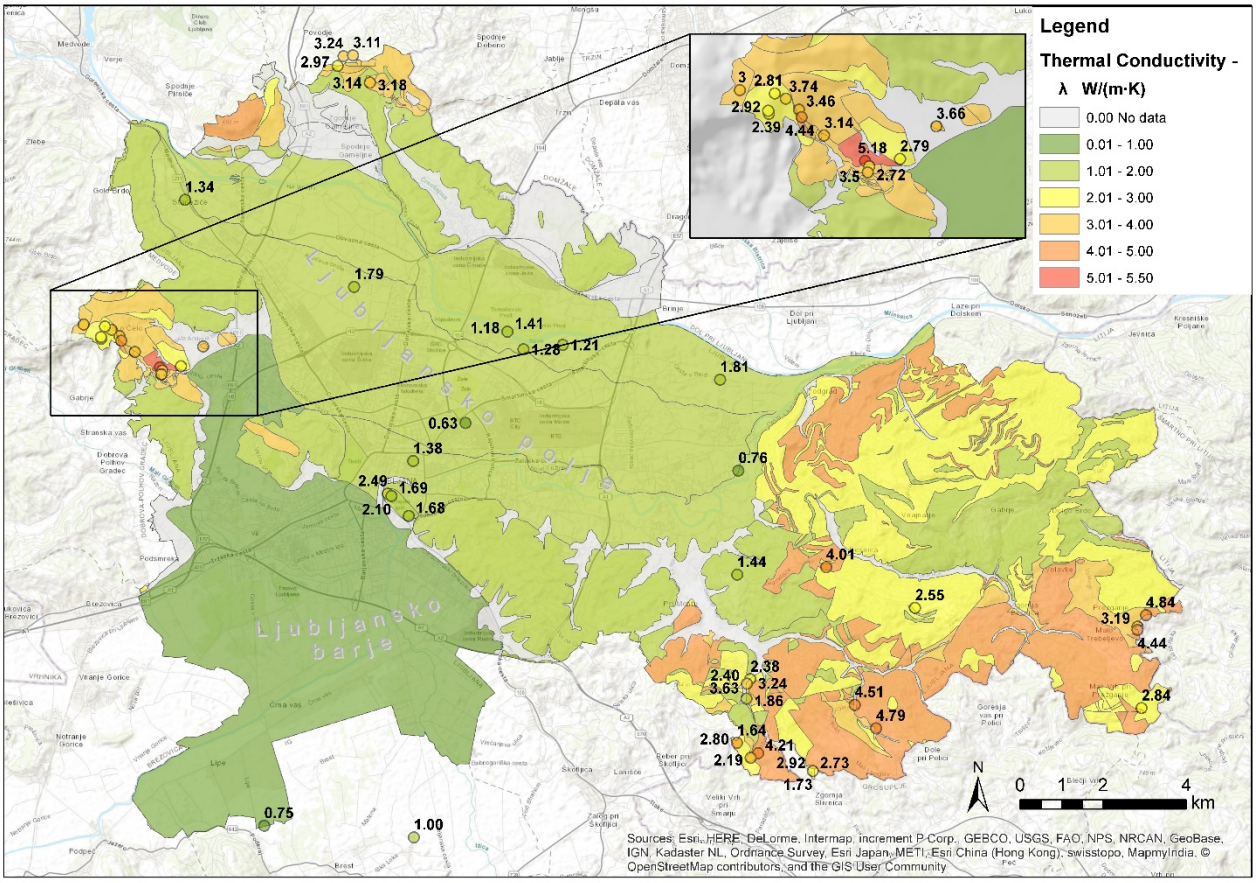

Figure 8. Thermal conductivity of rocks and sediments (adapted from Janža et. al. 2017).

2. Groundwater temperature

Groundwater temperature obtained from the monitoring network, which was set up for GeoPLASMA-CE project (Janža et. al. 2017) were used for estimation the thermal conductivity and volumetric heat capacity (Figure 9 and Figure 10).

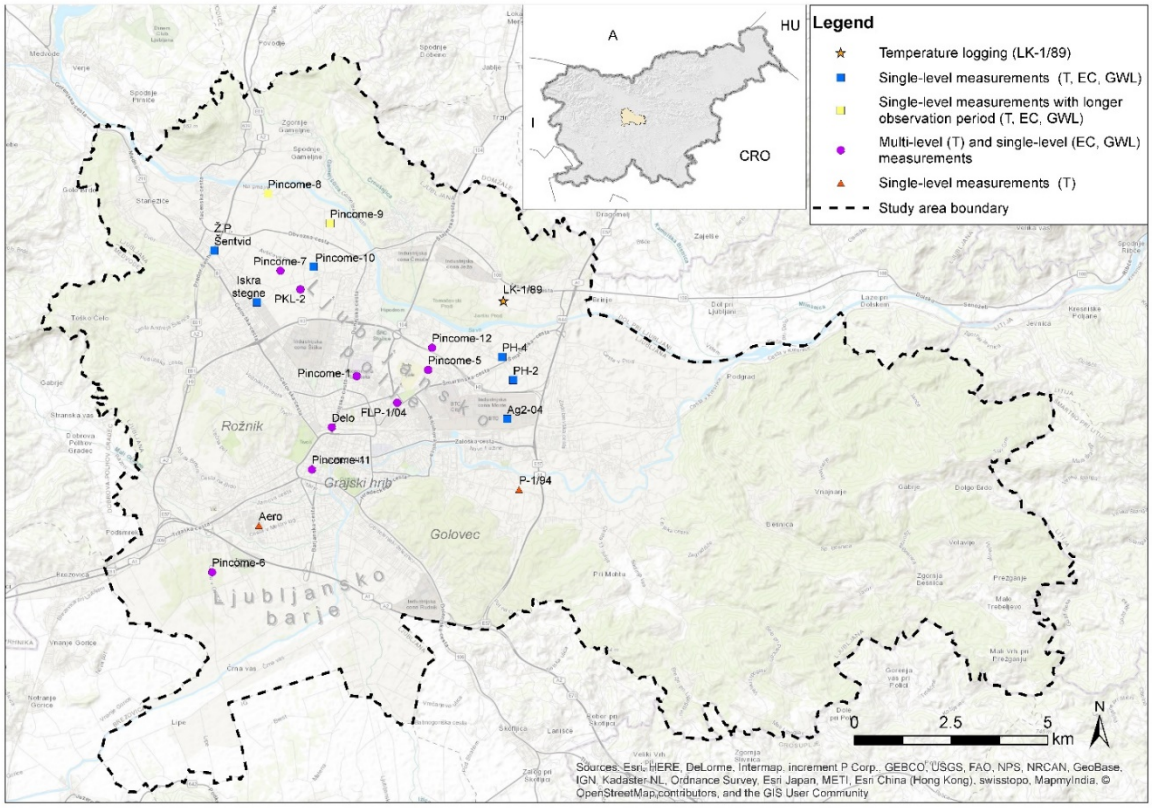

Figure 9. Location of temperature observation wells (adapted from Janža et. al. 2017).

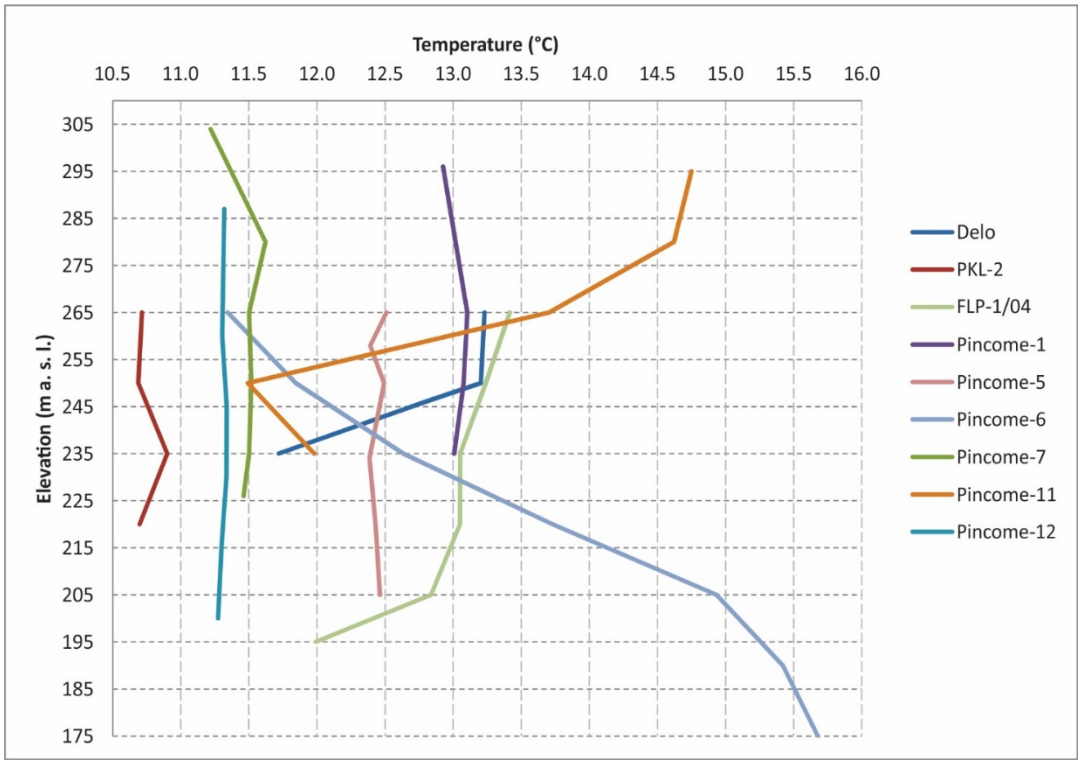

Figure 10. Measured temperature in observation wells (adapted from Janža et. al. 2017).

2.1.5. Simulations

Local model 2 in the North of the pilot area was used to simulate the infiltration of the River Sava to the aquifer based on the temperature fluctuation. Parameters from model 2 were used to set up hydraulic steady state simulation for the central part of the aquifer Ljubljansko polje (model 1) and the TRT simulation (model 3).

2.1.6. Calibration

Using FePEST, parameters in Table 2 were calibrated to the observation values for hydraulic head (steady state) and temperature (transient) at the observation wells.

Calibrated material properties are assigned separately for quaternary aquifer and bedrock as described in Table 2.

Table 2. Calibrated material properties.

Parameter	Aquifer (Unsaturated zone)	Aquifer (Saturated zone)	Bedrock
Hydraulic conductivity Hxx [m/s]	0.003-0.046	0.003-0.046	1.00E-08
Hydraulic conductivity Hyy [m/s]	0.003-0.046	0.003-0.046	1.00E-08
Hydraulic conductivity Hzz [m/s]	0.0003-0.0046	0.0003-0.0046	1.00E-08
In-transfer rate (Sava); flow [1/d]	2.10E+09	2.10E+09	0
Out-transfer rate (Sava); flow [1/d]	8.80E+07	8.80E+07	0
Longitudinal dispersivity [m]	0.1	10	10
Transverse dispersivity [m]	0.1	5	5
Thermal conductivity [J/m/s/K]	1.2	1.2	3
Volumetric heat capacity [MJ/m³/K]	2.7	2.7	3

The difference of observed and modelled groundwater elevation is less than 0.1 m on the 16 observation points and on 4 observation point the difference is up to 1 m.

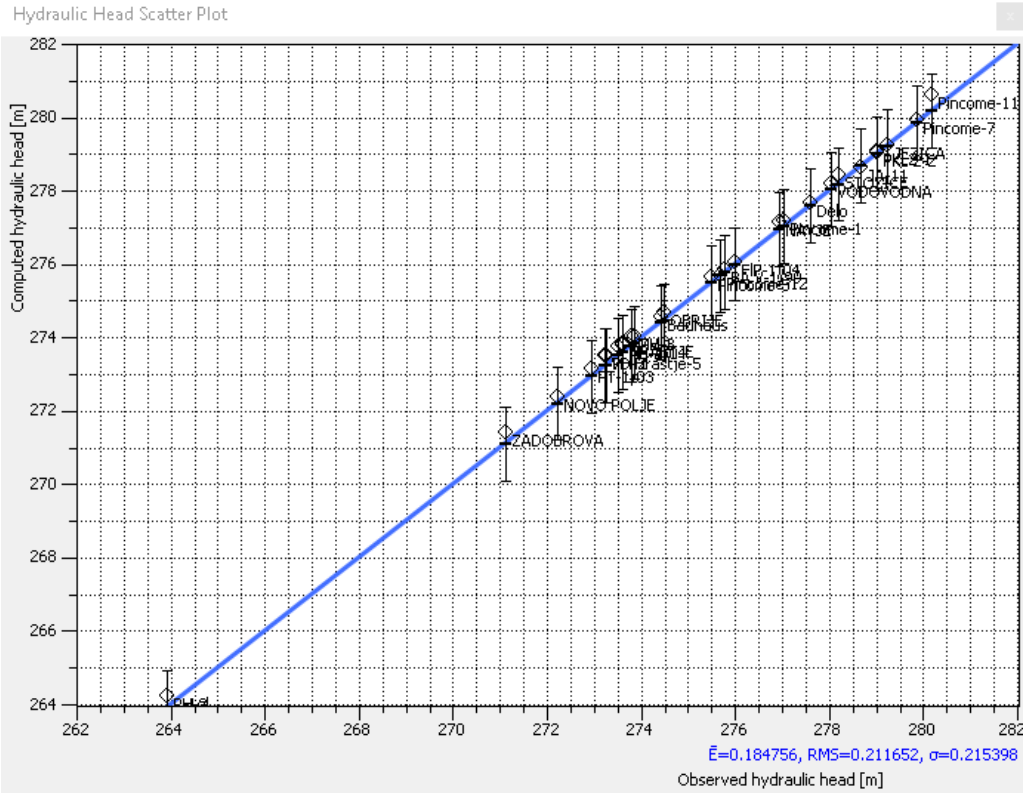

Figure 11. Simulated and observed values for hydraulic head in model 1.

Calibrated thermal parameters where validated with single datum vertical measurements from 10 observation wells. The difference in temperature is up to 1 °C.

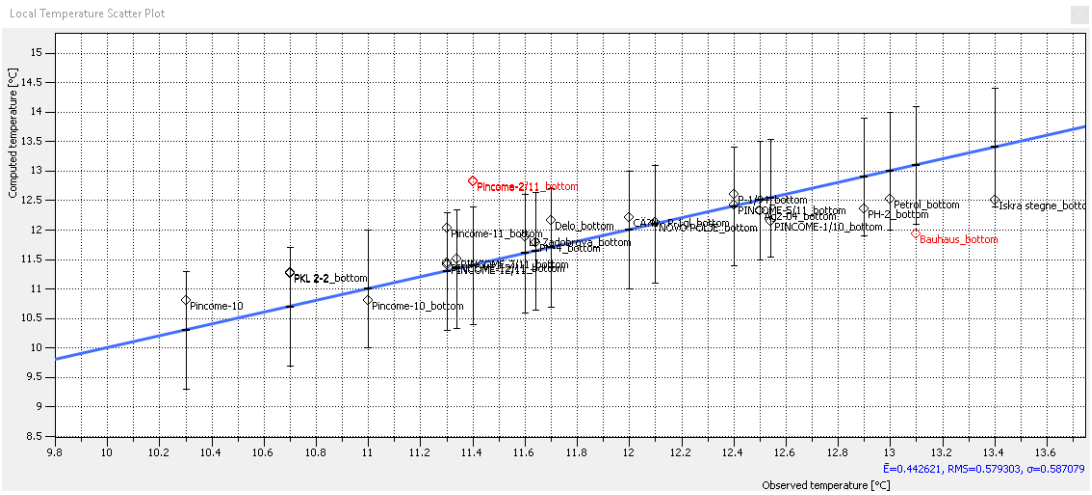

Figure 12. Simulated and observed values for groundwater temperature in Model 1.

2.1.7. Simulation results

Results from model 2 (Figure 18) show a good match of fluctuation of the temperature observed in the observation wells (Viz-2 and Pincome-8) near River Sava (Figure 13 and Figure 14). While measured (Figure 15) and simulated values show a time shift in the temperature for the observation well Pincome-9 (Figure 16). In observation wells Pincome-8 and Pincome-9 we also observed a dimmed temperature fluctuation with depth while the model does not mimic that effect, which we presume is the result of steady state hydraulic model. Results from model 1 (Figure 17) show steady groundwater temperature which is influenced also by groundwater flow.

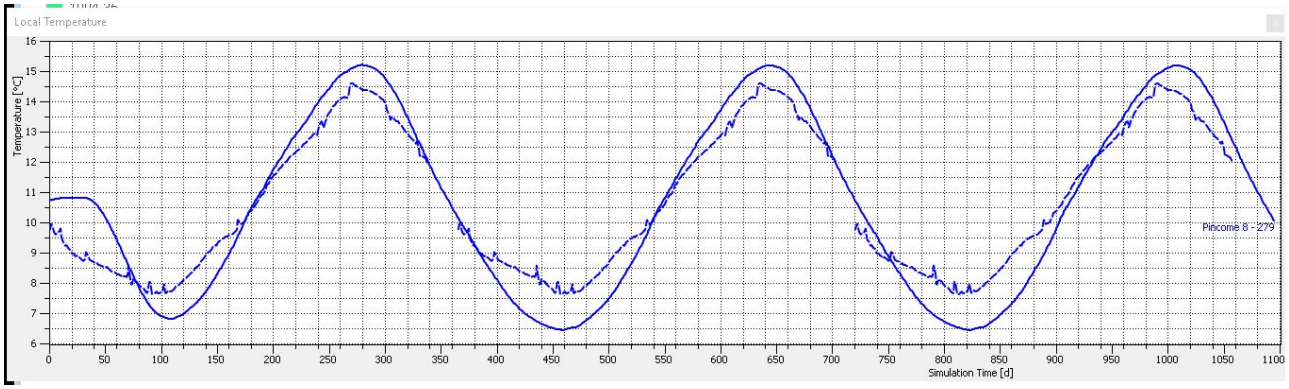

Figure 13. Modelled (solid line) and observed (dashed line) for observation well Pincome-8.

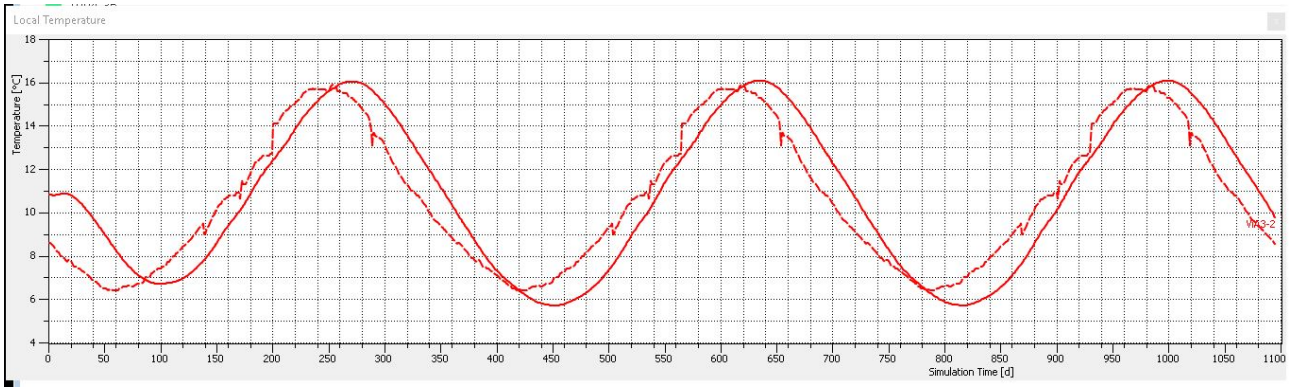

Figure 14. Modelled (solid line) and observed (dashed line) for observation well Viz-2.

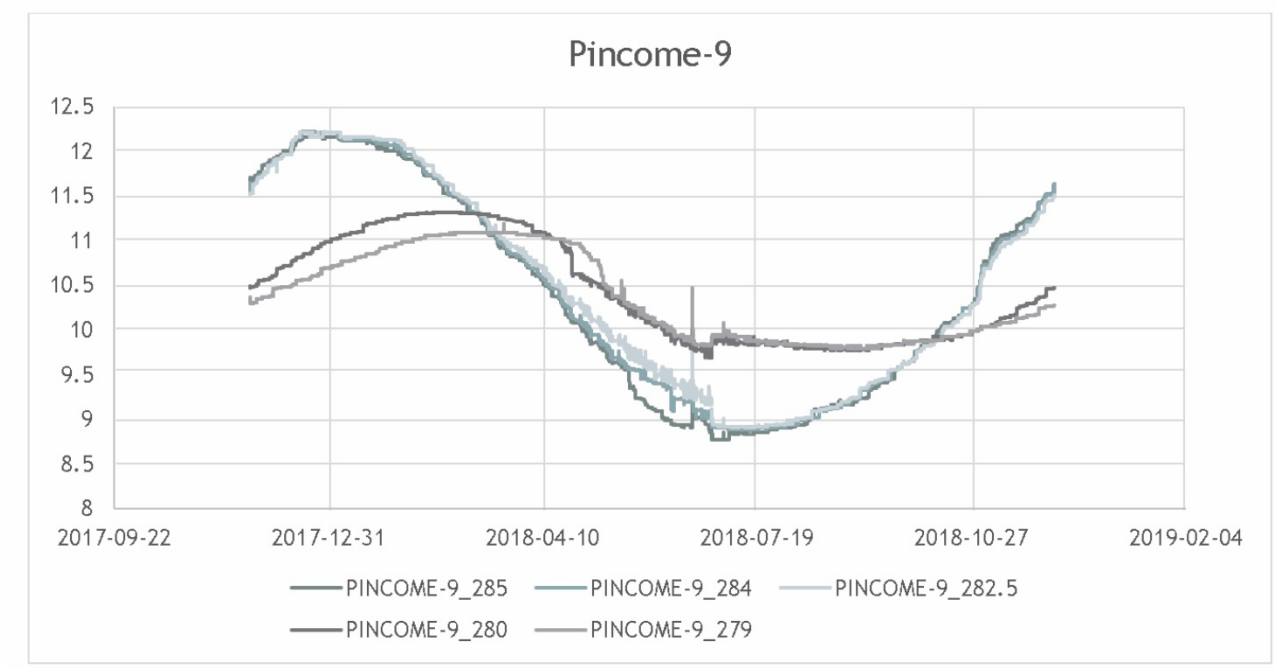

Figure 15. Observed values for observation well Pincome-9 with depth (m a.s. l.) .

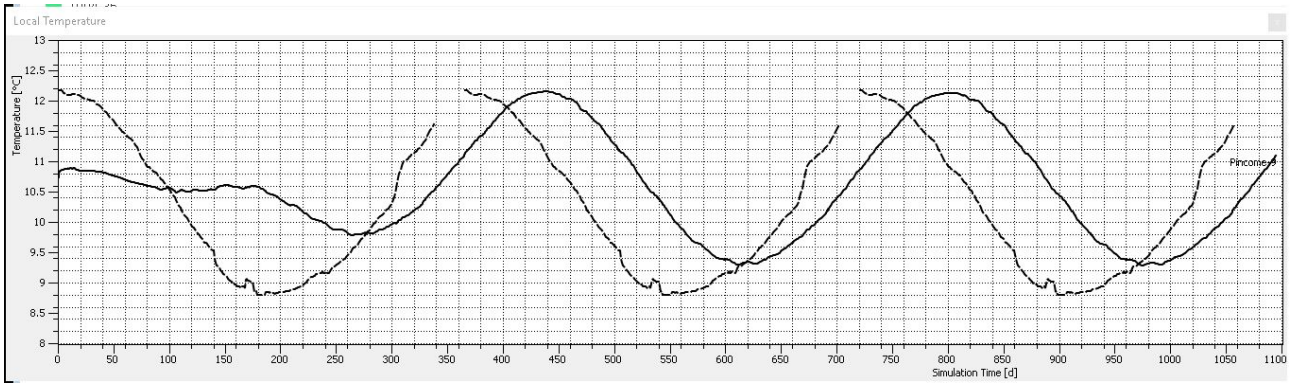

Figure 16. Modelled (solid line) and observed (dashed line) for observation well Pincome-9.

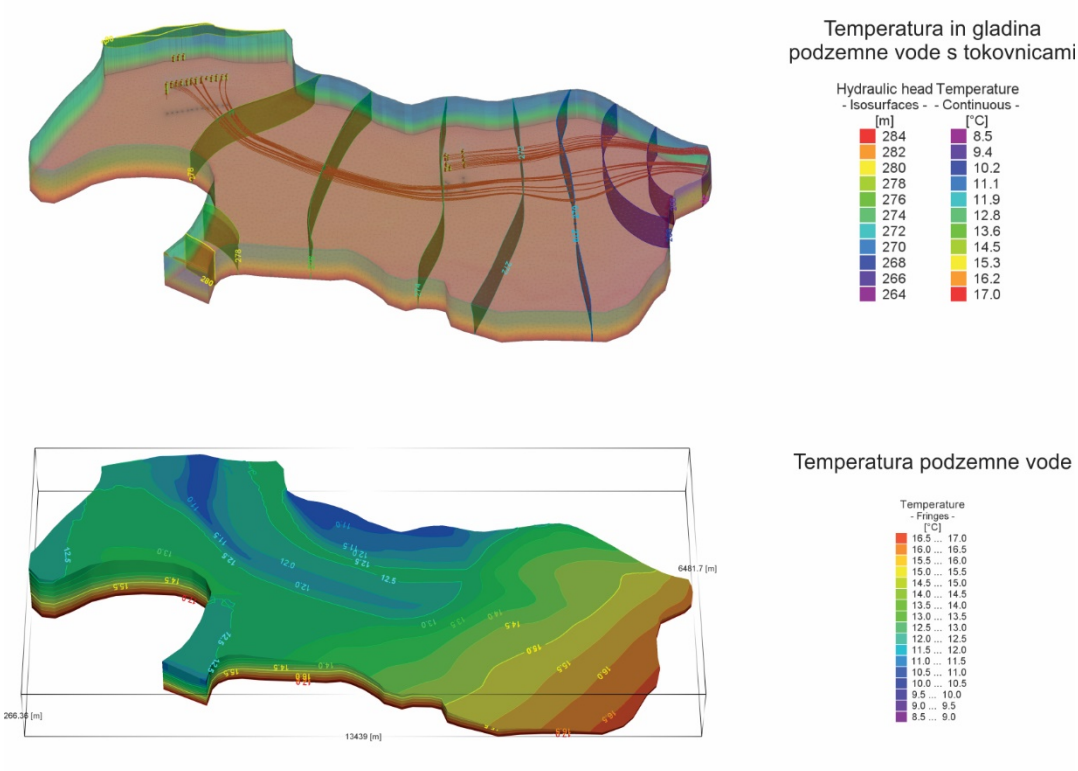

Figure 17. Hydrological and temperature results for Ljubljansko polje aquifer (model 1).

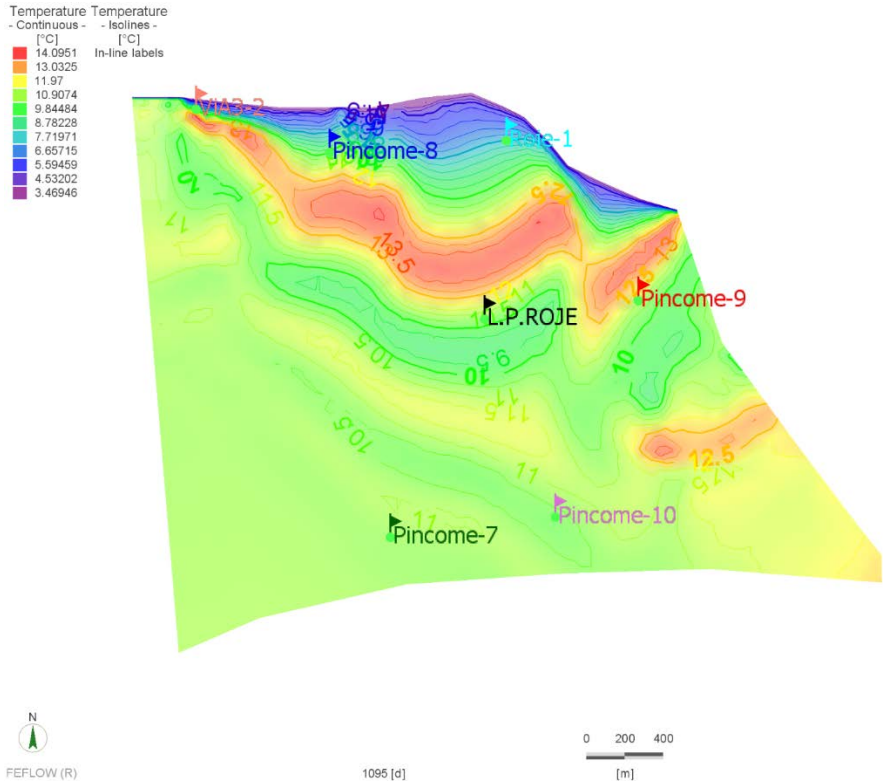

Figure 18. Modelled temperature from Northern part of Ljubljansko polje (Model 2).

A 3D hydraulic and heat transport model for quaternary alluvial aquifer of Ljubljansko polje was created and calibrated to observed groundwater level, temperature and thermal conductivity of sediments, using a FEFLOW software.

With numerical modelling we demonstrated the typical groundwater temperature profile in observation wells close to river Sava and constant temperature in the central part of the aquifer.

Considering the maximum temperature shift of 5 K and temperature limits of max change of temperature between 5 and 18 °C, whole area of Ljubljansko polje aquifer is suitable for cooling and heating. Due to strong groundwater flow, the thermal plume effect disperses fast after reinjection and has low impact to potential neighbouring installations, which has favourable effect on heating and cooling potential for shallow geothermal installations.

Observed temperature values shows vertical temperature shift close to the river Sava, which still cannot be modelled with the presented numerical models. Probably the main reason is static hydraulic model, which can significantly change the groundwater level (up to few meters) on the relevant observation wells.

2.2. Pilot area Vienna

2.2.1. Introduction

One aim of numerical modelling activities in the pilot area Vienna was to create a map of the mean groundwater level. It serves as input parameter for the potential calculations for open loop systems. Furthermore, we tested the predictability of large-scale numerical models regarding the thermal behaviour of a shallow aquifer in an urban environment. We simulated the natural seasonal behaviour of groundwater temperatures. Temperatures of a shallow aquifer mainly depend on the seasonal variations of the air temperature. In the city of Vienna, anthropogenic heat sources in the underground also influence the groundwater temperatures more and more. In order to be able to analyse and quantify the changes of the groundwater temperature over time due to this urban-heat-island-effect (UHI), we compared natural temperatures from the numerical model with groundwater temperature maps derived from field measurements. Observation wells consulted for this comparison are located partly in areas with known anthropogenic heat impacts.

Knowledge about the groundwater temperatures and its seasonal variations is important to be able to assess the potential of the groundwater body Marchfeld in Vienna for applications of open loop systems. Therefore, our results of the numerical model can be useful inputs for strategies in the city of Vienna about a sustainable use of groundwater for heating and cooling. The numerical model can further become a basis for detailed planning of new shallow geothermal energy applications and it can serve as initial model to include existing shallow geothermal applications to get an overview of the energy content of the aquifer, which has already been consummated.

We used the software FEFLOW 7.1 to prepare the numerical model and the plug in FePest for calibration. After calibrating the hydraulic model in 2D, we expanded the modelling domain into 3D for modelling the thermal behaviour of the aquifer. This approach allows considering heat storage effects in surrounding underground.

2.2.2. Input data

Table 3. Input data for numerical model of PA Vienna

No.	Dataset	Description	Implementation in FEFLOW	Source
1	Digital elevation model	Raster map of digital elevation model of Austria	Elevation of slice 1	Geological Survey of Austria
2	Top of aquifer	Raster map of the top of the "Danube gravel" in the PA Vienna	Elevation of slice 3	Vienna Water management
3	Bottom of aquifer	Raster map of the bottom of the "Danbue gravel" in the PA Vienna	Elevation of slice 10	Vienna water management
4	Bottom of surface water bodies	Compilation of the bottom of 9 surface water bodies in the PA Vienna	Elevation of slice 6	MA45 – Water management, compiled by GBA
5	Groundwater contour map	Groundwater isolines for mean groundwater level in the Marchfeld groundwater body in Vienna at representative day of 14.04.2005	Input to determine the Hydraulic head boundary conditions	MA45 - Water management
6	Groundwater level measurements at 14.04.2005	Groundwater level measurements in the Marchfeld groundwater body in Vienna of representative day 14.04.2005	Calibration data for the hydraulic head	MA45 – Water management
7	Hydraulic conductivity database	Database containing hydraulic conductivity values from pumping tests, sieving grain analysis for wells / samples in the PA Vienna	Input for initial hydraulic conductivity of the aquifer prior to calibration	Compiled by GBA
8	Groundwater abstraction wells	List of location and pumping rate of wells included in the groundwater contour map (5)	Input for multilayer well BC	Gruppe Wasser, 2014: Ausarbeitung von zwei Grundwasserschichtenplänen für das linksufrige Stadtgebiet unter Verwendung eines Grundwassermodells delivered by MA45 – Water management
9	Groundwater temperatures at wells	Database of groundwater temperature measurements from different organizations (GBA, MA45, Wienna Water	Calibration data for groundwater temperatures and	Compiled by GBA

		management, Marchfeldkanalgesellschaft)	interpretation of results	
10	Groundwater temperature maps	Two groundwater temperature maps for warm and cold conditions respectively prepared via interpolation with data (9) for PA Vienna	Interpretation of results	Compiled by GBA
11	Land surface temperature map	Land surface temperatures for Europe from 2014 (EuroLST) derived from MODIS data	Input for temperature BC on slice 1	http://www.geodati.fmach.it/eurolst.html
12	Air temperatures in Vienna	Trend of annual mean air temperatures for the city of Vienna from 1961 to 2017	Input for temperature BC on slice 1	ZAMG, 2018: Klimastatusbericht 2017, CCCA
13	Soil temperatures for Vienna	Time series of soil temperatures in 10 cm depth for soil measurement station Gross Enzersdorf	Input for temperature BC on slice 1	ZAMG
14	Groundwater level measurements time series	Groundwater level measurements at observation wells 21-75, 22-202, 22-52 and 331736 until 2015	Information for hydraulic model	https://ehyd.gv.at

2.2.3. Conceptual model

2.2.3.1. Modelling domain

The modelling domain comprises the western part of the groundwater body Marchfeld, which covers districts 21 and 22 of Vienna and extends further North East towards Lower Austria, see Figure 19. The mostly stagnant surface water body New Danube and the river Danube border the model domain to the Southwest. Alongside the New Danube there are two sheet piles, which are included in the model. The hill Bisamberg represents the northern boundary of the aquifer and the western boundary of the model domain follows a groundwater isoline from a mean groundwater contour map of the groundwater body Marchfeld in Vienna (representative day 14.04.2005). Aside from the River Danube and the New Danube, eight small lakes and the Old Danube are implemented in the model. The model furthermore includes 27 groundwater abstraction wells, which are used for drinking water and to lower the groundwater table.

A 2D model can already describe the hydraulic conditions of the Marchfeld groundwater body well. Therefore, the first numerical model domain consisted of aquifer top and bottom. For the thermal conditions, this 2D model domain was expanded into 3D. In vertical direction, the 3D model extends from 75 m a.s.l. to the ground surface and consists of three hydrogeological units (see Figure 20):

- Top layer: Unsaturated zone, comprises parts of the aquifer and overlying anthropogenic and natural sediments e.g. sand and clay.
- Aquifer: Saturated zone of the Marchfeld groundwater body. Holocene sand and gravel deposits of the rivers Danube and March, “Danube gravel”.

- Bottom Layer: Impermeable layer of Pliocene or Miocene silt and clay.

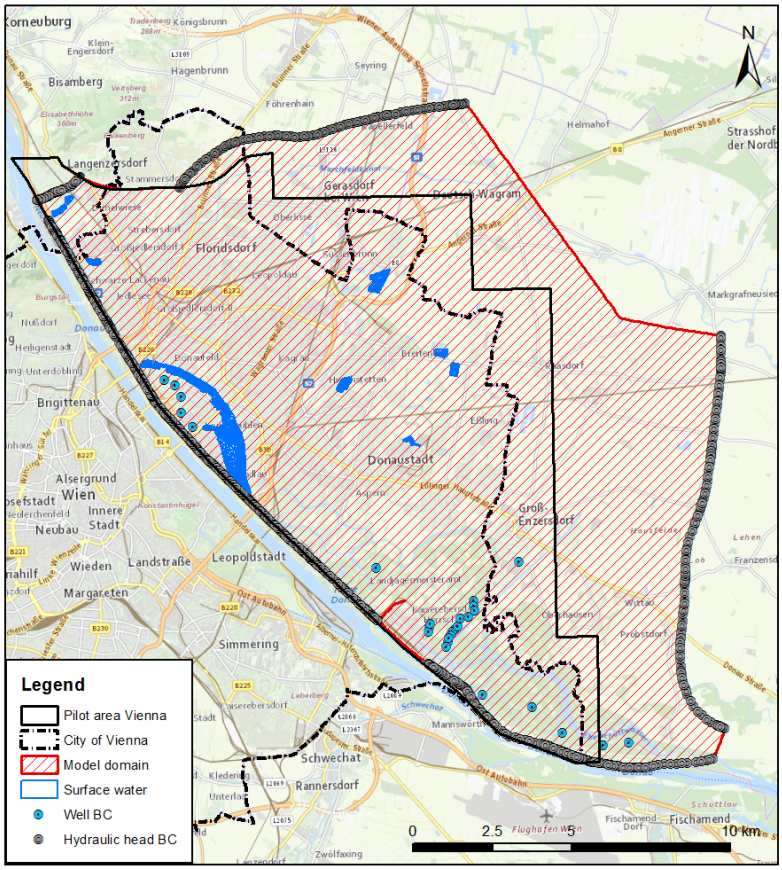

Figure 19. Model domain of the numerical model for the pilot area Vienna and hydraulic boundary conditions (BC). Sheet piles along the New Danube at the southwestern border and the border on the northeastern border are represented as no-flow boundary conditions (missing hydraulic head BC).

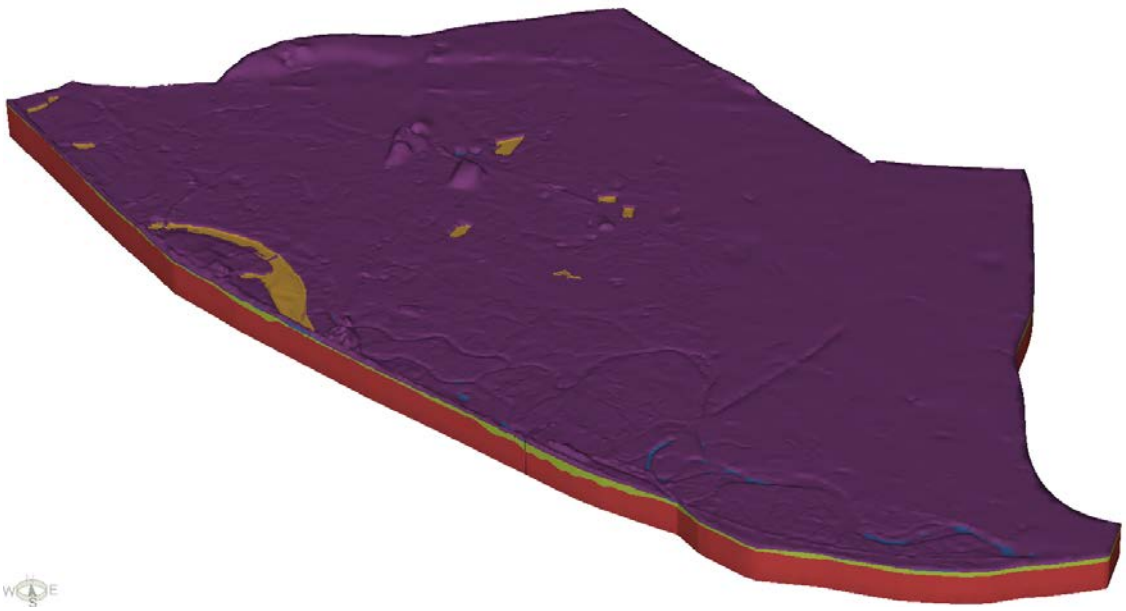

Figure 20. 3D model with surface water bodies (yellow), top layer (violet), aquifer (green), bottom layer (red). Vertical dimension is scaled by a factor of 5.

2.2.3.2. Modelling objectives

Objective of the hydraulic part of the model was to simulate the mean groundwater level of the aquifer. We chose the same representative day (14.04.2005) for the mean groundwater level as described in the report of input data No. 8. Authors of this report chose this date based on timelines for selected observation wells along the river Danube and in the hinterland as well as on the number of measurements available. The resulting groundwater isohypse map for a mean groundwater level is an input parameter to calculate the potential for open loop systems performed in D.T3.4.2. – Thematic maps showing potentials and conflicts at the pilot areas.

Major aim of the heat transport part of the model was to simulate the natural seasonal behaviour of the groundwater temperature. Main outputs of the model are temperature maps for warm and cold states of the aquifer. Two representative days (19.04.2016 - cold and 27.10.2016 - warm) were chosen based on the dates of minimum and maximum measured groundwater temperatures in the pilot area in 2016. To test the applicability of numerical modelling for this purpose in a large area and to identify anthropogenic heat impact on the aquifer, the simulated temperature maps on 19.04.2016 and 27.10.2016 were compared with the temperature maps based on measured data for the same dates.

Thermal modelling starts with steady state conditions for 1961 and continue with transient simulations from 1961 to 2017. The transient model includes a linear surface temperature increase from 1961 to 2007, according to the climate status report 2017 for Austria (Figure 21). The seasonal and spatial variation of the surface temperature from 2007 to 2017 is based on the land surface temperature map of 2014 (input No. 11) and a time series of the soil temperatures at the measurement station Gross Enzersdorf (input No. 13). The time series for the surface temperatures in the model is provided in Figure 22. This input data contains therefore the UHI of the surface. This effect however also applies to the subsurface. Increasing subsurface temperatures are also known in the pilot area Vienna due to different anthropogenic heat sources, such as sewage systems, district heating pipes, underground structures and shallow geothermal energy systems, especially thermal uses of the groundwater. Neither of those effects is included in the numerical model developed for GeoPLASMA-CE. It is planned to further implement these anthropogenic heat sources into the model in follow-up activities.

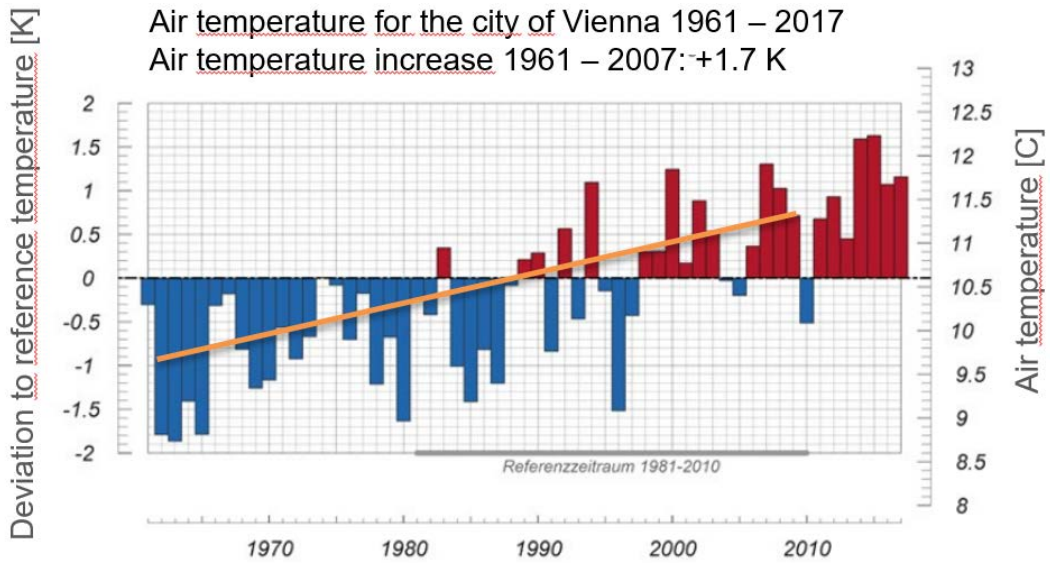

Figure 21. Time series of air temperature in the city of Vienna from 1961 to 2017. (source: Klimastatusbericht 2017, ZAMG)

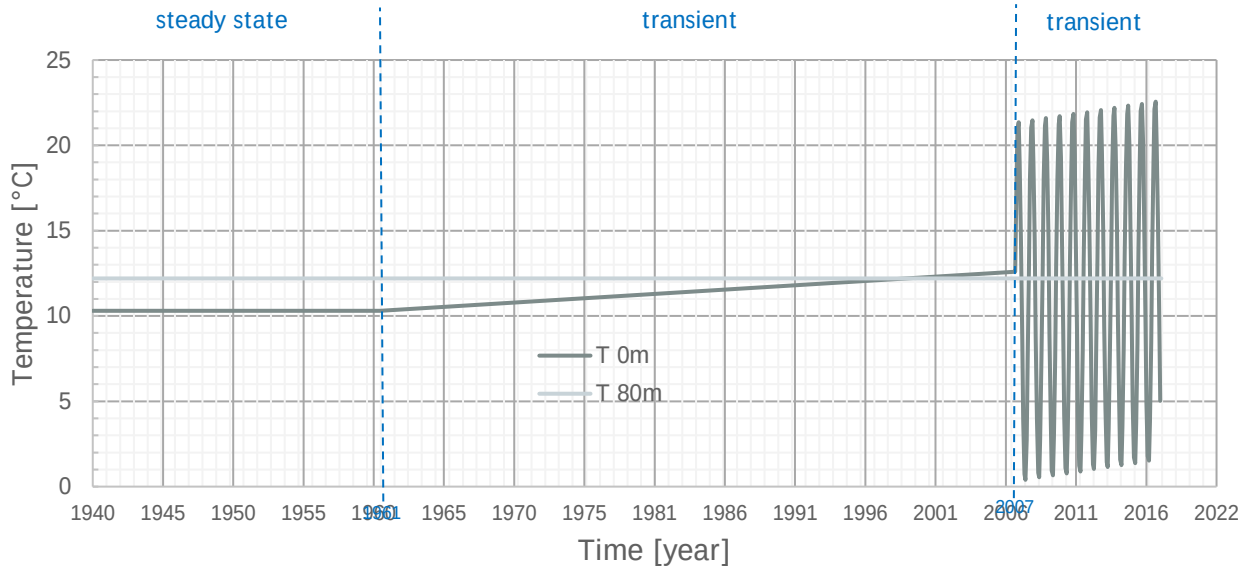

Figure 22. Time series of the temperature boundary conditions on the surface (T 0 m) and bottom of the model (T 80 m). From 1961 to 2007 the mean annual surface temperature increases from 10.3 °C to 12 °C. From 2007 to 2017 it includes monthly temperatures to simulate seasonal variations with a linear temperature increase of 0.12 K/year.

2.2.4. Numerical model

2.2.4.1. Model setup

The Marchfeld groundwater body is an unconfined (phreatic) groundwater system. The mean monthly groundwater level variation in the aquifer between 2007 and 2015 is low, around 1 m, according to data from four selected observation wells of input No. 14. Hence, we simulated the fluid flow for steady state conditions.

For heat transport, we chose a combination of steady state and transient conditions to be able to include the impact of climate change induced increase of surface temperatures on the temperature regime of the aquifer. The initial conditions for the transient simulations were simulated with steady state conditions for 1961. All simulations from 1961 on are transient. They contain transient temperature boundary conditions for the surface, the inflowing groundwater from the Northern boundary and two surface water bodies New Danube and Danube.

The numerical calculation uses an automatic time-step control to define the time step size. The time step size is limited to 1095 days for the simulation from 1961 to 2007. The time series of the boundary conditions in the simulation from 2007 to 2018 automatically limit the time step size to 30 days. The growth factor between subsequent time steps is unrestricted, 0.001 is the error tolerance for Euclidian L2 integral norm and the maximum number of iterations per time step is 40 for both transient simulations.

2.2.4.2. 3D configuration

Main input for the 3D configuration of the model are the maps listed in Table 2. The elevation of the bottom slice of the model, slice 14, is at a constant height of 75 m a.s.l..

Table 4. Main units of the 3D layer configuration. No. of input data according to Table 1. Slices in-between depend on the main input maps.

Input map	No. of input data	Slice No.
Digital elevation model	1	1
Top of aquifer	2	3
Bottom of surface water bodies	4	6
Bottom of aquifer	3	10

The raster maps are imported into FEFLOW as point data. Top and bottom of the aquifer are only available for the pilot area Vienna and to cover the entire modelling domain kriging was used to interpolate within FEFLOW. This has to be kept in mind for the interpretation of the results, which are therefore only reliable inside the pilot area.

We divided these overall model units into additional layers to ensure a stabile numerical solution for heat transport. A short distance between layers with changing material properties facilitates a stabile numerical calculation. Therefore, we inserted one layer of 0.2 m thickness respectively, below aquifer top and aquifer bottom slices. Aside from those two layers, the model units were split evenly. The aquifer contains most layers, since it is the target area of the model. The model unit top layer consists of 2 layers, the aquifer of 7 layers and the bottom layer contains 4 layers. In total the 3D model has 13 layers and 1 440 740 nodes.

2.2.4.3. Meshing

The outlines of the surface water bodies in the pilot area Vienna were included in the mesh as polygons. The preparation of this data was performed in ArcGIS. Point data included in the mesh are observation wells with available temperature und water level data, abstraction wells and locations of existing open loop systems. Material properties change at the boundaries of the polygons and the points are prepared for boundary conditions, therefore we refined the mesh around those polygones and points, to facilitate stabile numerical calculations.

The mesh was smoothed several times to reduce the elements violating the Delaunay criterion and to optimize the maximum interior angle of triangles. After smoothing, only a few elements (1321 of 204725 for each slice) still violate the Delaunay criterion and most triangles have a maximum interior angle of 60 to 70 (ideal interior angle is 60). Figure 23 shows the final mesh with its densely meshed areas.

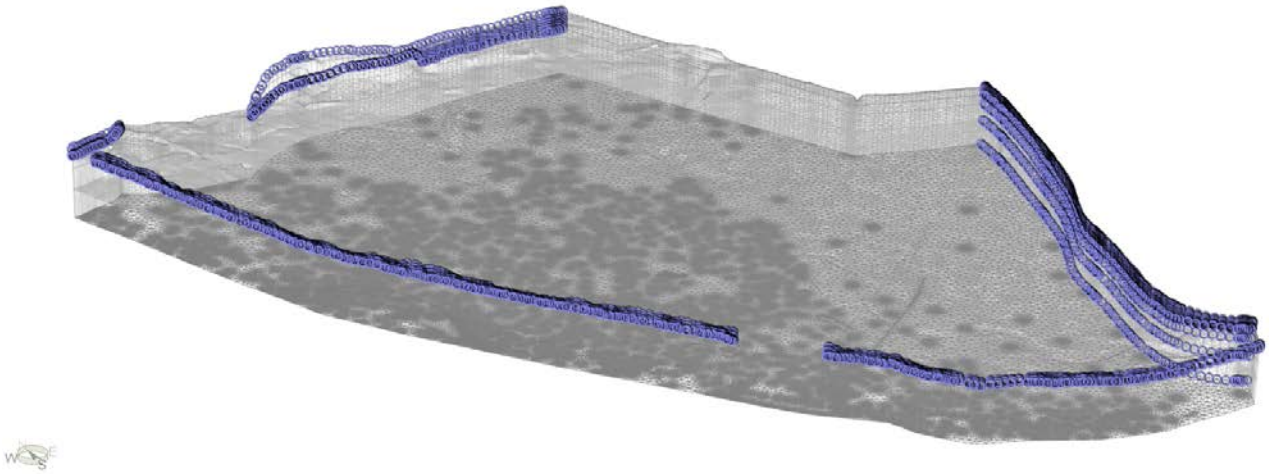

Figure 23. Mesh of numerical 3D model for PA Vienna. It consists of 13 layers and 1 440 740 nodes. Purple dots mark hydraulic head boundary condition.

2.2.4.4. Boundary conditions

The following two subchapters describe the boundary conditions for fluid flow and heat transport separately.

2.2.4.4.1. Boundary conditions – fluid flow

The numerical model solves the fluid flow for steady state conditions and hence all boundary conditions are constant over time. Main input for the boundary conditions for fluid flow was the report of Gruppe Wasser for a project, which elaborated a mean groundwater table for the Marchfeldgroundwater body in the city of Vienna (input No. 5). Large existing groundwater extraction wells are included in the report and are implemented into the 3D model as multilayer wells (Input No. 8). Table 3 shows the abstraction rates of the wells. They are multilayer wells in the numerical model and cover the entire aquifer (slice 3 to slice 10) with a uniform radius of 0.25 m.

All other boundary conditions in the numerical 3D model are no-flow and hydraulic head boundary conditions set at the model boundaries. The boundary conditions along the western and the southeastern model borders correspond to the groundwater contour map of input No. 5. At the western border, the hydraulic head boundary condition comprises slices 1 – 5, which are within the New Danube and the Danube. The hydraulic head boundary conditions along the southeastern model border extend from slice 1 to slice 14. The two gaps along the western border are no-flow conditions, due to sheet piles in this area along the New Danube. The northeastern border and a small part of the northern border are no-flow boundary conditions as well, since the groundwater contour lines run perpendicular to these model boundaries. The remaining border in the North is also a hydraulic head boundary condition. However, there are no continuous groundwater contour lines available for this border from Input No. 5. Prior to the calibration process, it was implemented as fluid flux boundary condition and calibrated with in- and out-transfer rate along the border. The hydraulic heads along the border simulated with the calibrated model complete the boundary conditions for the 3D model. These hydraulic head conditions are set on slice 1 and slices 6 – 14. The slices were selected, because there are temperatures available for boundary conditions of the heat flow. Heat transport boundary conditions have to be set on all nodes with hydraulic head boundary conditions located upstream of the model.

Table 5. Abstraction wells included as multilayer wells in the for steady state conditions in the numerical model for PA Vienna. Well radius is 0.25 m for all wells.

Well	UTM_easting	UTM_Northing	Usage of well	Pumping rate [l/s]

Br.01	13457.88	337213.7	Lowering groundwater table	15
Br.02	13479.31	337358.86	Lowering groundwater table	15
Br.03	13495.48	337477.77	Lowering groundwater table	14
HFB-NW6	16327.50	339393.00	Industrial use	150
LB1	14883.37	338174.75	Lowering groundwater table	9
LB12	14142.77	337105.57	Lowering groundwater table	8
LB13	14096.28	337010.91	Lowering groundwater table	6
LB15	14050.14	336870.64	Lowering groundwater table	20
LB16	13994.52	336739.91	Lowering groundwater table	16
LB2	14882.77	338000.4	Lowering groundwater table	6
LB3	14906.47	337853.94	Lowering groundwater table	10
LB4	14704.27	337672.5	Lowering groundwater table	15
LB5	14447.43	337608.78	Lowering groundwater table	14
LB6/7	14370.13	337367.38	Lowering groundwater table	7
LB8	14298.21	337284.21	Lowering groundwater table	6
LB9	14209.59	337202.17	Lowering groundwater table	6
LBHFB_GANS	17605.30	333946.30	Drinking water well	167
LBHFB_MARK	11837.70	339269.50	Drinking water well	47
LBHFB_ROHR	16671.40	334791.00	Drinking water well	61
LBHFBKREU	15123.70	335197.50	Drinking water well	62
LBHFBSCH1	18893.00	333530.00	Drinking water well	61
LBHFBSCH2	19708.00	333600.00	Drinking water well	61
SB01	5257.03	345318.26	Lowering groundwater table	23
SB02	5574.27	345133.09	Lowering groundwater table	19
SB03	5774.12	344777.79	Lowering groundwater table	8
SB04	5762.53	344255.44	Lowering groundwater table	17
SB05	6127.10	343819.80	Lowering groundwater table	4

2.2.4.4.2. Boundary conditions – heat transport

Boundary conditions for heat transport vary for steady and transient simulations. One steady state simulation serves to determine the initial temperature distribution for the transient simulations. It represents the temperature regime in 1961 assuming a constant surface temperature of 10.3 °C and a temperature of 12.2 °C at the bottom of the model in the entire modelling domain. The surface temperature is set as temperature boundary condition on all nodes of slice 1 and all nodes with a hydraulic head boundary condition at the inflow of the model (at the northern border and at the New Danube and Danube). The temperature at the bottom of the model (slice 14) is determined by a heat transfer boundary condition. A combination of this heat transfer boundary condition and the in- and out-transfer rate together with an assumed thermal gradient of 0.023 K/m lead to a virtual extension of the model of 100 m below the bottom of the model. This additional extension enables a heat transport outwards and inwards of the model instead of fixing the temperature at the bottom of the model. The heat transfer boundary condition on the bottom of the model remains the same for all thermal simulations, whereas the temperature boundary conditions vary for the transient simulations.

For the simulation time from 1961 to 2007 a linear increase of the air temperature from 10.3 to 12 °C according to the climate state report of Input No. 12 and Figure 21 is included as a time series for all nodes on slice 1 and for the New Danube and the Old Danube. For the northern boundary, the inflowing groundwater was also assumed to show increasing temperatures. Therefore, the temperature boundary conditions here are set on slices 6 – 10 and increase from 10.8 to 11.3 °C.

Temperature boundary conditions for the simulation time from 2007 to 2018 are more precise, they include seasonal and spatial variation of the surface temperatures. Basis for the spatial distribution is the land surface temperature for 2014 (Input No. 11) and the time series from 2007 to 2018 for the soil temperature measurement station Gross Enzersdorf (Input No. 13). A first step to prepare the boundary conditions for this time span was to fit a sine wave including a linear trend to the time series of the soil temperature. The following equation describes the soil temperatures with a determination coefficient of (R^2) 0.91 and a linear temperature increase of 0.12 K/year:

*Temp_soil = Intcp - 3.41206 * sin(2 * π * time / 365.25) - 10.15457 * cos(2 * π * time / 365.25) + 0.0003325 * time*

Time is the day starting from 01.01.2007, for which the temperature is to be calculated. *Intcp* is the mean temperature of 2007. A variation of *Intcp* is used to derive spatially different time series for the surface temperature. Therefore, the land surface temperature map was classified into 4 categories and the temperature map was recalculated for 2007 in ArcGIS, considering this linear temperature change with the following equation:

*Land surface temperature (2007) = -0.12 * (2014 – 2007) + Land surface temperature (2014)*

This land surface temperature map for 2007 now represents the mean values for the sine wave function to calculate time series including a linear trend for each land surface temperature category. These 4 time series are applied on the respective nodes on slice 1 and on the nodes of the New Danube and the Danube. Figure 24 shows the mean land surface temperatures for 2007, which are included in the time series.

Time series for temperature of inflowing groundwater at the northern boundary was derived from the observation well with the most data available in the northern part of the modelling domain: GT331777. It is set on slices 6 – 10. Temperature measurements of one measurement location in the New Danbue (Donaustadtbrücke at weir 1) were analysed and converted into a time series for slices 2 – 5 at the Western boundary of the model. Data of the New Danube do not show increasing groundwater temperatures for the 2012 – 2018 and therefore no positive trend was included in the time series. Figure 22 shows a rough overview of heat transport boundary conditions implemented in the model. Figure 25 shows the temperature boundary conditions of 2007 – 2008, as an example for the simulations from 2007 – 2018. Time series for the New Danube / Danube and the Northern inflow are cyclic (no trend) and the surface temperatures increase 0.12 K /year.

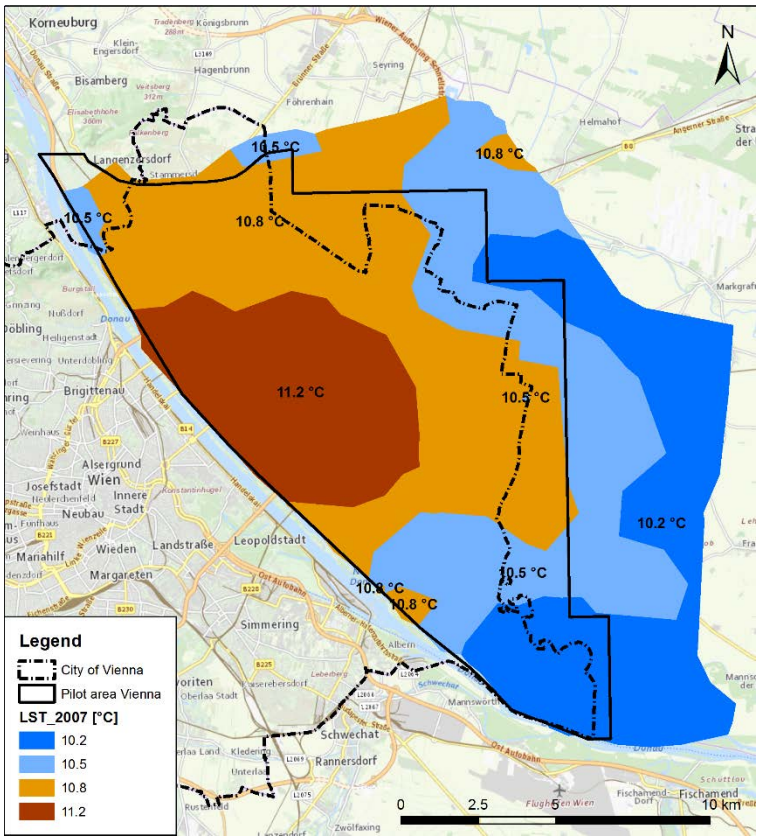

Figure 24. Mean land surface temperature for 2007 implemented in time series for temperature boundary condition on the surface of the model

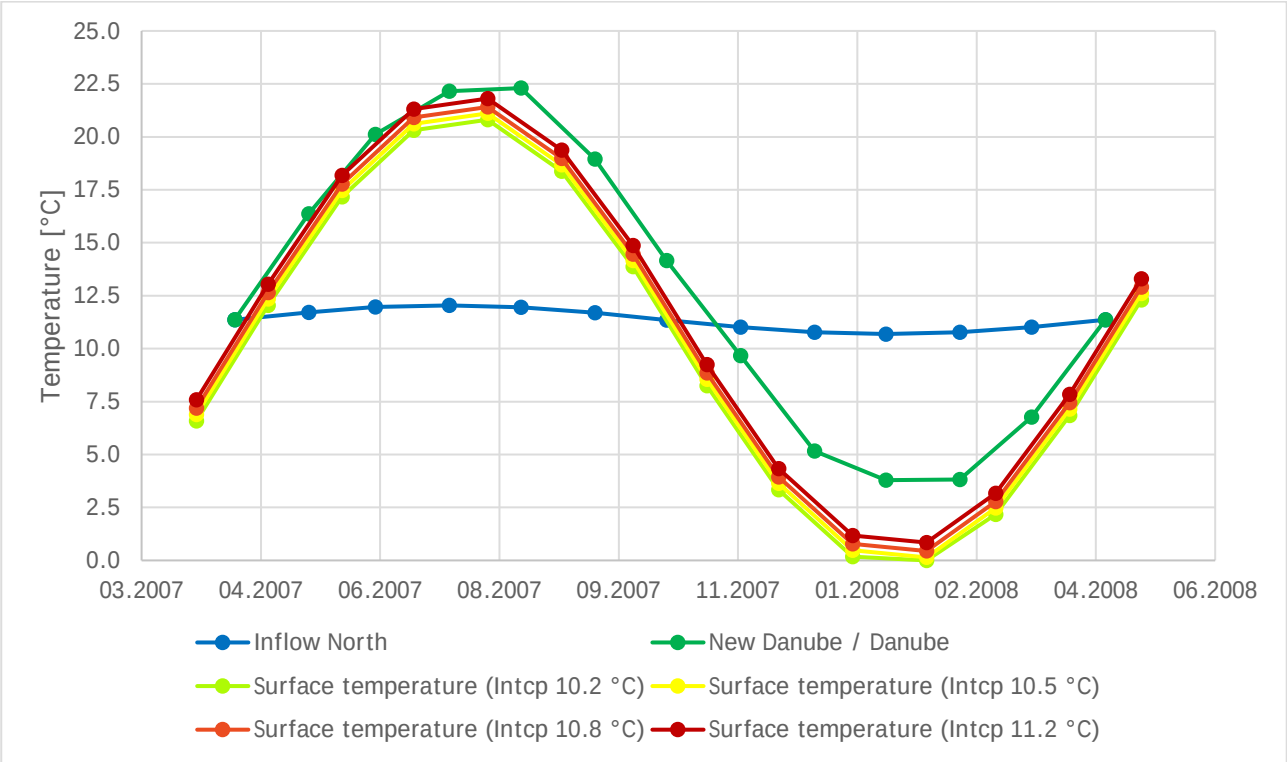

Figure 25 Temperature boundary conditions as examples for 2007 - 2018. Surface temperatures increase 0.12 °K, others are cyclic.

2.2.4.5. Material properties

The following two subchapters describe the material properties for fluid flow and heat transport separately.

2.2.4.5.1. Material properties – fluid flow

The hydraulic conductivity of the aquifer in the 3D moel is based on the calibration performed for the 2D model. The lower and upper boundary of values for the calibration were fixed to 2.3 * 10^{-3} m/s and 1.7 *10^{-2} m/s respectively. Hoelting, 2013 and the German guideline VDI 4640 part 1 (Verein Deutscher Ingenieure, 2010) contain tables of hydraulic conductivities for unconsolidated sediments, which provided input values for the top layer and bottom layer.

The surface water bodies are implemented into the model as areas with a very high hydraulic conductivity. The hydraulic conductivity was set to factor 100 higher than the initial value of the aquifer prior to the calibration. One exception is the Old Danube, it is heavily sealed on the South Eastern shore, as the first runs of the numerical model show. This area of low hydraulic conductivity was determined in the calibration separately, the lower and upper boundary were fixed to 1.0 * 10^{-9} m/s and 7.0 * 10^{-1} m/s. The hydraulic conductivities are the same for all directions (x, y and z-direction). Table 3 summarizes all material parameters for fluid flow.

Table 6. Material parameters for fluid flow of the numerical model pilot area Vienna. Hcond = Hydraulic conductivity in x, y and z-direction.

Layer	Hcond [m/s]
Top layer	1 * 10^{-5}

Aquifer	$2 * 10^{-2} - 2 * 10^{-3}$
Bottom layer	$1 * 10^{-7}$
Surface water bodies (except Eastern shore of Old Danube)	$7 * 10^{-1}$
Eastern shore of Old Danube	$5 * 10^{-3} - 2 * 10^{-9}$
Constant values	
Porosity	0.2

2.2.4.5.2. Material properties – heat transport

Input for the material properties of heat transport are thermal conductivity maps of the pilot area, elaborated in GeoPLASMA-CE, previous FEFLOW models in the area, especially from project DEGENT-NET and literature values, mainly the German guideline VDI 4640 part 1. The calibration process of the thermal model led to an update of the thermal properties in the upper part of the model. The unsaturated zone, derived from the mean groundwater level, was included as new unit for the heat transport and replaced the top layer. The calibration found a better match with the time series of observed temperatures with lower mean heat capacity and lower mean thermal conductivity for the unsaturated zone than the initial values for the top layer (mean volumetric heat capacity = 1.8 MJ/m³/K, mean thermal conductivity = 1.4 W/m/K). Thermal properties of the model differ between the hydrogeological units as stated in Table 5, but inside the unit, there is no spatial variation. This assumption is justified for the thermal conductivity as the thermal conductivity maps of the pilot area show very little variation. Thermal conductivities range between 1.6 W/m/K and 2.1 W/m/K with a mean value of 1.9 W/m/K.

In-transfer rate and out-transfer rate are set on the bottom most slice. These properties are related to the heat transfer boundary condition, which was set to 14.5 °C on slice 14. A combination of this heat transfer boundary condition and the in- and out-transfer rate together with an assumed thermal gradient of 0.023 K/m lead to a virtual extension of the model of 100 m below the bottom of the model. Table 4 summarizes all material properties for the heat transport.

Table 7. Material properties of the numerical model for heat transport: Cap = Volumetric heat capacity of fluid, solid and mean value [MJ/m³/K], Tcond = Thermal conductivity of fluid, solid and mean value [W/m/K] and transfer rate [W/m²/K].

Model unit	Cap_fluid	Cap_solid	Tcond_fluid	Tcond_solid	Cap_mean	Tcond_mean
Unsaturated zone	1.5	1.5	1.3	1.3	**1.5**	**1.3**
Aquifer	4.2	1.83	0.59	2.1	**2.3**	**1.8**
Bottom layer	4.2	2.08	0.59	2.35	**2.5**	**2**
Constant values		**Slice**				
Porosity	0.2	All slices				
In-transfer rate	0.0235	Slice 14				
Out-transfer rate	0.0235	Slice 14				

2.2.5. Simulations

2.2.5.1. Hydraulic model

The hydraulic model simulates the groundwater table at the representative day 14.04.2005, this date represents the mean groundwater level. The model assumes steady state conditions. Chapters 3.2.4.4 and 3.2.4.5 provide detailed information about the boundary conditions and material properties for fluid flow.

The calibration results of the 2D hydraulic model became the basis for the 3D model. The simulation of the fluid flow of the 3D model showed the same generally low residuals (difference between observed and simulated hydraulic heads) as the 2D model. This indicates a good quality of the hydraulic model. For more information about the calibration of the hydraulic model, see chapter 3.2.6.

Another indicator of the model quality is the balance of fluid flow into and out from the entire model domain. A balance for the entire model domain in steady-state models should show an imbalance close to 0 m^3/d, as it only includes a residual numerical error. The resulting imbalance of our hydraulic 3D model +0.73 m^3/d fits this criterion rather well, especially considering the large volume of the model. Table 6 shows all sources and sinks of the fluid flow.

Table 8. Balance of the fluid flow into and out from the 3D model. Imbalance is +0.73 m^3/d.

Boundary Condition	Outflow [m^3/d]	Inflow [m^3/d]
Hydraulic head	75 659	148 840
Wells	73 181	

2.2.5.2. Thermal model

The thermal model shows groundwater temperatures from 1961 to 2017 including a linear increase of surface temperatures. The last 10 years additionally include seasonal temperature changes on the surface. Chapter 3.2.4 describes all boundary conditions and material properties. During multiple simulation runs, the boundary conditions and material properties were updated. For the last simulation run we selected 18 observation wells to conduct a detailed analysis of the model results for 2015 - 2016. Chapter 3.2.7 discusses this analysis, a comparison of groundwater temperature maps derived for two dates – 29.04.2016 and 27.10.2016 - and a comparison of temperature measurements at the location Oase 22+ in a borehole heat exchanger of simulation data and measured data respectively.

2.2.6. Calibration

We calibrated the fluid flow of the 2D hydraulic model. Goal of the calibration was to determine hydraulic head boundary conditions at the Northern boundary and a hydraulic conductivity map of the aquifer. Therefore, representative parameter groups were set-up according to Figure 26 in the calibration process. Table 7 lists the properties of each parameter group. The calibration was conducted with the operation mode “estimation” and used the regularization method of Prior Information Tikhonov. Table 8 lists the termination criteria of the calibration. MA45 provided a total number of 794 observation points (input data set 6) with hydraulic head measurements of 14.04.2005, which we included in the calibration. 704 of the observation points are located in the pilot area Vienna. The hydraulic boundary conditions of the model

were derived from a groundwater isohypse map of the same day (input data set 5), which enables a direct comparison of the data.

The first simulation run showed a relatively high deviation of simulated and measured groundwater temperatures. Simulated temperature time series and measured time series differed in wavelength, amplitude and mean value. Therefore, we reworked the thermal properties and implemented the thermal properties for heat flow stated in Table 5. We abstained from a detailed calibration with FePEST for thermal conductivity and heat capacity, because an anthropogenic influence on the observation wells cannot be ruled out. There are already around 500 existing open loop systems in the pilot area and a large number of additional already mentioned sources of the underground UHI could influence the temperature at the observation wells.

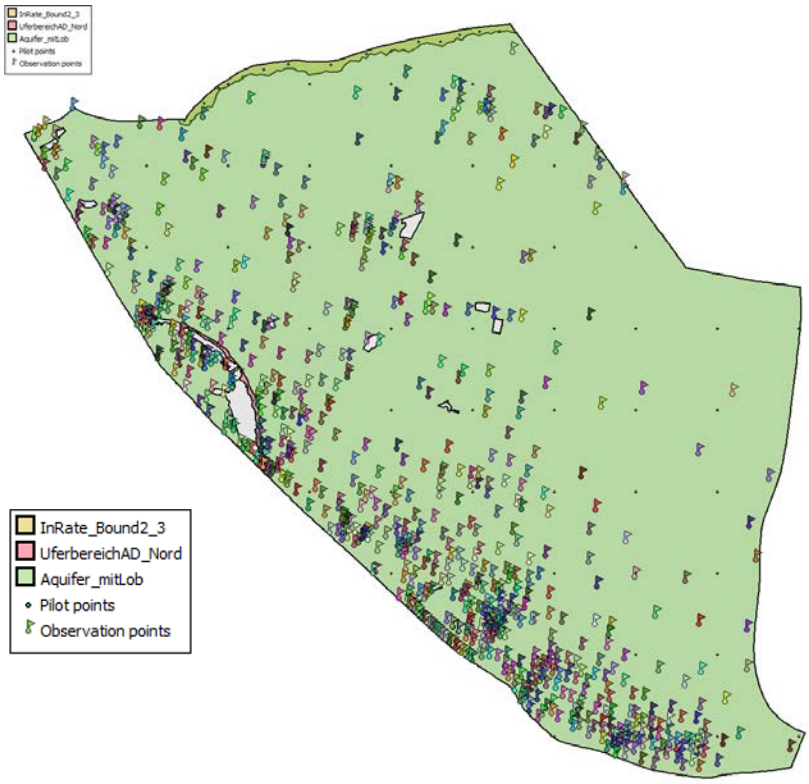

Figure 26. Parameter groups, pilot points and observation points used to calibrate the in-transfer rate at the northern model boundary and the hydraulic conductivity of the aquifer.

Table 9. Parameter groups to calibrate the hydraulic 2D model of the pilot area Vienna.

Parameter group	Parameter to be estimated	Pilot points	Lower bound	Upper bound
Northern boundary	In-Transfer rate	13	$1 * 10^{-8}$ 1/d	$1 * 10^{8}$ 1/d
Old Danube	Hydraulic conductivity	9	$9 * 10^{-5}$ m/d	60480 m/d
Aquifer	Hydraulic conductivity	53	200 m/d	1500 m/d

Table 10. Termination criteria to calibrate the hydraulic 2D model of the pilot area Vienna.

Termination Criteria	Value
Maximum number of optimization iterations	30
Relative Phi reduction indicating convergence	0.005
Number of Phi values required within this range	5
Maximum number of consecutive failures to lower Phi	5
Maximum relative parameter change indicating convergence	0.01
Number of consecutive iterations with minimal parameter change	5

The above stated calibration set-up led to a good calibration result. Half of all observation wells located in the pilot area show a deviation of < 10 cm and 75% of all wells inside the pilot area show a deviation of < 20 cm. A high determination coefficient (R^2) of 0.9948 was reached (see Figure 27). The distribution of positive and negative residuals is almost balanced. Hydraulic heads at 51 % of the observation points are lower than the measured hydraulic head. A map of the residuals in Figure 28 shows that most of the observation wells with simulated hydraulic heads outside the confidence interval of ±20 cm are located in clusters.

Following reasons explain the simulated hydraulic heads outside the confidence interval of ±20 cm:

1) Along the New Danube, there are some critical points for the groundwater flow, such as sheet piles, for example at the Northwestern corner of the numerical model and at the more Southern border. Residuals of the hydraulic head in this area are due to missing knowledge about exact location and permeability of the sheet piles.
2) In the middle of the New Danube, at the Southern end of the Old Danube, there is a weir constructed in the water body. The impact of the weir onto the groundwater body leads to residuals in the close vicinity of the construction.
3) A large area with also higher deviations in the Southeastern part of the numerical model is a result of some of the implemented extraction wells in this area and of many cutoff lakes. The communication with the groundwater and therefore the impact of these cutoff lakes on the groundwater level is not well known.
4) Residuals outside the pilot area are due to missing input data about the aquifer geometry.

At the majority of the observation wells, modelled heads underestimate the measured hydraulic head. This leads to a more conservative hydraulic model. This situation and generally low deviations of ±20 cm between simulated and measured water level and the reasonable explanations for areas with comparable higher deviations leave us satisfied with the hydraulic model. The calibration results (hydraulic conductivities for aquifer and Old Danube and hydraulic head at the Northern boundary) serve as input data for the 3D model. The residuals of the hydraulic head in the 3D model were the same as in the 2D model and therefore no further calibration of the 3D model was necessary.

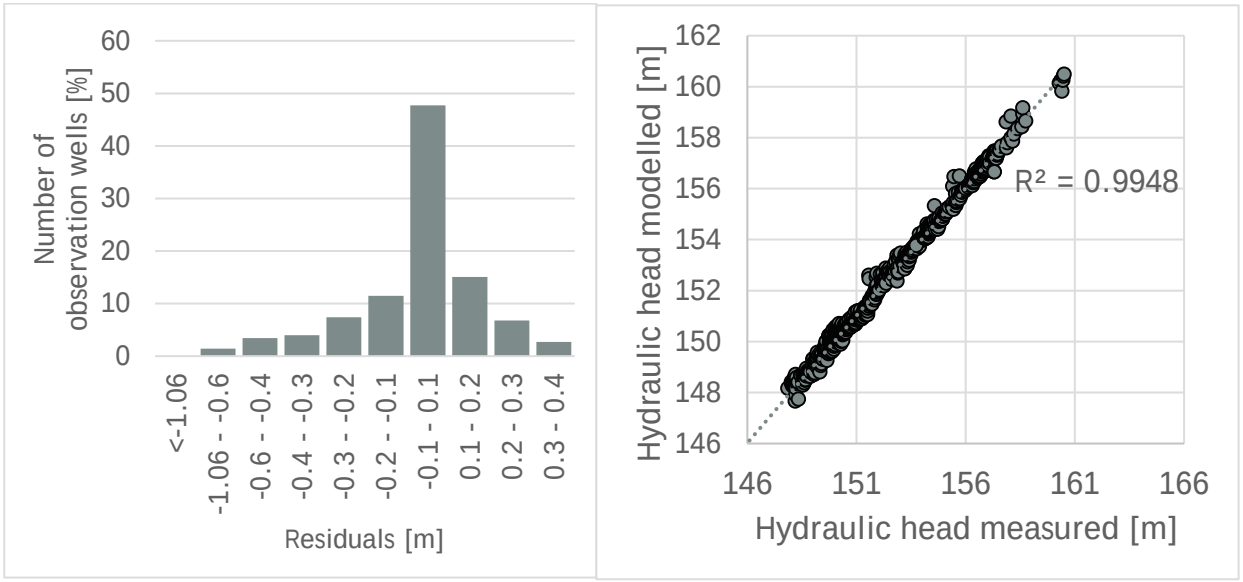

Figure 27. Calibration results for the mean groundwater level in the pilot. Left: Histogram of residuals. Right: Hydraulic head measured vs. hydraulic head modelled.

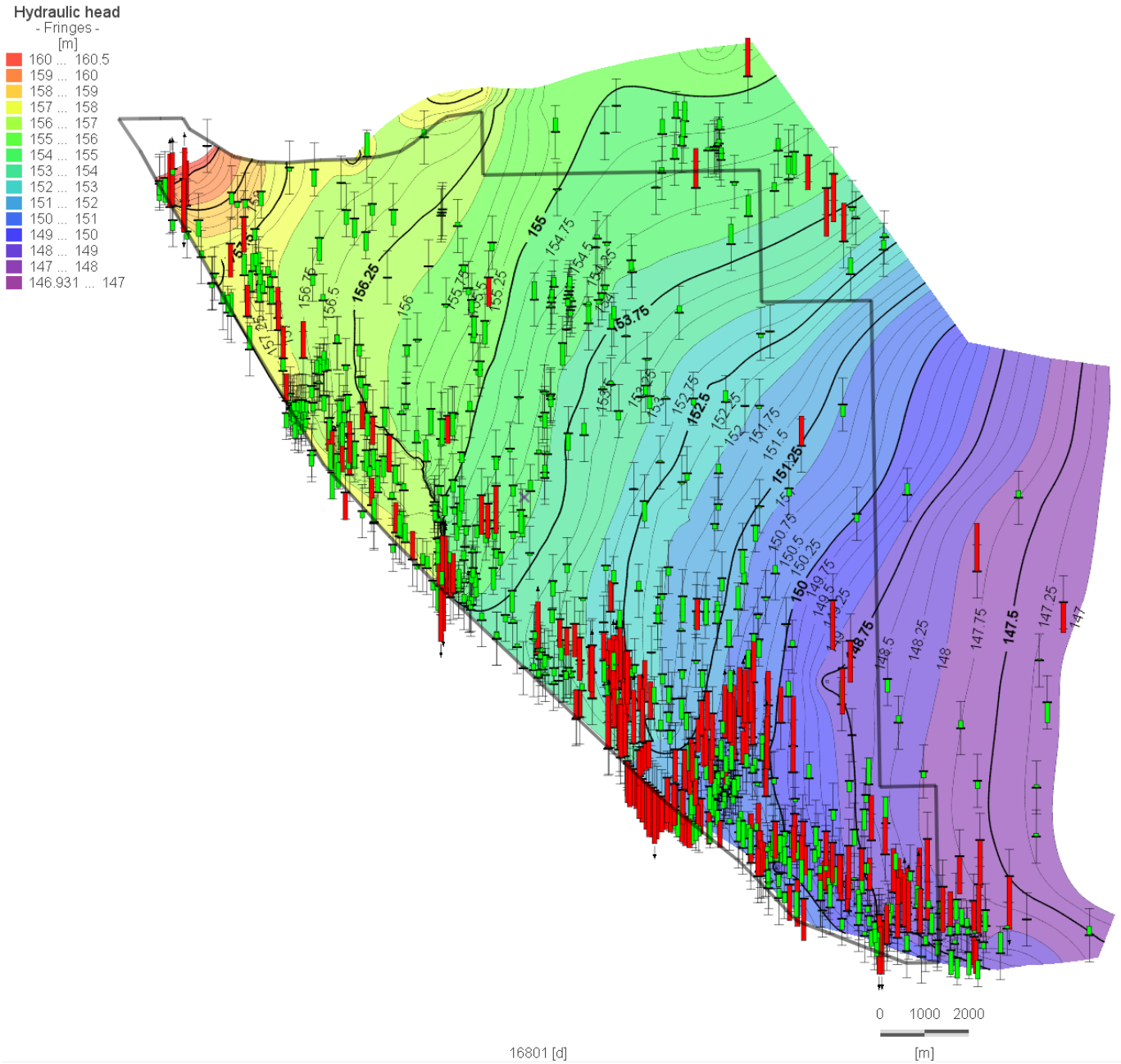

Figure 28. Bars show the calibration results for the mean groundwater level. Red bars indicate a simulated value outside a ±0.2 m confidence interval (black lines).

2.2.7. Simulation results

The simulated mean groundwater level for steady state conditions on the reference day 14.04.2005 is presented in Figure 29. Groundwater flows generally from Northwest to Southeast, parallel to the river Danube. Implemented groundwater abstractions (mainly in the Southeastern part of the model), the weir in the New Danube and a layer with low permeability on the Eastern shore of the Old Danube cause deviations of the general groundwater flow direction.

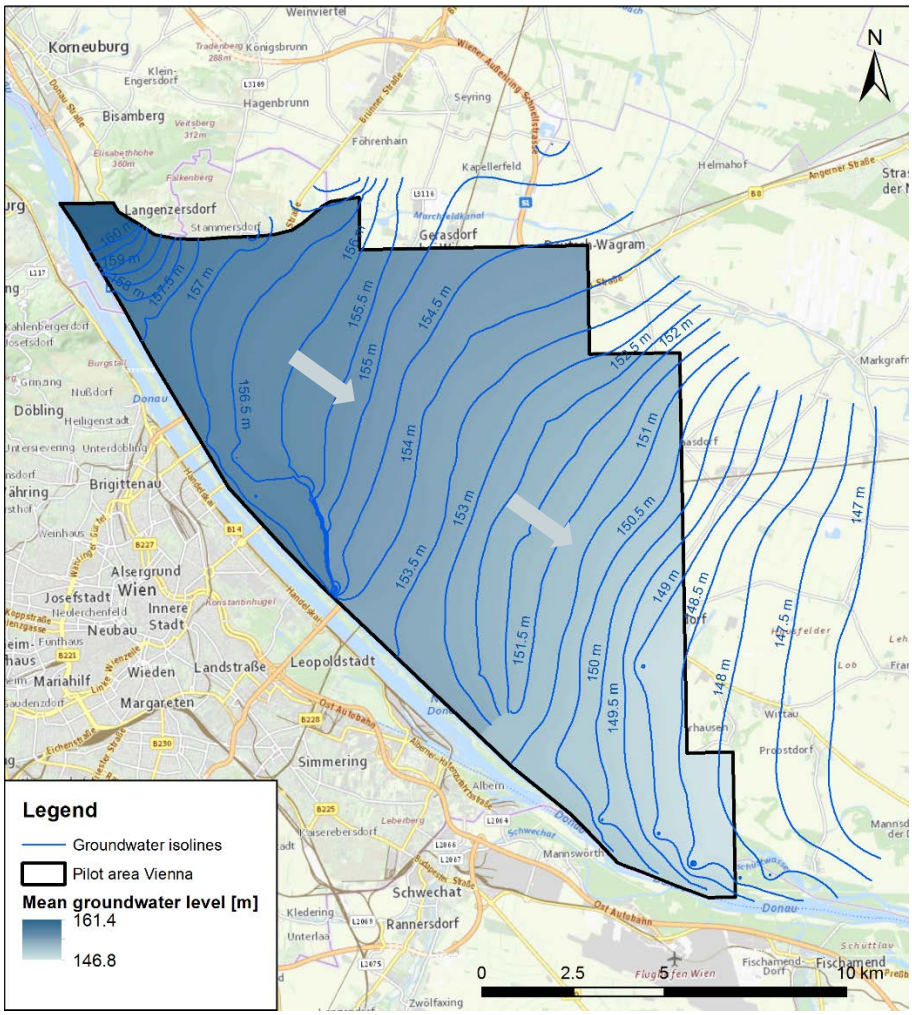

Figure 29. Mean groundwater level (representative day: 14.04.2005) derived from FEFLOW model for the pilot area Vienna. Grey arrows indicate general groundwater flow direction.

According to the calibration results and the imbalance of the 3D model, the resulting hydraulic head represents the mean groundwater level well for the entire model domain. Errors of the mean water level range between -20 and +20 cm. Higher deviations in the southern part of the pilot area are of minor concern, due to the national park "Donau-Auen", which hinders use of shallow geothermal energy use in this area anyways. Uncertainties of the model outside the pilot area are insignificant for the project GeoPLASMA-CE as well. The simulated water level is at most observation points lower than the measured water level and we prefer this conservative hydraulic model compared to an overestimation. We used the resulting map of mean groundwater table as input data set to calculate the shallow geothermal potential for open loop systems in D.T3.4.2.

The thermal model reproduces seasonal fluctuation of groundwater temperatures due to seasonal surface temperature variations and overall increasing temperatures, according to increasing surface temperatures in Vienna related to climate change according to climate status report 2017 for Austria (Figure 21). Therefore, it contains the UHI of the surface. However, this effect also applies to the subsurface. Increasing subsurface temperatures in the pilot area Vienna are due to different anthropogenic heat sources, such as sewage systems, district heating pipes, underground structures and shallow geothermal energy systems, especially thermal uses of the groundwater. Neither of those effects is included in the numerical model developed for GeoPLASMA-CE. Field measurements in the pilot area indicate increasing temperatures as

consequences of the underground UHI. This complicates a comparison of measured and simulated temperatures.

We analysed the simulation results for 2015 and 2016 and compared them with field measurements. Trend analysis of measured groundwater temperatures in the pilot area show a temperature increase of 0.11 K/year from 1990 to 2017. Therefore, we selected 2016 to produce temperature maps as up to date as possible and to use as many data points available as possible. These temperature maps and time series of field measurements served as comparative data set for our numerical thermal model. Furthermore, we compared time series of 20 selected observation wells with time series of our model.

Temperature maps from the numerical model were produced for slice 8, which represents the deeper parts of the aquifer. A slight negative aspect of these temperature maps is, that slice 8 (and all other slices as well) does not have a uniform elevation, due to the geometry of the hydrogeological layers. Elevation of slice 8 varies from 157 m a.s.l to 133 m a.s.l. In a first approach, we calculated an average groundwater temperature map of all slices inside the aquifer, however the resulting map did not match the measured temperature map as well as the temperature map of slice 8 did. Figure 30 shows the temperature maps derived numerically and from field measurements and Figure 31 a comparison of those maps for the same reference days. We selected the reference days based on analysis of field measurements. They represent days of minimum (29.04.2016) and maximum (27.10.2016) groundwater temperatures. In general, both temperature maps of the numerical model underestimate measured temperatures. Especially more to the city centre, modelled temperatures are lower than measured data. This data comparison confirms our assumption, that various sources of the underground UHI effect raise groundwater temperatures in the pilot area.

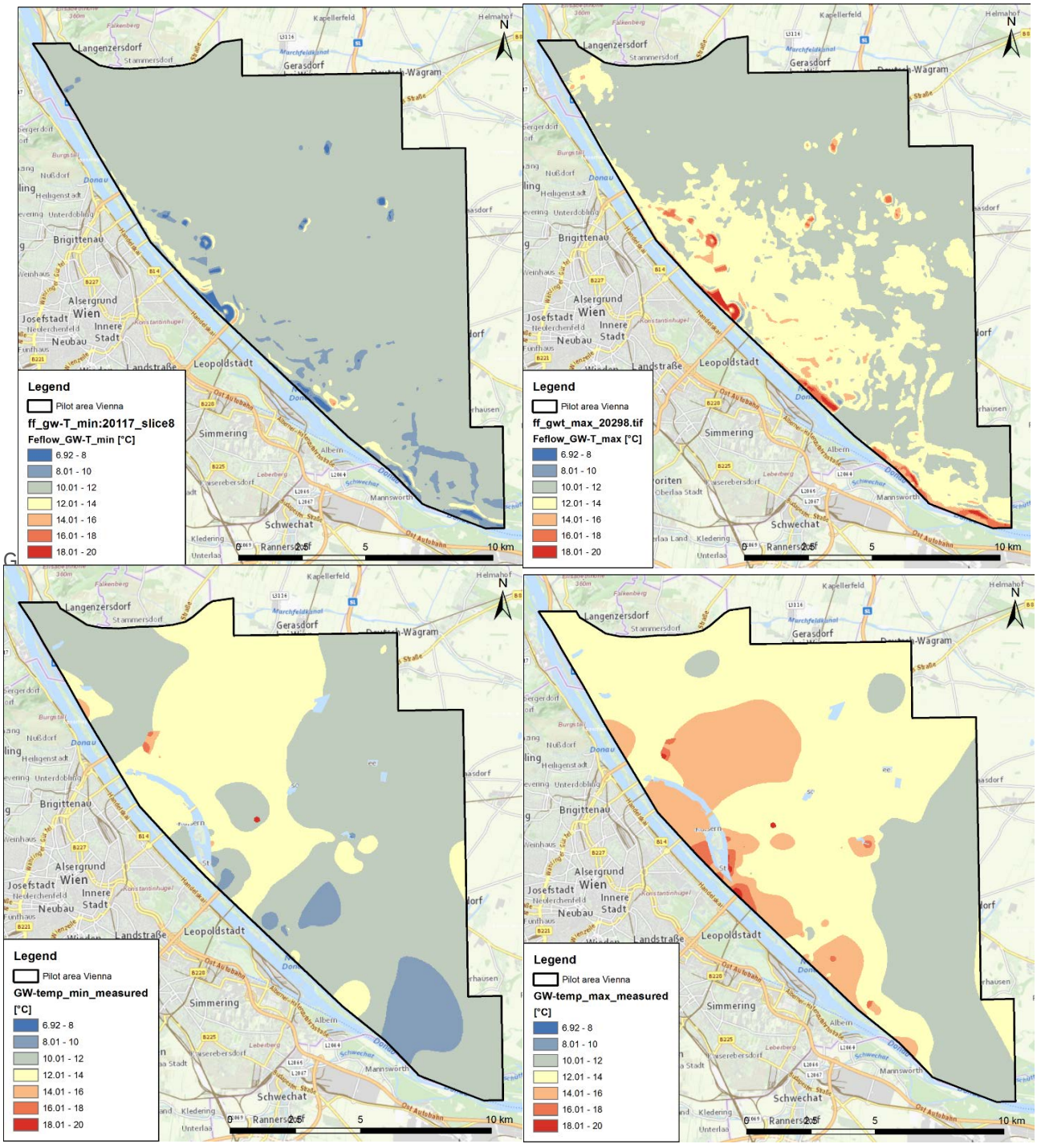

Figure 30. Minimum (left) and maximum (right) groundwater temperature maps for pilot area Vienna derived for representative days 29.04.2016 and 27.10.2016 respectively from numerical model (above) and measured data (below).

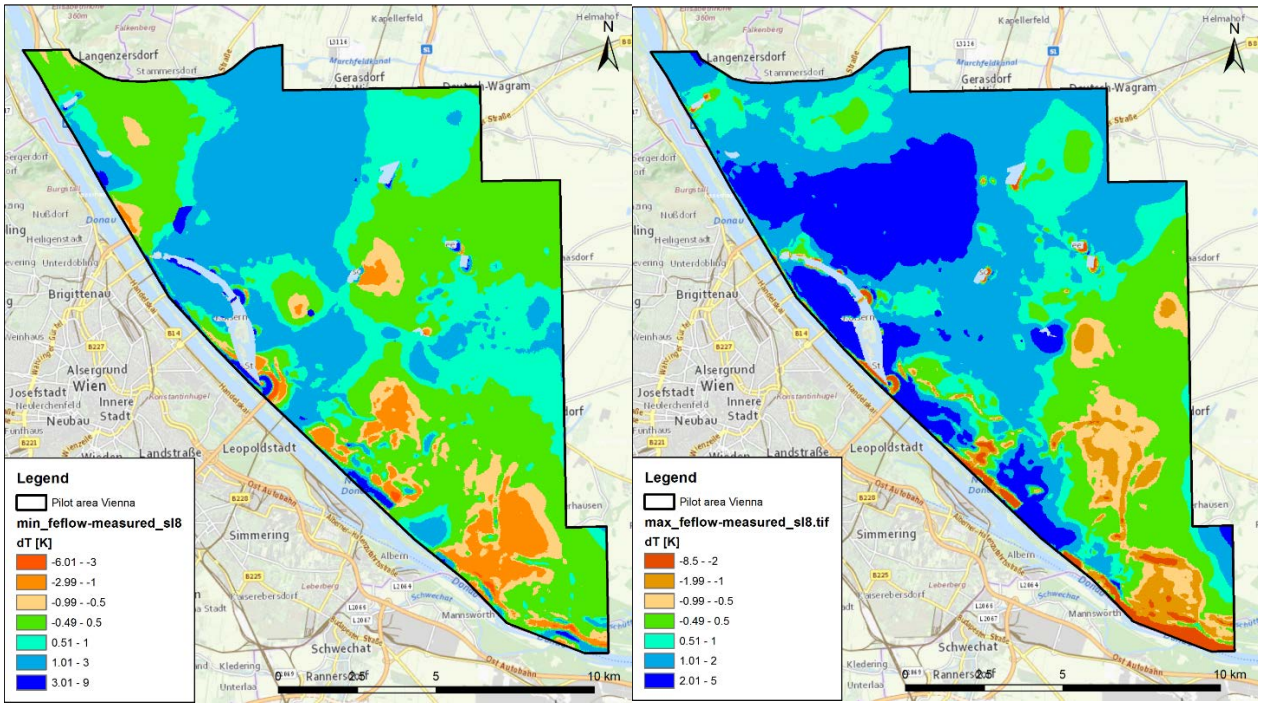

Figure 31. Differences of temperature maps derived from numerical model and field data. Green areas indicate a good match of the maps (±0.5 °K). Negative values show higher temperatures and positive values lower temperatures of the numerical model compared to the field data.

This raise of groundwater temperatures is also visible at two additional comparisons we conducted of simulated and measured temperature data. Oase 22+ is the only location in the pilot area where temperature measurements extend deeper than the quaternary aquifer. GBA measured the temperature in a borehole heat exchanger at Oase 22+ several times in 2017. Figure 32 shows the temperature profiles measured and derived from the simulations for winter and summer times respectively. Modelled groundwater temperatures are around 2 K lower in the upper 20 m than field measurements and with increasing depths, modelled and measured temperatures fit better. This trend implies that surface temperatures are too low in the model or that additional heat sources in the upper part of the model are missing.

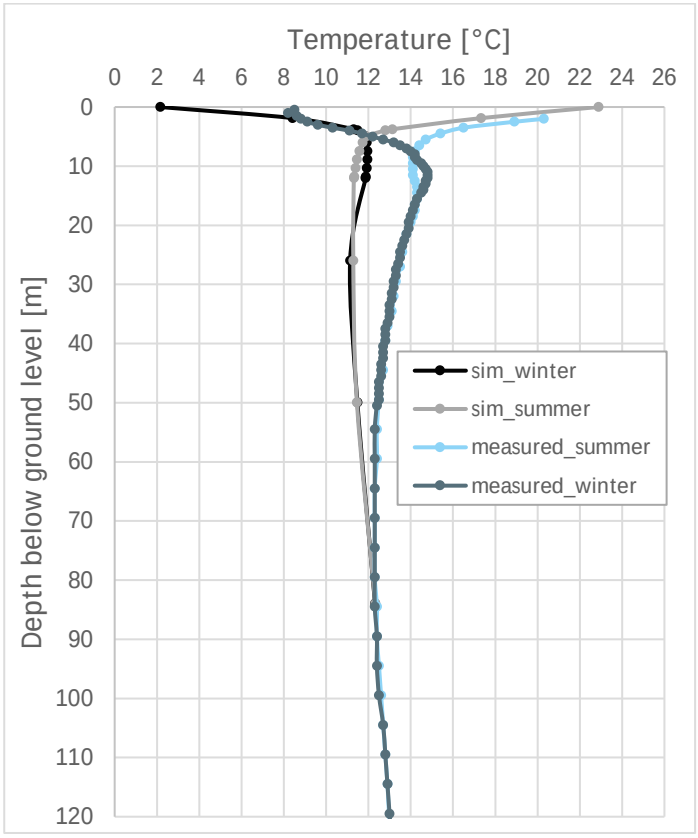

Figure 32. Simulated and measured temperatures for summer- and wintertime at location Oase 22+.

We compared time series of 18 observation wells located at crucial points in the pilot area. They are situated close to temperature boundary conditions and surface water bodies to check their implementation in more detail. Figure 33 provides an overview of the wells' locations, including the borehole heat exchanger Oase 22+. Depth levels (slices) of the model temperatures corresponded to the depth levels of the groundwater temperature measurements. Therefore, only wells with known ground level and depth of measurements could be included. We categorized the observation wells depending on the boundary conditions with highest impact on the temperature. Table 11 includes this categorization and an estimation of how well simulated temperatures match measured data (1 – very good match, 2 – good match, 3 – poor match). Figure 34 shows one time series for each category. Model temperatures at observation wells next to the New Danube have poorest quality. However, the two wells influenced by both the New and Old Danube match measured data well. Implementation of the New Danube could therefore be slightly improved. An improvement of the temperature boundary condition for inflowing groundwater at the Northern model boundary is also suggested to achieve a better fit for the Northern part of the model area. Observation wells with surface temperatures as main impact on the groundwater temperature fit measured data best. Overall, simulated time series tend to have lower temperatures than measured. Wavelength and phase shift match in more than half of the observation wells. Amplitude also matches in half of the observation wells; the other half tends to be smaller.

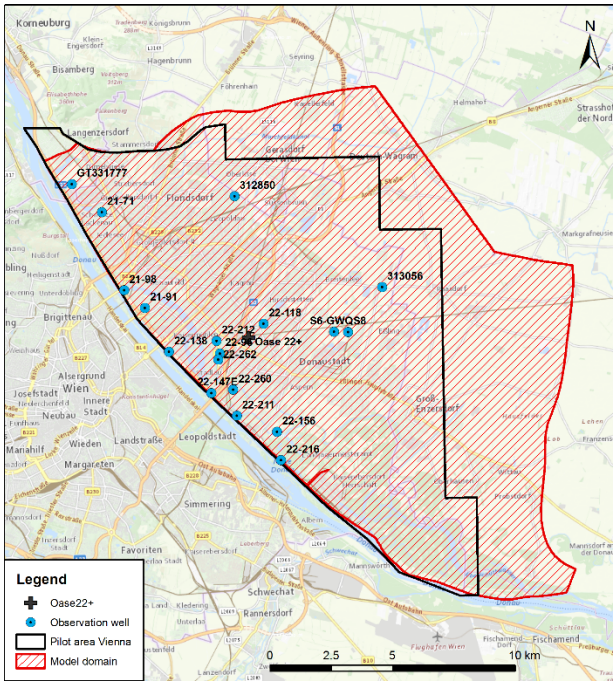

Figure 33. Overview of locations where we compared measured and simulated groundwater temperature time series (observation wells) and temperature profiles for summer and winter (Oase 22+).

Table 11. Selected wells for analysis of simulated and measured data, classified according to the temperature boundary condition with main impact on the groundwater temperatures. Model quality: 1 - very good match, 2 - good match, 3 - poor match of simulated and measured temperatures.

Well	Elevation FEFLOW [m]	Main impact of T-BC	Model quality
312850	153.5	Aquifer inflow	2
GT331777	157.01	Aquifer inflow	2
22-260	148.8	New and Old Danube	1
22-147E	148.6	New and Old Danube	1
21-91	153.23	New Danube	3
22-138	152.1	New Danube	2
21-98	151.48	New Danube	3
22-216	149.3	New Danube	3
22-211	150.4	New Danube	3
22-212	149.76	Old Danube	2
22-262	150.17	Old Danube	2
22-96	150.3	Old Danube	2
21-71	153.9	Surface	3
S6	146.7	Surface	1
S8	147.6	Surface	1
22-118	150.9	Surface	1
22-156	146.94	Surface	1
313056	147.89	Surface	2

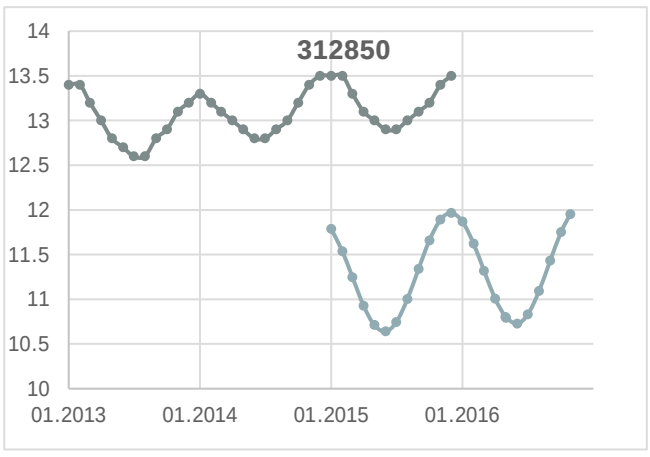

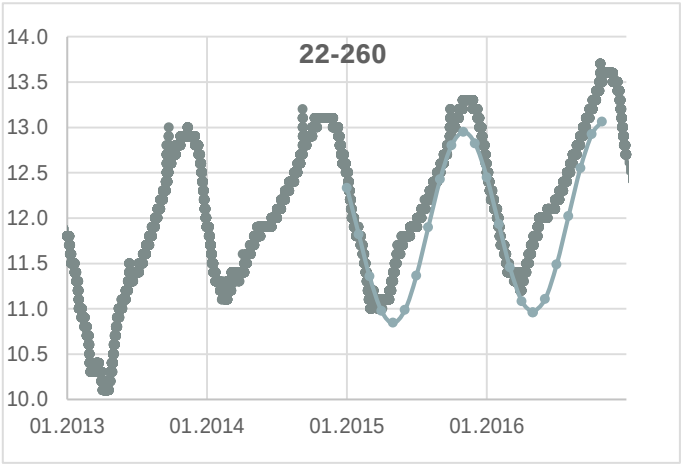

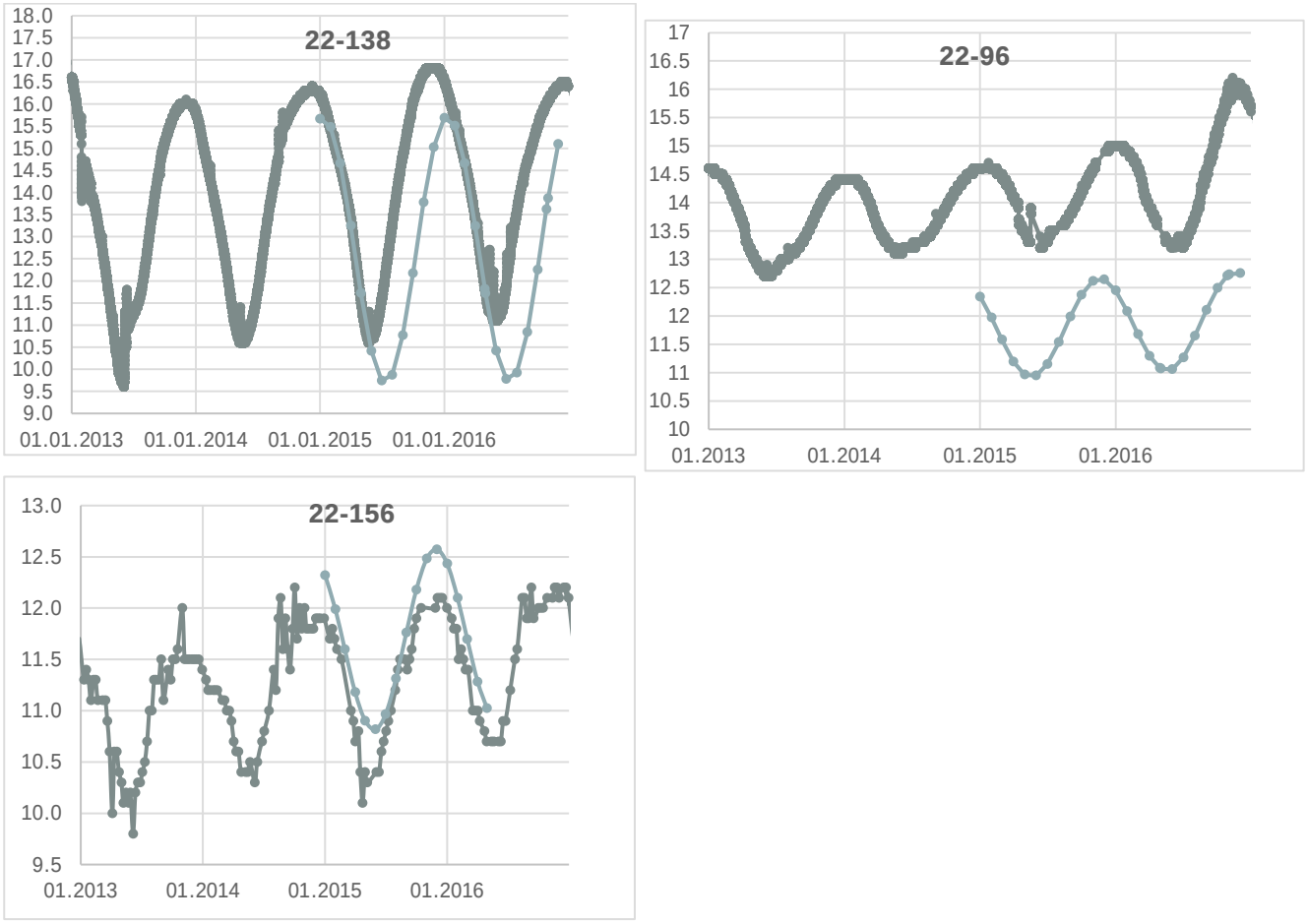

Figure 34. Time series of simulated (light) and measured (dark) groundwater temperatures at corresponding depth levels of selected observation wells.

Spatial variation of surface temperature is included, but very roughly. We applied the time series of one surface temperature measurement station to the entire model area and changed only the mean value (interception) of the sine wave according to the surface temperature map of one year. The thermal model could be significantly improved with measured data for the surface temperature variations over time and space. However, due to lack of data, we applied this simplified approach.

Another source of errors is the applied uniform heat capacity and thermal conductivity within the hydrogeological layers. Even though large variations of those parameters are not to be expected in the model area, as prior studies show, also small variations of thermal properties influence heat transfer in the underground.

Higher deviations between measured and simulated groundwater temperatures are found close to the New Danube. The model inadequately represents the temperature influence of the New Danube. In this area the groundwater temperatures strongly depends on the temperature boundary condition along the New Danube. One reason for the high deviations could therefore be that the temperature data available for the New Danube at weir 1, which was taken for the time-series, is not very representative for the entire surface water body. Another explanation could be an incorrect thermal connection of the New Danube to the groundwater body. A rework of thermal properties along the New Danube could therefore also lead to an improvement of the model quality in this area.

Overall we summarize that, according to our various spatial and temporal data comparison with field measurements, our model adequately represents groundwater temperatures of from underground UHI effect undisturbed conditions. It provides a basis for future implementations of the underground UHI including

already existing open loop systems. The 3D mesh is already prepared for it. Originally, it was planned to include the underground UHI and existing open loop systems already in this model for GeoPLASMA-CE. Data preparation of the wells including the mode of operation and licensed yield takes more time than expect. Therefore, we postponed these additional modelling activities to future projects.

2.3. Pilot area Bratislava – Hainburg

2.3.1. Introduction

Aim of numerical modelling in the pilot area Bratislava – Hainburg was mainly to simulate groundwater flow in the uppermost (Quaternary) aquifer and thus provide groundwater table across the pilot area, that would serve as input to many subsequent calculations and maps of GeoPLASMA-CE published on the web portal. Similarly, the model should help to estimate distribution of hydraulic parameters of Quaternary and Neogene sediments and assess hydraulic productivity needed in thermal potential quantification. Auxiliary goal was to deliver boundary conditions for 3D thermal model.

The groundwater model requires a tight approximation of complex faulted geology with discrete line and point features, such as rivers and point water abstractions, where steep pressure and temperature gradients are unavoidable. Therefore, a finite element model was chosen as the most appropriate. Program FEFLOW version 7.1 (update 9, Diersch 2006) is capable of solving coupled groundwater flow, mass transfer and heat transfer problems in three dimensional porous domains. Its powerful mesh generators enable to construct good quality triangular meshes with inclusion of discrete finite elements representing wells, faults, etc. The program uses finite element analysis to solve the groundwater flow equation of both saturated and unsaturated conditions as well as mass and heat transport, including fluid density effects and chemical kinetics for multi-component reaction systems.

Estimation of parameters was performed using FePEST version 7.1.9.2701 (DHI-WASY 2012), which acts as a pre- and postprocessor for numerical code PEST (Doherty et al. 1994). Program PEST enables for calibration, sensitivity and predictive analyses as well as uncertainty analysis (Monte Carlo), independently from the model software used.

For geostatistical modelling of main lithologies in Neogene sediments, the transition probability software T-PROGS version 2.1 (Carle 1999) was used.

Computations over grids were performed using Python programming language with libraries Numpy (Oliphant 2006) and FloPy (Bakker et al. 2016).

Data used for model creation consisted of various topographic, geologic, hydrogeological, meteorological and groundwater abstraction datasets from different sources. The topographical surface was taken from SRTM digital elevation model (Jarvis et al. 2008). The main geological framework was adopted from the 3D geological model of the pilot area. Databases of boreholes from Austria and Slovakia were indexed and merged together to provide a set of 1216 boreholes with lithological profiles (Figure 35).

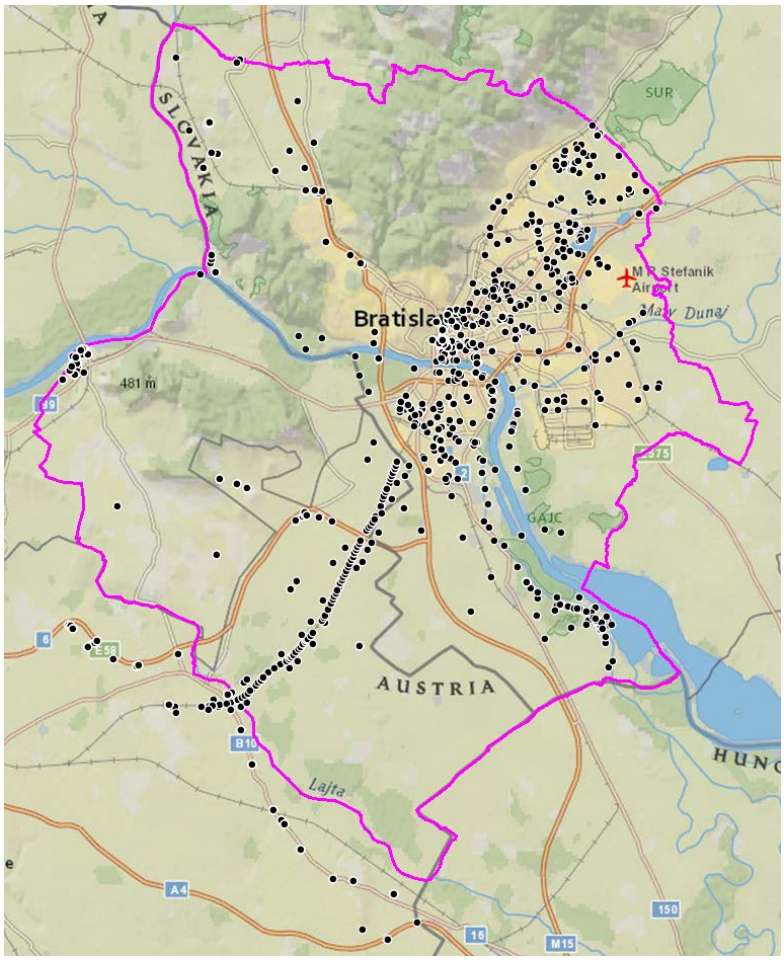

Figure 35. Location of geological borehole profiles for 3D geological model.

River stages, groundwater table measurements were obtained from Slovak Meteorological Institute and Federal Ministry of Republic of Austria for Sustainability and Tourism, respectively. Because input datasets are referenced in different geographic and height systems (in Slovakia S-JTSK/Krovak, vertical reference is Baltic after adjustment Kronstadt gauge, in Austria MGI/Austria Lambert, vertical reference is Adriatic – Trieste gauge), it needed to be transformed prior use into a common system, in our case ETRS89/ETRS TM33, EVRF2007.

The potential recharge of aquifers was estimated based on datasets calculated by Malík & Švasta 2010 (Figure 36). Because the effective rainfall data presented in this paper cover the territory of Slovakia only, it was extended for Austrian part of the pilot area by assuming a trend with a topographic elevation (Figure 37).

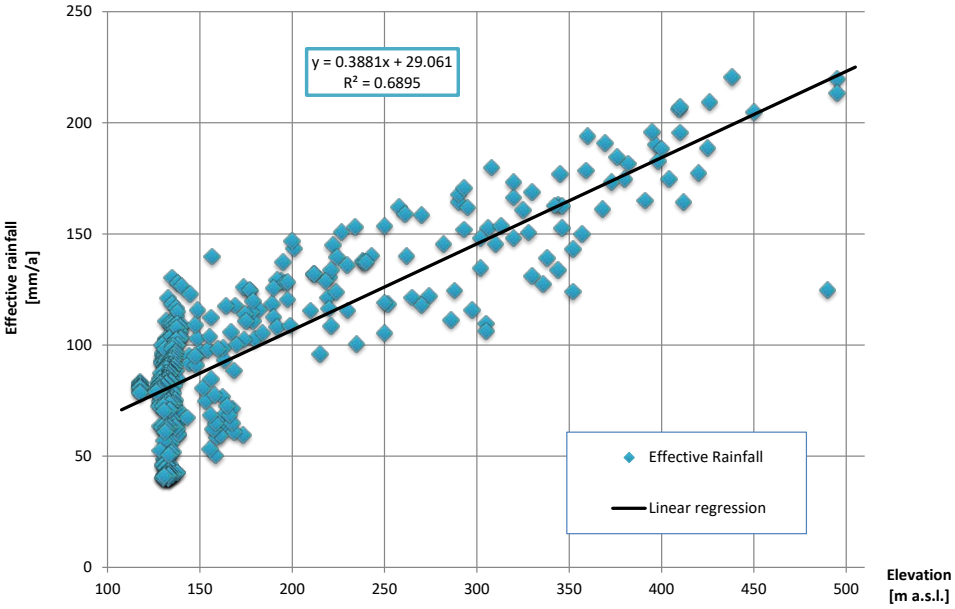

Figure 36. Linear regression of effective rainfall with topographic elevation.

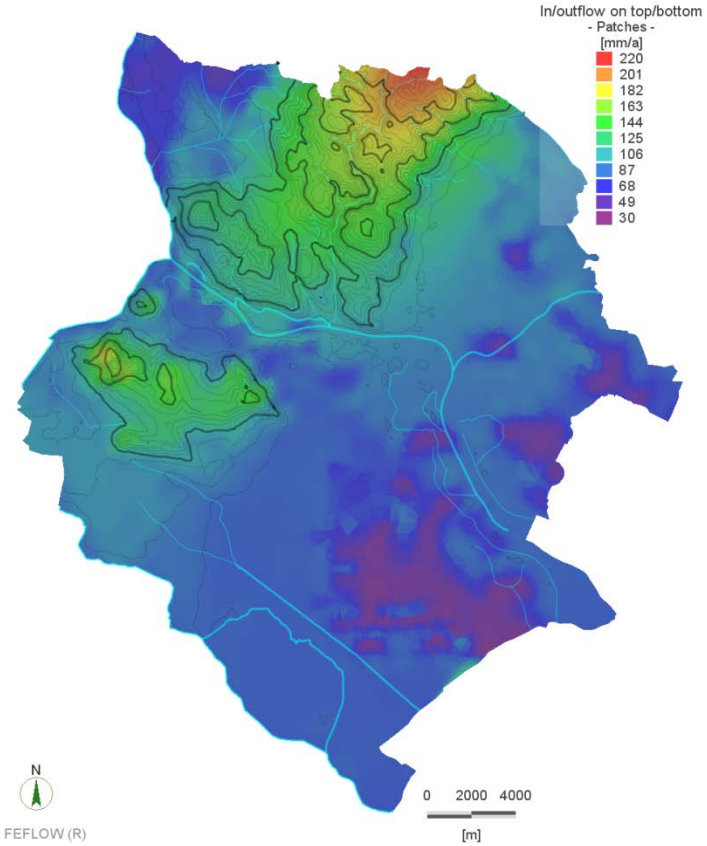

Figure 37. Map of groundwater recharge implemented into the numerical model.

2.3.2. Conceptual model

2.3.2.1. Modelling domain

The model area is outlined in accordance with the GeoPLASMA project pilot area Bratislava – Hainburg. It encompasses all important sedimentary structures predominantly of Quaternary and Neogene age, which host the main aquifers. The pilot area boundary was demarcated earlier in accordance with all hydrogeological knowledge, along well defined hydrogeological limits. Areas without relevant aquifers, mostly hilly areas with outcropping bedrock or thin quaternary cover, were excluded from the model.

The topographical surface limits the top of the model. It is adopted from the digital elevation model SRTM. The model extends down to a depth of -25 m a.s.l.

Although the aquifer of interest is Quaternary, the interaction of phreatic groundwater with underlying less permeable strata, including Neogene sediments, Mesozoic carbonates and quartzites and Paleozoic granites, cannot be neglected. Therefore, the model concept includes also these domains, acting like a buffer.

2.3.2.2. Modelling objectives

The main objective was to simulate the groundwater table of the uppermost (shallow) aquifer, where possible groundwater heat pumps may be installed. It serves as input data for subsequent groundwater potential calculations.

2.3.3. Numerical model

2.3.3.1. Model setup

The model was conceived as an unconfined (phreatic) and steady state model. Technically, it is a 3D model, but because the vast majority of groundwater flow occurs in a single layer and is almost horizontal and the model is therefore quasi 2D.

2.3.3.2. 3D configuration

The model consists of 3 layers: Quaternary aquifer and pre-Quaternary bedrock subdivided into two layers. The top of the two is a 20 m thick layer representing a weathered zone with higher permeability. Below is an unaltered rock, extending up to the bottom of the model, arbitrary set to -25 m a.s.l.

2.3.3.3. Boundary conditions

Waters of major rivers, like Danube, March, Little Danube and Leitha are in a direct contact with groundwater, therefore these were assigned a Cauchy (third type) boundary condition, with assigned hydraulic conductance of a clogging layer. Water elevations were interpolated from several river stage measurements. Other small creeks and streams act mostly as groundwater drains, so a Dirichlet boundary conditions with a flow constrain was set there. At the eastern boundary of the model groundwater is freely flowing across. To simulate this phenomenon in a model a Dirichlet boundary condition was set there, with heads taken from existing groundwater contour maps. The rest of the outer model boundary follows groundwater divides and was defined as no flow (Neumann type) boundary condition. Groundwater abstractions were included in the model as nodal sinks. Figure 38 shows the boundary conditions implemented in the model.

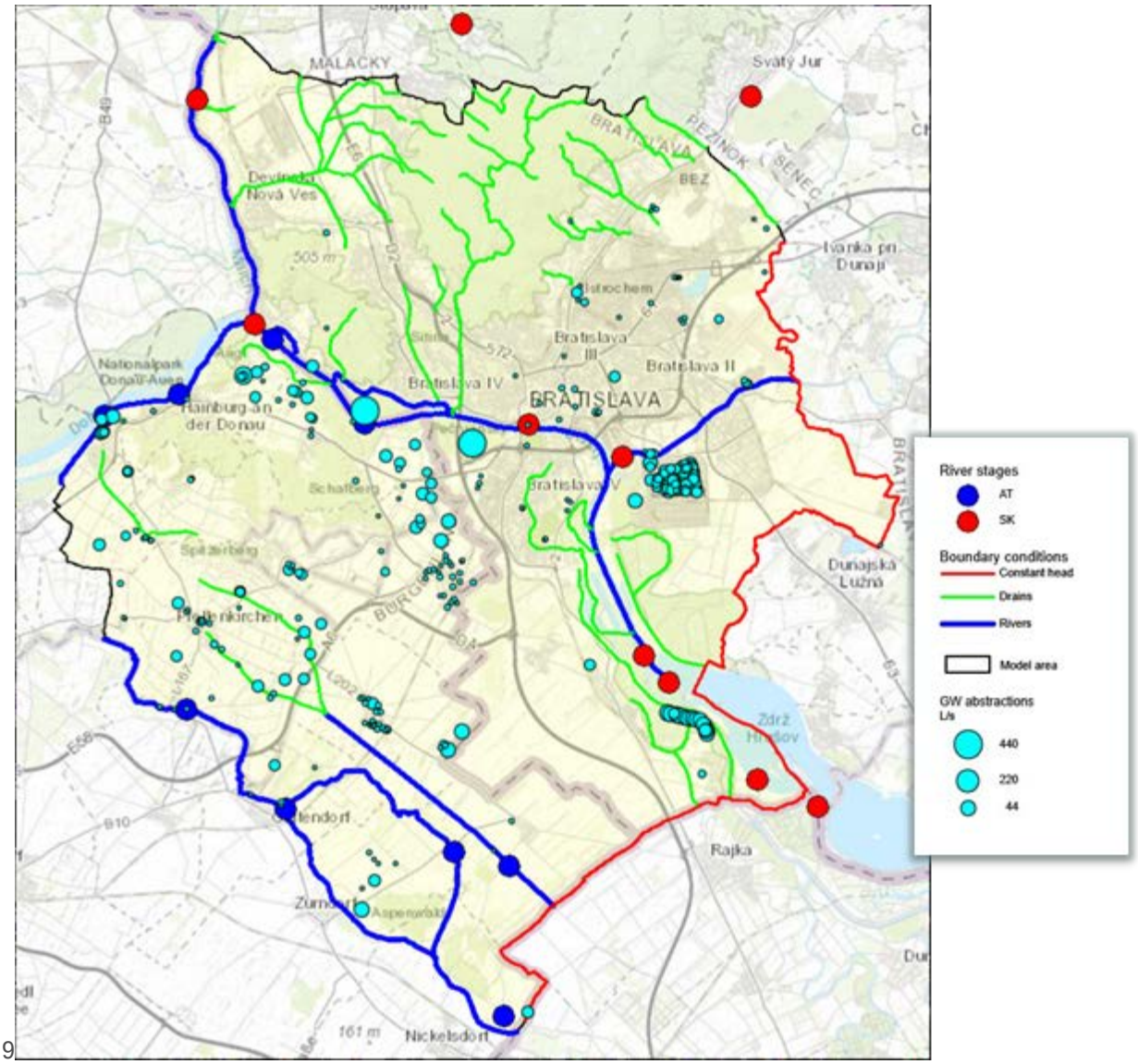

Figure 38. Boundary conditions included in the numerical model. Magnitude of groundwater abstractions are expressed by point size.

An important feature affecting groundwater flow near the river Danube is an artificial flood protection wall constructed throughout the history on both riverbanks. Unfortunately, the underground construction of these walls, which are of different types, is unknown and so their hydraulic function is unknown. Hence, they were neglected in the model. Figure 39 shows the approximate location of the flood protection walls.

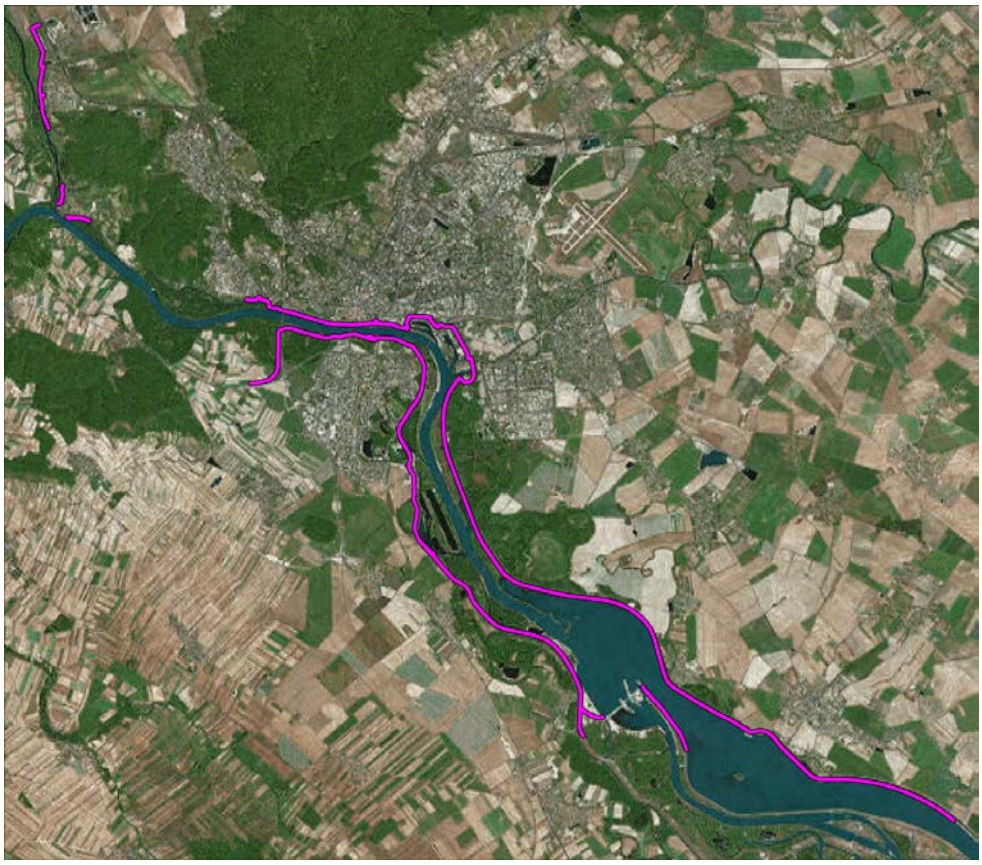

Figure 39. Flood protection walls along Danube in Bratislava.

2.3.3.4. Meshing

The triangular prismatic model mesh was constructed using two-dimensional mesh generator Triangle 1.6 (Jonathan Richard Shewchuk, University of California, Berkeley). Due to expected elevated hydraulic gradients close to rivers and wells, the computing mesh needed to be locally refined around these features. Thus the generated mesh, consisting of triangular prisms, ended up counting 98,058 nodes per slice (in total 392,232), forming 192,239 elements per layer (total 576,717).

Previously created 3D geologic model was transformed into numerical modelling software by means of exporting individual horizons from GoCAD software, importing them into FEFLOW and interpolating elevations to mesh nodes. Pinching-out or missing strata were represented by layers with negligible thickness. Figure 40 shows the mesh in FEFLOW.

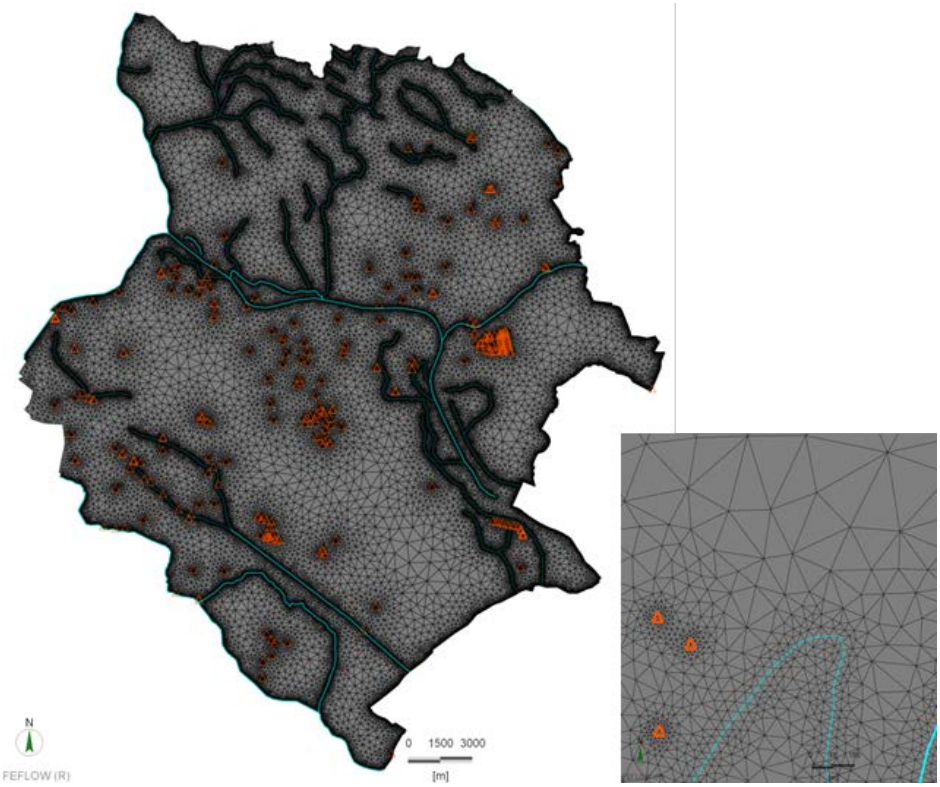

Figure 40. Computational mesh in FEFLOW with detail of refinement around wells (red) and rivers (blue).

2.3.3.5. Material properties

The Quaternary aquifer covering a large territory encompasses a wide range of lithological types (gravels, sands, clays). The hydraulic conductivity coefficient exhibits a very large variability (Table 10). Due to this fact, together with insufficient hydraulic test data from Austrian territory, a decision was made to estimate hydraulic conductivities of the Quaternary aquifer from inverse modelling. The vertical hydraulic conductivity anisotropy was estimated to 10.

Table 12. Hydraulic conductivities in pilot area Bratislava-Hainburg.

Stratigraphy	No. of records	Hydraulic conductivity k_f					
		Min.	Max.	Geom. mean	St. Dev.	Lower bound	Upper bound
Quaternary	512	2.87E-07	1.26E+00	2.14E-03	8.23	2.60E-04	1.76E-02
Quaternary to Paleozoic	3	1.19E-05	8.31E-05	3.29E-05	2.22	1.49E-05	7.30E-05
Quaternary to Tertiary	2	2.45E-07	2.64E-03	2.55E-05	103.72	2.45E-07	2.64E-03
Neogene as a whole	8	7.88E-07	2.05E-04	2.54E-05	6.88	3.69E-06	1.75E-04
Neogene sediments	2	1.99E-05	1.66E-04	5.74E-05	2.89	1.99E-05	1.66E-04
Paleozoic	4	6.74E-07	2.60E-05	6.52E-06	4.03	1.62E-06	2.63E-05

The Neogene sediments underlying Quaternary are composed of intercalated layers and lenses of clay, marl, sand and gravel, which possess very different hydraulic properties. To encounter for such great heterogeneity of hydraulic conductivity, a stochastic approach to model the distribution of facies was applied, because simple interpolation would lead to unacceptable neglecting of flow variability. Moreover, the borehole data is scattered very unevenly over the area with most of the boreholes having a very limited

depth. To accomplish this, a transition probability geostatistical simulation of three main lithologies of Neogene basin filling was performed. Figure 41 shows the boreholes with lithologies in the pilot area and Figure 42 the artificial distribution of Neogene facies after the geostatistical simulation. The resulting 3D grid of lithologies was transferred into materials of a FEFLOW model and assigned hydraulic conductivities based on statistical data from wells database.

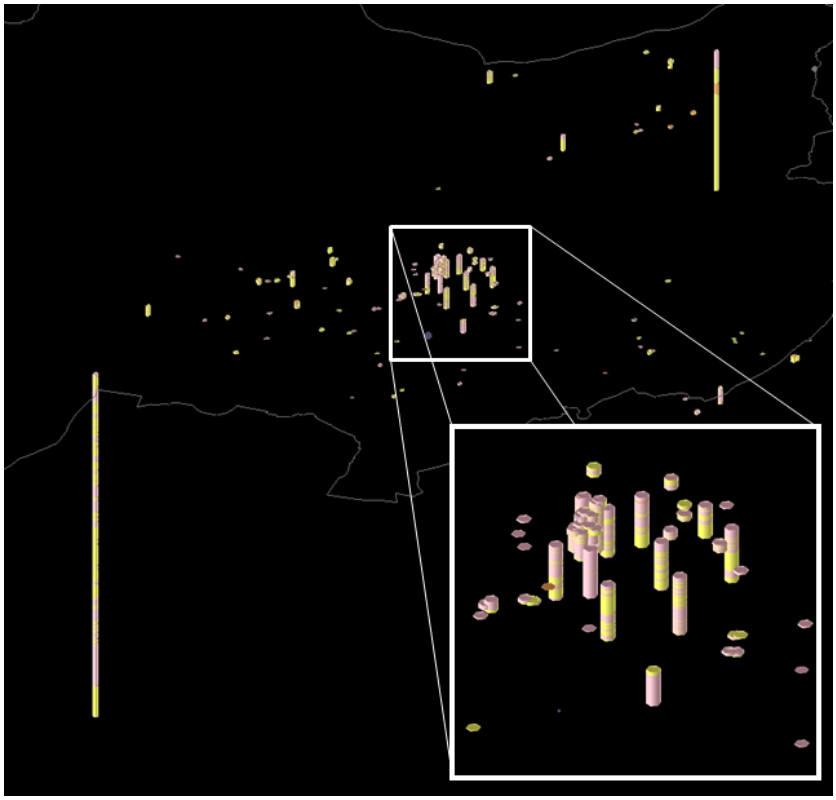

Figure 41. Perspective view on boreholes with lithology.

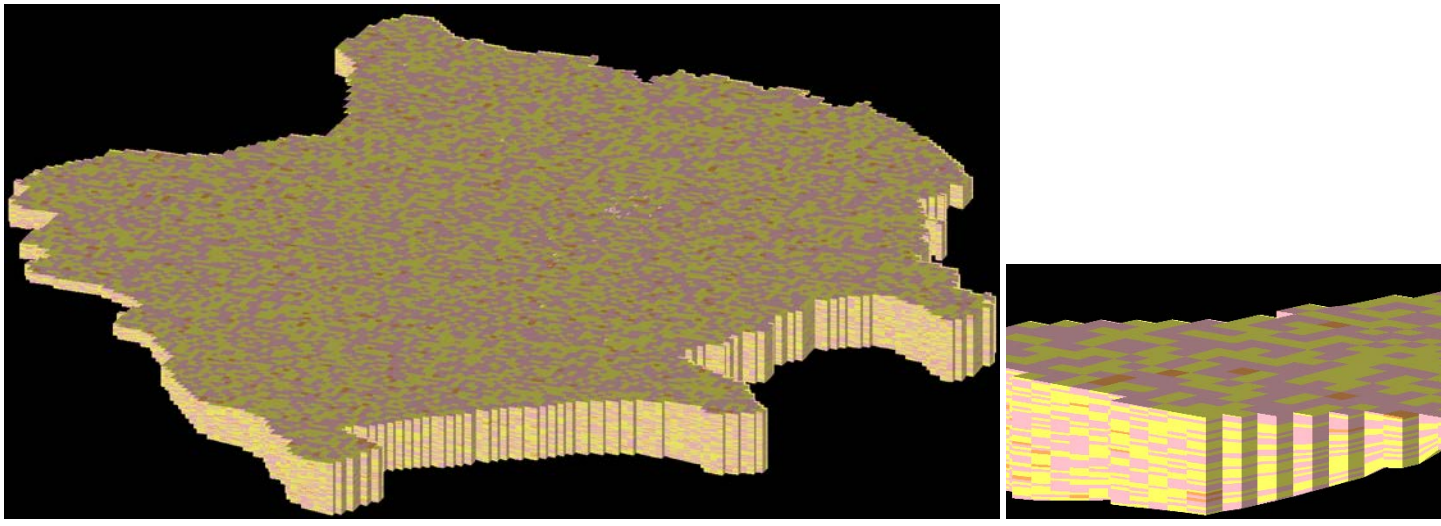

Figure 42. Left: Artifical distribution of Neogene facies resulting from geostatistical simulation in the entire pilot area Bratislava-Hainburg. Right: Detailed view of vertical facies distribution.

2.3.4. Simulations

Several steady state simulations fine-tuned the model set-up before the final calibration. An algorithm for differential equations approximation Algebraic multigrid SAMG was employed, which proved to be reasonable fast and converging successfully.

2.3.5. Calibration

Inverse modelling with FePEST, adjusted the initial distribution of hydraulic conductivities, in order to find the best match between modelled groundwater level and observed piezometric levels measured in boreholes. More than 900 observation measurements were used for this purpose.

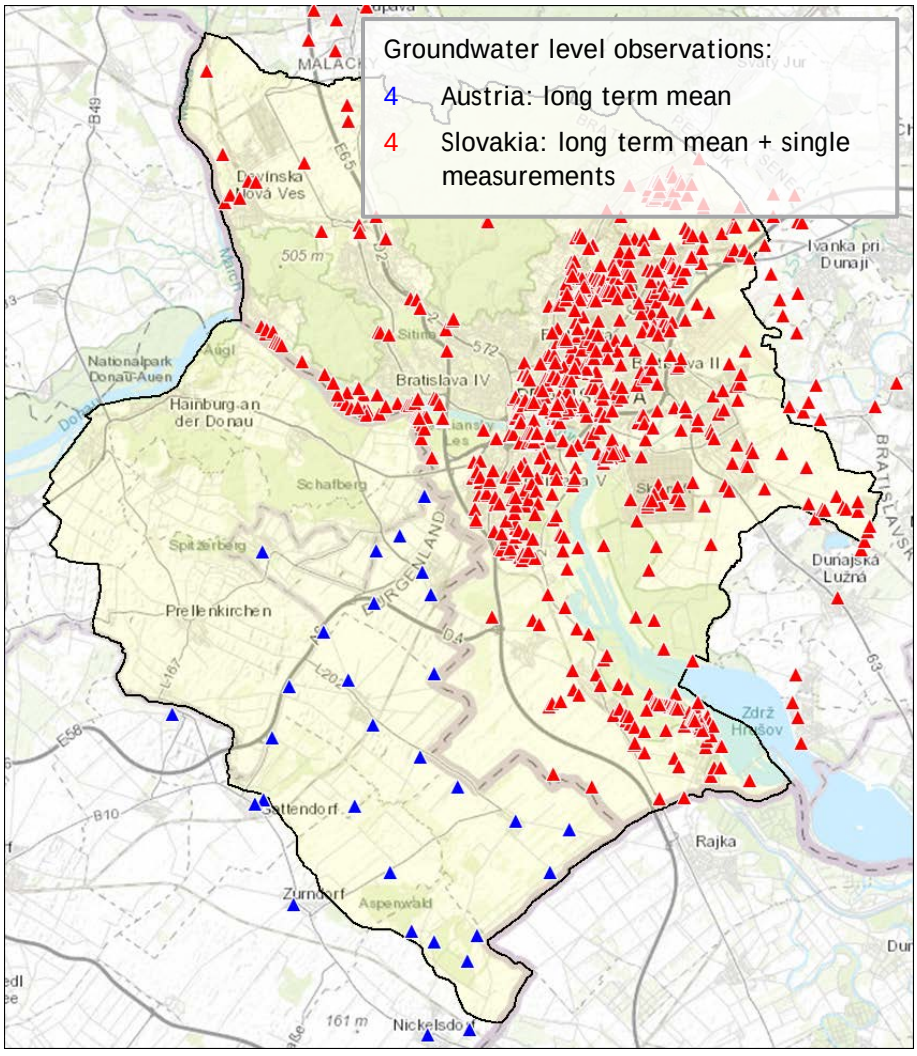

Figure 43. Location of groundwater observation wells.

Piezometers screening both Quaternary aquifer and pre-Quaternary bedrock were considered. It must be noted, that the quality of head measurements is very limited. Most of the values come from historical single measurements and only few come from long term monitoring. The difference in quality of data was accounted for by setting different weights in the parameter estimation process. Results of the calibration show an acceptable match between calculated and observed heads (Figure 44).

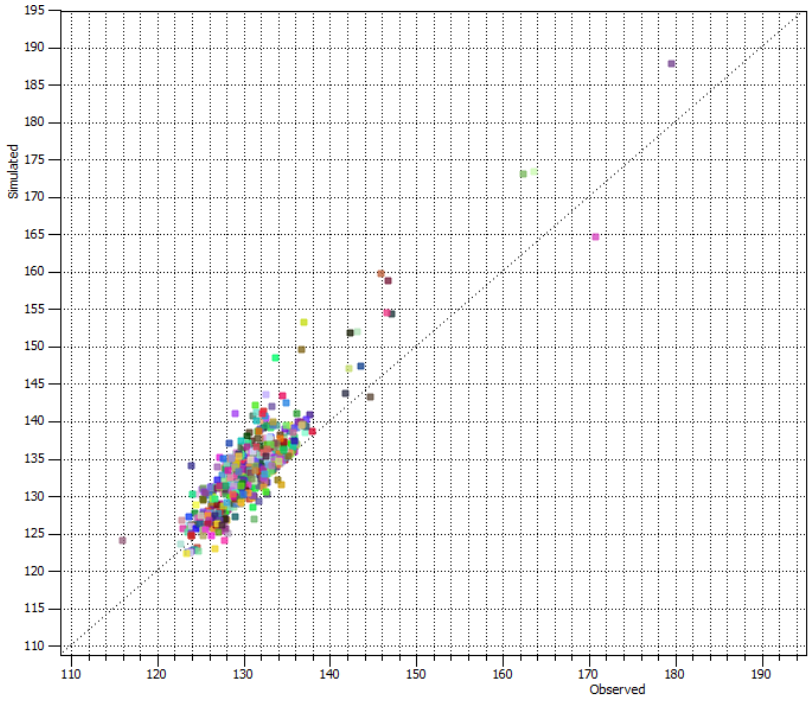

Figure 44. Result of final calibration shows fit of simulated and measured groundwater levels at observation wells.

The resulting distribution of hydraulic conductivities (Figure 45) shows an increasing trend towards the deepening Danube basin, which is in accordance with the real situation.

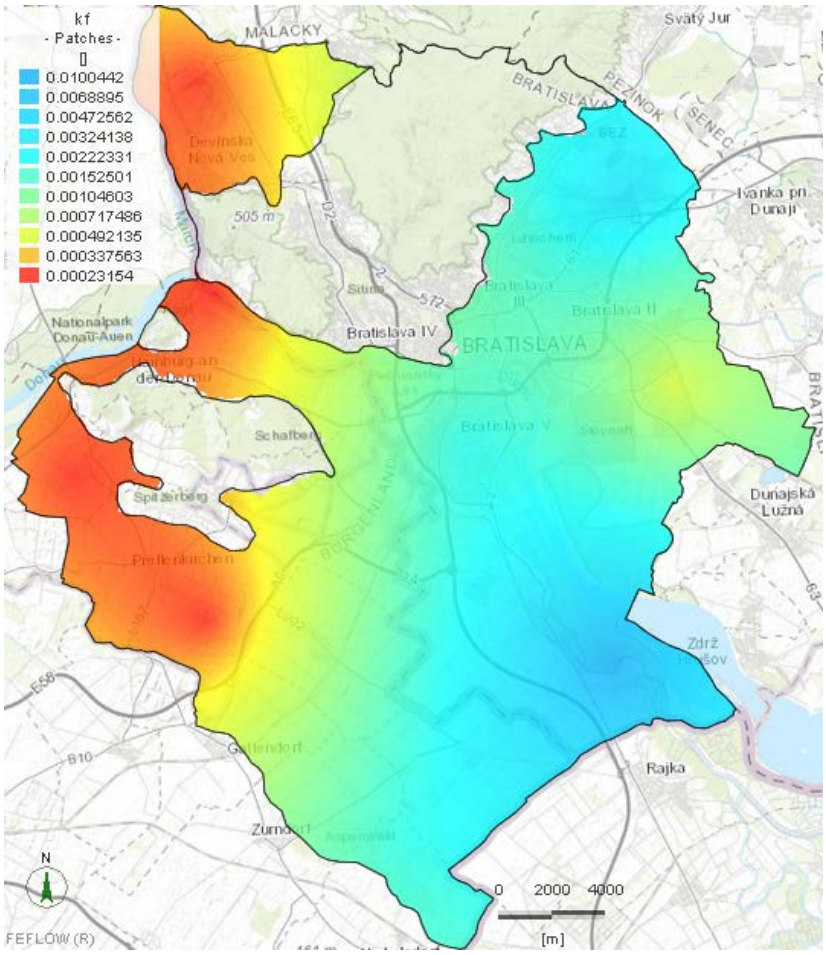

Figure 45. Distribution of calibrated hydraulic conductivities (kf in m/s) of the Quaternary aquifer (Layer 1).

2.3.6. Simulation results

The final groundwater model of Bratislava – Hainburg pilot area shows a general pattern of groundwater flow in the Quaternary aquifer. It confirms the unprecedented role of river Danube in groundwater circulation in fluvial gravels in rivers alluvium. The hydraulic function of the river changes along its path. Upstream the river mostly donates ground water by bank infiltration, while downstream, when it enters Pannonian basin, river water infiltrates into sediments and surpluses groundwater. What is also evident is the impact of major groundwater abstractions. Near drinking water supply wells or around the hydraulic curtain of Slovnaft oil refinery, groundwater table depression develop as a result of excess pumping. These depressions dramatically change the groundwater flow direction and total water budget in the area.

The resulting groundwater table serves as input data for subsequent calculations of groundwater and thermal potentials for shallow geothermal installations, for open loop and closed loop systems in the pilot area.

Another result of the model is the map of groundwater table depth. Generally, the groundwater table is very shallow, up to 4 m, but in prolluvial cones or in elevated regions it can be several tens of meters deep. Figure 46 shows both maps (groundwater contour lines and depth of groundwater table).

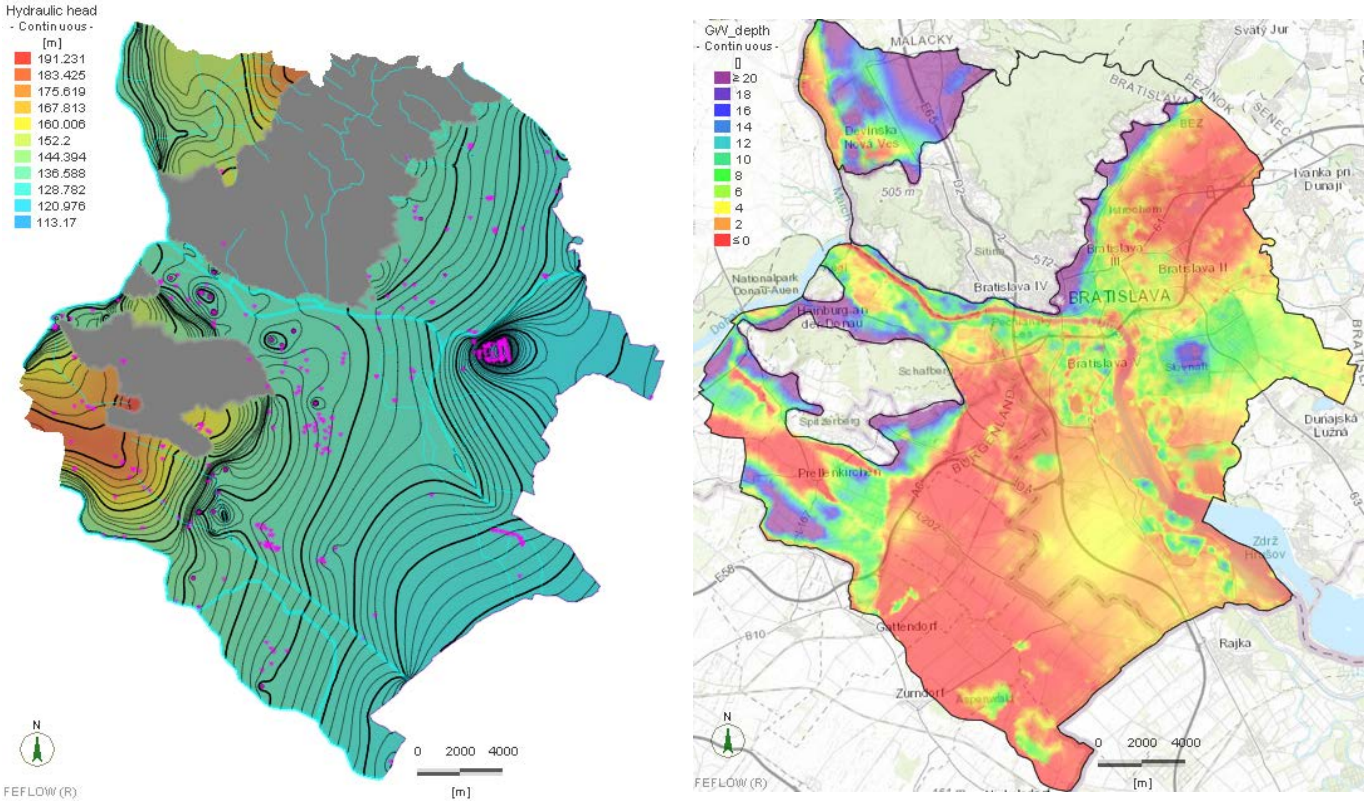

Figure 46. Left: Simulated groundwater levels of the Quaternary aquifer. Groundwater abstractions are shown as pink dots. Right: Depth of groundwater table.

2.4. Pilot area Krakow

2.4.1. Introduction

Main aim of numerical modelling is to obtain reliable and broad information about productivity and expected temperature of water bearing layers in the Upper Vistula River basin, for catchments surrounding Kraków. For that effect, Schlumberger Petrel and VisualModFlow will be applied. Structural geological modelling and numerical modelling will be performed, respectively.

2.4.2. Conceptual model

2.4.2.1. Modelling domain

Model consists of 189600 blocks, covering in total about 1900 km^2, of which about 1100 km^2 are active in the modelling process. Figure 47 provides an overview of the model domain. Main model units for Krakow area will be as follows: Quaternary, Flysch, Miocene, Upper Cretaceous, Upper Jurassic, Carboniferous and Upper Devonian, in common divided into 16 permeable and semipermeable layers.

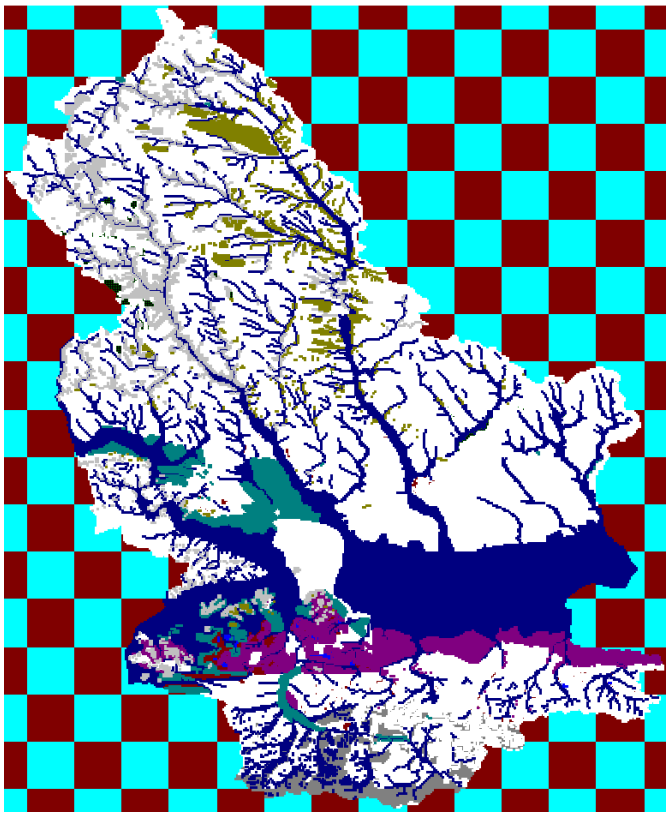

Figure 47. Model overview for pilot area Krakow.

2.4.3. Numerical model

2.4.3.1. Model setup

The steady state regional hydrogeological model has been developed. It gives general information about aquifer's permeability and expected water levels, which was used to calculate the potential productivity.

2.4.3.2. 3D configuration

Geometrical models will be imported from Petrel in the form of applicable file format, most probably surfaces converted into ASCII grid files.

2.4.3.3. Boundary conditions

Three kinds of constrains are applied:

I^{s}t kind – H=constans – Vistula River water level is assumed to be constant (according to 2007 conditions), as this river is main regional drainage

IInd kind – Q=constans – effective infiltration (plus) and water intake exploitation (minus), is established in catchment borders (practically identical to underground flow borders)

IIIrd kind – rivers influencing groundwater level or vice versa – drainage or water supply is limited by hydraulic conductivity of river bed (values set automatically)

2.4.3.4. Meshing

Entire process will be performed in grid conditions, arbitrarily divided into 395x480 blocks (dx=dy=100m, dz depending on thickness of a given layer (total thickness of a layer in one block)). Figure 48 shows an exemplary model cross section.

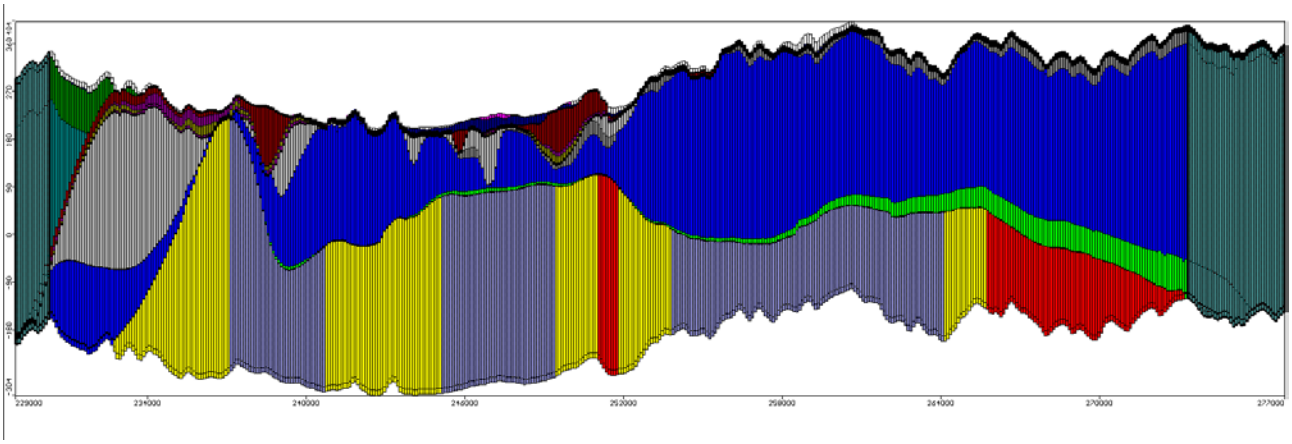

Figure 48. Examplary model cross section.

2.4.3.5. Material properties

Material properties have been preliminary assigned according to the recognised parameters' distribution. The data used was obtained from hydrogeological wells performed over the considered area (Figure 49). Then, the permeability was manually calibrated to get high accordance of watertable level in the model with quasi-natural state observed in the hydrogeological maps.

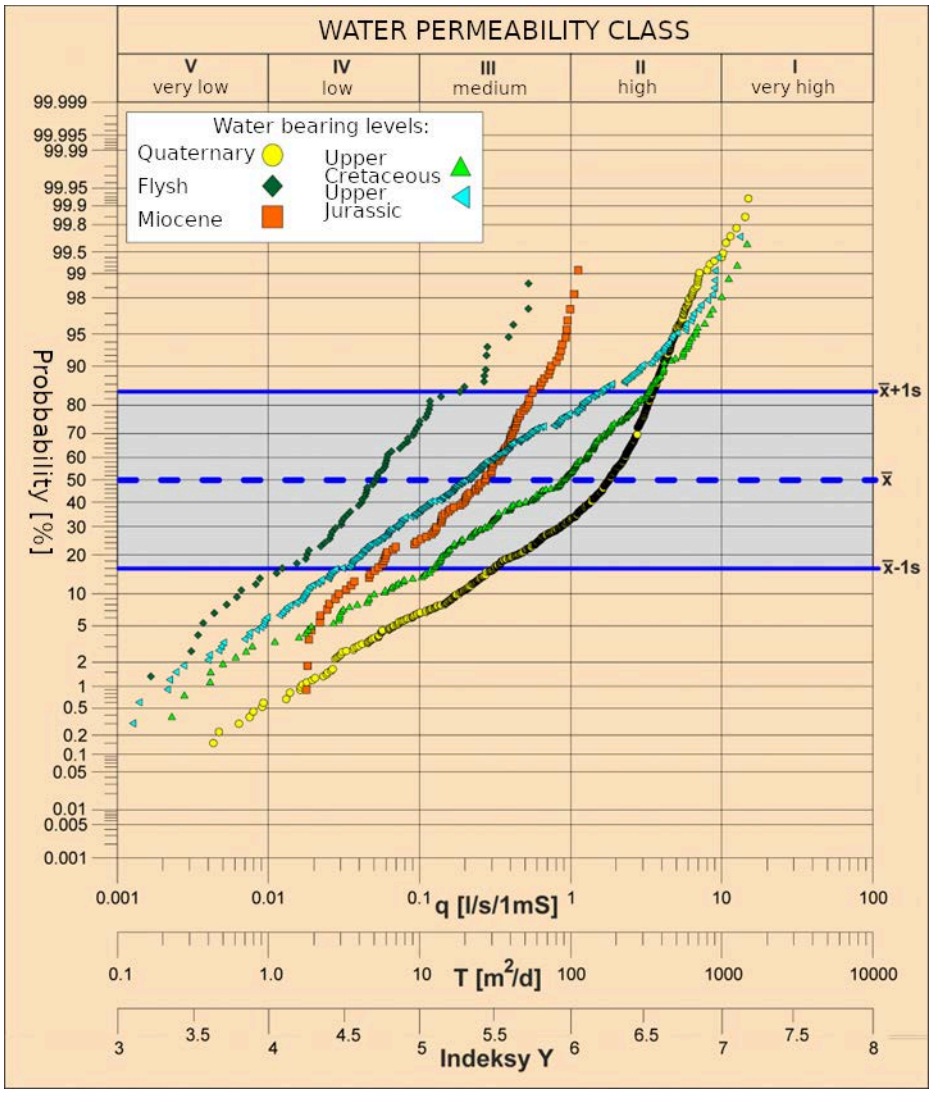

Figure 49. Water permeability classes for pilot area Krakow.

2.4.4. Calibration

Model will be calibrated with regard to hydrogeological maps from years 2005-2007 (mainly summer 2006) and benchmarking measurements, expected accuracy is within 10%. Maps used for calibration were compiled with data obtained in measurements, which typically lasted not longer than 1 month and is recognised as quasi natural state. Measurements under the GeoPLASMA-CE were performed in 2017 and 2018, mainly in summer season. Their purpose was to compare provide independent, modern data for model benchmarking.

2.4.5. Simulation results

The following hydrogeological outputs for Kraków pilot area are derived from static hydrogeological model and geological model:

- aquifers' outlines
- water pressure in each water bearing level (expressed as unconfined water table level),
- artesian aquifers,
- confined aquifers,

- areas, where multiple aquifers occur,
- hydraulic productivity of each aquifer

Once the model was finished, outlines of aquifers were clipped to relevant thickness occurrence (above 1m). Then, adequate layers were intersected, compared and multiplied in order to obtain required outputs.

3. Summary and conclusions

Four 3D numerical groundwater models were produced for the pilot areas Vienna, Ljubljana, Bratislava - Hainburg and Krakow. They all focused on shallow Quaternary aquifers in the respective areas, since they are most important for the use of open loop systems. Aside from providing groundwater level contour maps, an additional goal of the models was to deliver boundary conditions for thermal models. Regional thermal models should include heat transport to and from the surface and underlying layers. Therefore, all models were prepared in 3D.

Most important results of the numerical models are maps of mean groundwater level for all pilot areas and thermal models providing groundwater temperatures for the pilot areas Vienna and Ljubljana. Groundwater level and temperature measurements in observation wells were used to calibrate the models. Accuracy of the mean groundwater level maps varies inside the pilot areas, depending on local features such as e.g. sheet piles, and between the pilot areas. High accuracies up to ±0.1 m could be reached in some pilot areas. Thermal models consider the urban heat island effect from the surface to a fair amount, but neglect the underground urban heat island effect. Since urban heat islands are known in both cities, model calibration was difficult and highest uncertainties of the thermal models are related to anthropogenic heat impact. Nonetheless, models achieved a good fit with around ±1 °C in most parts of the models. The inclusion of anthropogenic heat sources proved to be more challenging than expected and could not be accomplished. However, the thermal models provide a basis for detailed planning of new shallow geothermal energy applications. They can serve as initial models to include existing applications to estimate the energy content of the aquifer, which has already been used, and to implement other anthropogenic heat sources causing an underground urban heat island effect. This makes these models an ideal supportive tool for sustainable management of subsurface resources. Groundwater level maps and maps of saturated zone thickness are input parameters for the calculation of the shallow geothermal potential for open loop and closed loop systems.

4. References

Baker, H. (2014): JewelSuite modelling manual. DELFT, 953 p.

Bakker, M., Post, V., Langevin, C. D., Hughes, J. D., White, J. T., Starn, J. J. and Fienen, M. N. (2016): Scripting MODFLOW Model Development Using Python and FloPy: Groundwater, v. 54, p. 733–739, doi:10.1111/gwat.12413.

Carle, S.F. (1999): TProGS: Transition Probability Geostatistical Software, version 2.1. Department of Land, Air and Water Resources, University of California, Davis, CA.

Decree (2012): Decree on the water protection area for the aquatic body of the aquifers of the Ljubljansko barje and the surroundings of Ljubljana

DHI-WASY (2012): FEFLOW finite-element subsurface flow and transport simulation system. User's Manual/Reference manual/White Papers, v. 6.1. Technical Report, DHI-WASY GmbH, Berlin.

Diersch H.J.G. (2006): FEFLOW Finite Element Subsurface Flow and Transport Simulation System. Reference Manual. WASY GmbH Institute for Water Resources Planning and Systems Research, Berlin.

Doherty, J., Brebber, L. and Whyte, P. (1994): PEST: model independent parameter estimation. Watermark Numerical Computing, Corinda, Australia.

Esri (2014): ArcGIS Desktop: Release 10. Redlands, CA: Environmental Systems Research Institute.

Hoelting, B. and Coldewey, W.G. (2013): Hydrogeologie – Einführung in die Allgemeine und Angewandte Hydrogeologie. 8. Auflage, Springer, Berlin Heidelberg.

Janža, M. (2015): Environ Earth Sci 73. 3763. https://doi.org/10.1007/s12665-014-3662-2

Janža, M., Lapanje, A., Šram, D., Rajver, D. and Novak, M. (2017): Research of the geological and geothermal conditions for the assessment of the shallow geothermal potential in the area of Ljubljana, Slovenia. Geologija. 60. 309-327. 10.5474/geologija.2017.022.

Jarvis A., H.I. Reuter, A. Nelson and E. Guevara (2008): Hole-filled seamless SRTM data V4, International Centre for Tropical Agriculture (CIAT), available from http://srtm.csi.cgiar.org.

Malík, P. and J. Švasta (2010): Spatial distribution of potential aquifer recharge from precipitation for the period of 1951–1980 over Slovakia. V: Andrzej ZUBER, Jarosław KANIA a Ewa KMIECIK, ed. XXXVIII IAH Congress „Groundwater Quality Sustainability", Krakow, 12–17. Krakow: University of Silesia Press, s. 1273–1275. ISBN 978-83-226-1979-0.

Oliphant, T.E. (2006): A guide to NumPy, Trelgol Publishing USA.

Šram, D., Brenčič, M., Lapanje, A. and Janža, M. (2012): Perched aquifers spatial model: a case study for Ljubljansko polje (central Slovenia). Geologija. 55. 107-116. 10.5474/geologija.2012.008.

Šram, D., Janža M., Novak, M. and Lapanje A. (2019a): Deliverable D.T3.3.1 Activity report on 3D modelling (detailed description of static and numerical models including estimation of errors). (https://portal.geoplasma-ce.eu/content/outputs)

Šram, D., Koren K., Janža, M., Rajver, D. and Novak, M. (2019b): Deliverable D.T3.3.1 Activity report about field measurements in the pilot area Ljubljana (https://portal.geoplasma-ce.eu/content/outputs).

Verein Deutscher Ingenieure (2010): Thermal use of the underground – Fundamentals, approvals, environmental aspects. Beuth Verlag GmbH, Berlin.

Web 1: http://vode.arso.gov.si/hidarhiv/pov_arhiv_tab.php (last access: 12.08.2019)

Web 2: http://www.feflow.info/html/help71/feflow/mainpage.htm#t=09_Parameters%2FMaterial_Properties%2Fflow_parameters.html (last access: 26.08.2019)

5. Annexes

Interreg CENTRAL EUROPE
GeoPLASMA-CE
European Union
European Regional Development Fund

ANNEX 1

Numerical modelling of TRT measurments and estimation of Heat extraction capacity in the pilot area Ljubljana

Version 1

05 2019

Geologische Bundesanstalt
LANDESAMT FÜR UMWELT, LANDWIRTSCHAFT UND GEOLOGIE
Freistaat SACHSEN
CZECH GEOLOGICAL SURVEY
GeoZS Geološki zavod Slovenije
AGH University of Science and Technology
geoENERGIE Konzept
GiGa infosystems
Bundesverband Geothermie
City of Ljubljana

The involved GeoPLASMA-CE team

PP Accronym	**Person**
PP07 - GeoZS	Mitja Janža Dejan Šram

Table of contents

1. Introduction

In scope of GeoPLASMA-CE, project partner geoENERGIE Konzept GmbH has preformed the TRT test in PA06 (Ljubljana). The TRT test took place on days 6.8.2018 – 9.8.2018.

Based on the TRT measurements results a local numerical model with FEFFLOW software was constructed. The aim of the modelling was to estimate the effect of groundwater flow and effective thermal conductivity (TC; l (W/mK) and potential heat extraction capacity – HEC (W/m).

2. TRT measurements

BHE settings

Drilling length: 100 m

Tubing length 40 m

Mean drilling diameter: 152 mm

Type of tubing: Double PE100-RC: 40*3.7

Grouting material: Gravel

TRT setting:

Input power: 6.7 kW

Flow rate: 27 l/min

2.1. Results

Time of first temperature measurement: not possible

Inlet temperature: 21 °C (after ca. 5h)

Outlet temperature: 17 °C (after ca. 5h)

Due to strong groundwater flow and consequently rapid stabilisation of temperature in the BHE the measurement of temperature difference was not possible (Figure 1).

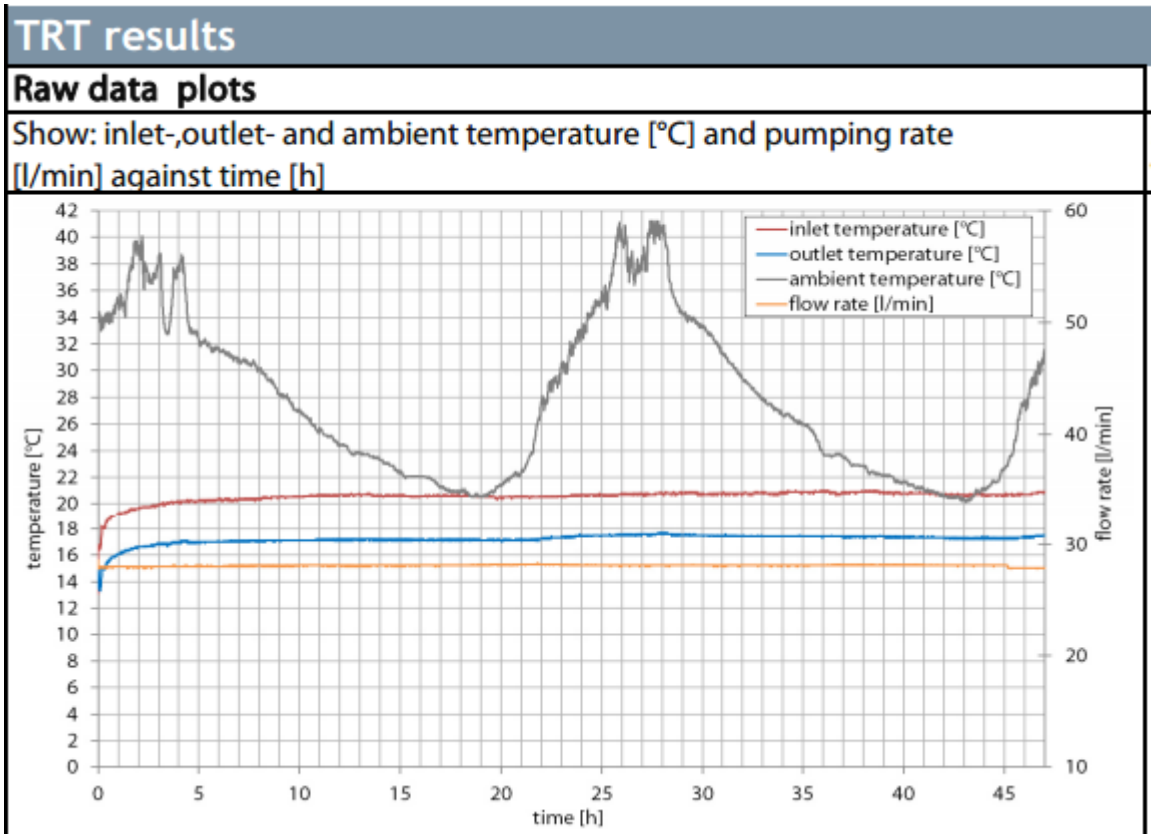

Figure 1: Results from TRT measurments.

3. FEFLOW numerical model

A small numerical model was constructed in the area of the BHE (Univerzitetni rehabilaticijski center SOČA). Two scenarios were simulated, first one with present groundwater flow and second one without groundwater flow.

Calibration of the model with TRT measurements

Simulation of TRT measurements on the local numerical model.

BHE top (depth): 40 m

BHE bottom (depth): 100 m

Input power: 6.7 kW

Flow rate: 27 l/min

Borehole diameter: 152 mm

Hydraulic model: steady state (Head on West 278m, on East 276 m)

Temperature model: Transient – 365 days

Temperature boundary conditions:

constant on top, bottom of the model, constant on inflow and outflow of the model.

Results Calibration

Results of calibration are presented in Figure 2. Inlet and outlet temperature stabilize fast at the value of 20 °C and 16.3 °C respectively (Figure 2 and Figure 3). Simulated temperatures in BHE are 1 K lower than measured values from TRT (Figure 1).

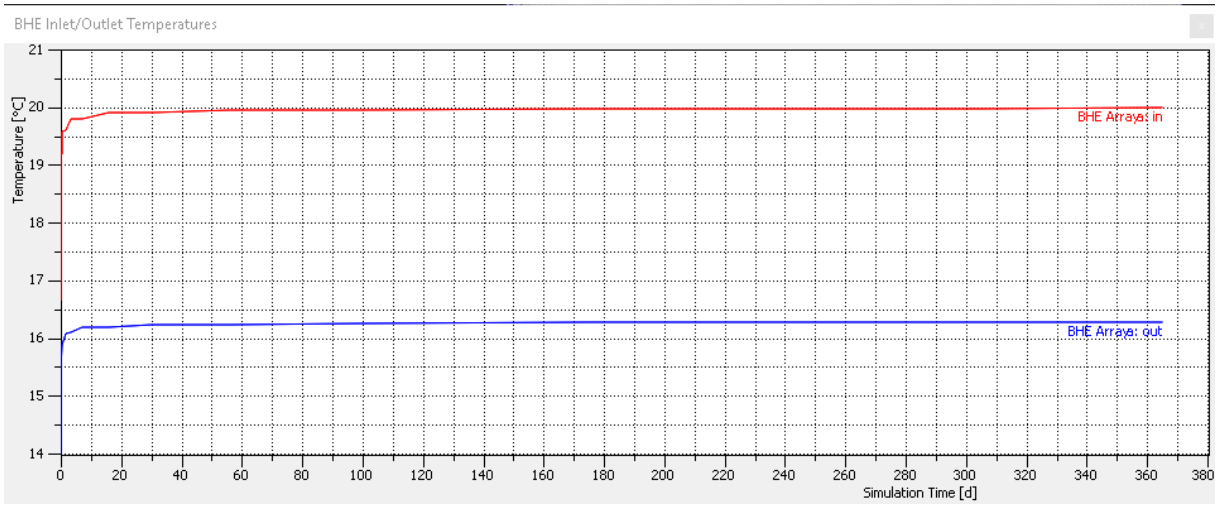

Figure 2: Inlet and outlet temperature in BHE (TRT simulation).

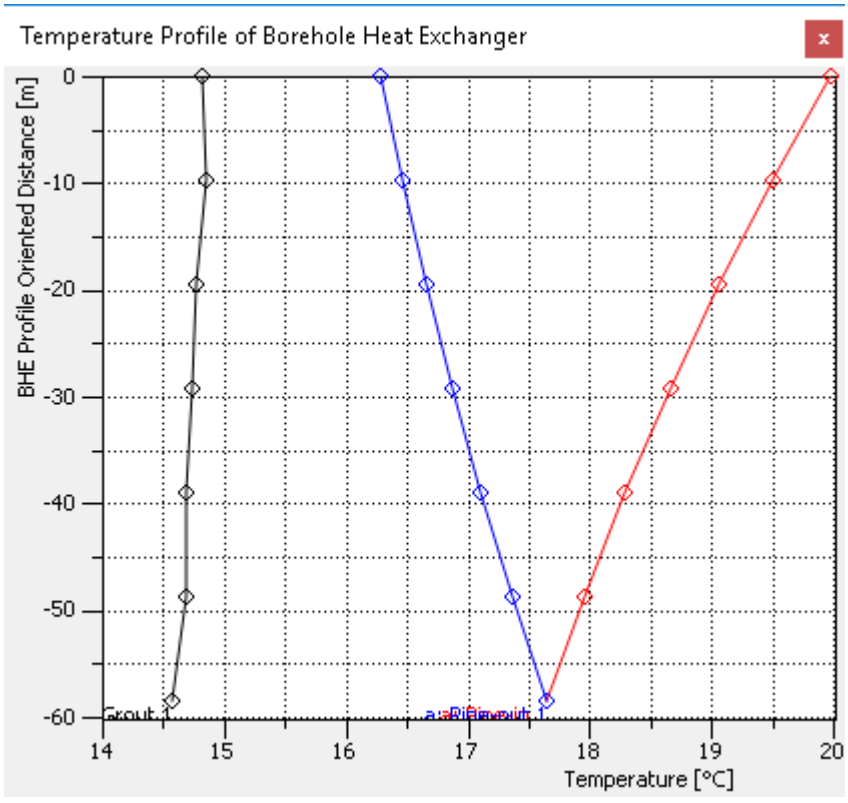

Figure 3: Temperatures in BHE (TRT simulation).

Scenario 1: Simulation of conditions with GW flow (v_D=1.28 m/d)

Parameter values:

BHE top (depth): 40 m

BHE bottom (depth): 100 m

Inlet temperature: 5 °C

Flow rate: 24 l/min

Borehole diameter: 152 mm

Hydraulic model: steady (Head on West 278m, on East 276 m)

Temperature model: Transient – 365 days

Temperature boundary conditions:

constant on top, bottom of the model, constant on inflow and outflow of the model.

Results Scenario 1:

Temperature on the BHE on the inlet is constant 5 °C meanwhile the outlet temperature is stabilised at 9.5 °C (Figure 4). Extracted power is equivalent to 7.27 kW (Figure 5).

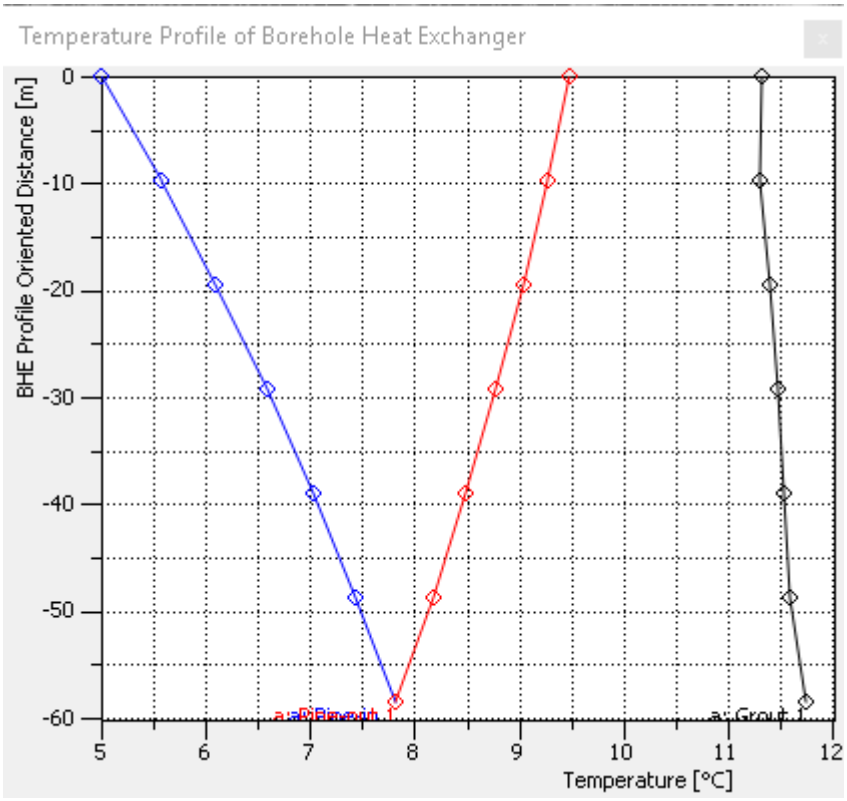

Figure 4: Temperatures in BHE (Scenario 1).

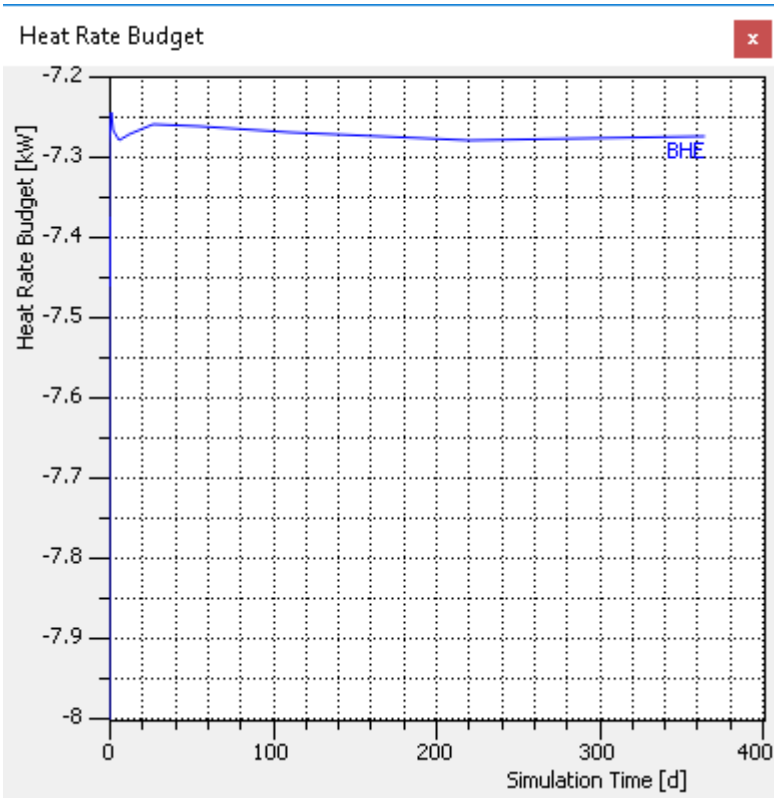

Figure 5: Extracted power at constant inlet temperature 5 °C (Scenario 1).

Scenario 2: Simulation of conditions with no GW flow

Parameter values:BHE top (depth): 40 m

BHE bottom (depth): 100 m

Inlet temperature: 5 °C

Flow rate: 24 l/min

Borehole diameter: 152 mm

Hydraulic model: steady – no flow

Temperature model: Transient – 365 days

Temperature boundary conditions:

constant on top, bottom of the model, constant on inflow and outflow of the model.

Results Scenario 2

Temperature on the BHE on the inlet is constant 5 °C meanwhile the outlet temperature is stabilised at 6.15 °C (Figure 6). Extracted power in equivalent to 1.8 kW after the 365 days (Figure 7).

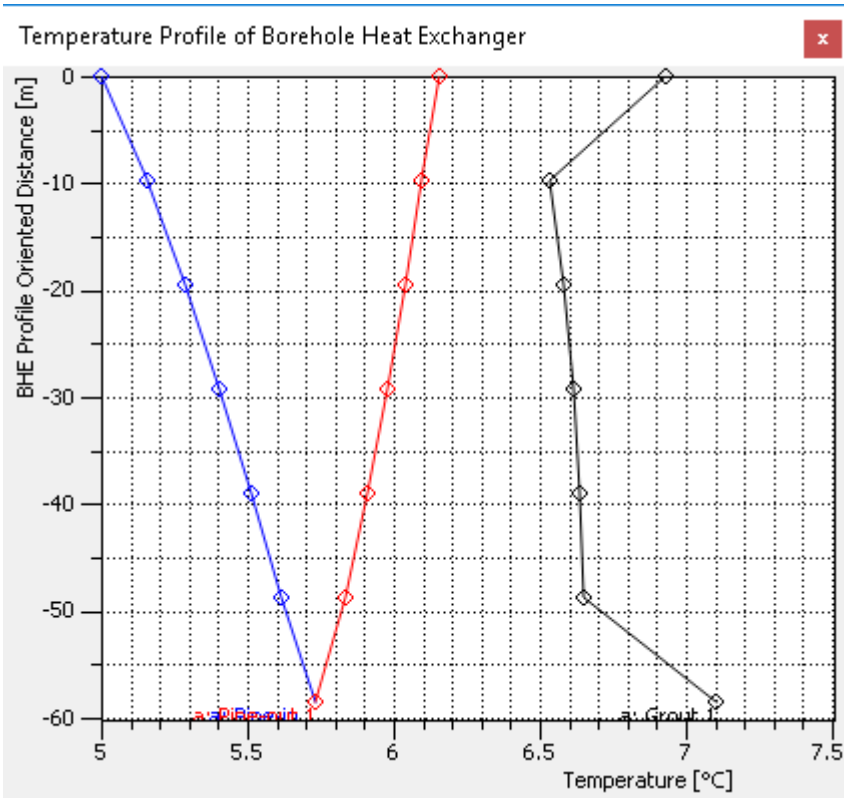

Figure 6: Temperatures in BHE (Scenario 2).

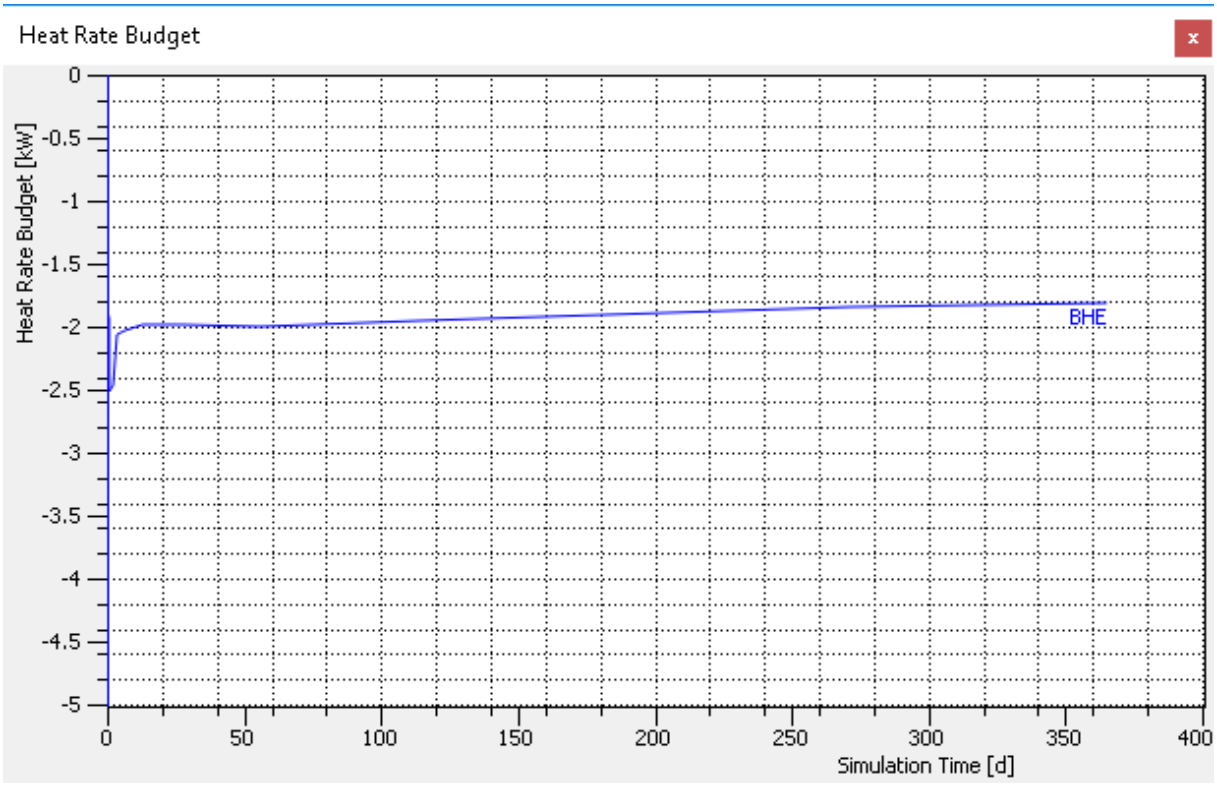

Figure 7: Extracted power at constant inlet temperature 5 °C (Scenario 2).

4. Groundwater effect on Heat Extraction Capacity (HEC)

Borehole for BHE was drilled 100 m deep and cased to 40 m depth. In the section 40 – 100 m it is open hole in saturated zone of highly productive open aquifer. Grouting of BHE is gravel and sand from the aquifer. With the numerical model we have evaluated the amount of extracted heat from the BHE with same parameters once with groundwater flow and once without groundwater flow at the constant inlet temperature of 5 °C.

	Scenario 1	Scenario 2
Input	vD = 1.28 m/s	no GW flow
Inlet temperature (°C)	5	5
Outlet temperature (°C)	9.5	6.15
BHE section (m)	40 - 100	40 - 100
Output		
Extracted heat (kW)	7.27	1.8
Calculation		
W/m	121.1667	30
Ground waterflow factor	4	/